We thank the referees for their consideration of our manuscript. Below are our responses (in red) to each of the **comments (in black)**, followed by the proposed changes and additions to our revised manuscript and supplementary information (with tracked changes in response to the comments highlighted in red).

Response to Anonymous Referee #1

Introduction: I think it's worth remarking (with appropriate references) that the "simple scheme" is fairly similar to what is used in most climate and earth system models submitted to CMIP6 (NorESM, HadGEM3/UKESM1, I think also GFDL AM4), while a couple of climate models (CESM and E3SM as far as I know) have configurations that are more similar in at least some important respects to the complex scheme (such as including the volatility basis set for semi-volatile SOA).

This is a good point; we have added a statement in the introduction with an appropriate reference from the 2014 Tsigaridis model intercomparison that can point readers to various ESMs that use similar OA schemes.

L103 "we perform a series of simulations from 2008 to 2017 using two distinct model scheme": It would be helpful to include a table summarizing the simulations that were performed (one simple, one complex, then some simulations in which the simple scheme was modified, the simple SOA with complex POA, etc.), and a more detailed explanation of which periods were simulated – just the times of the flights, or the whole year.

We have added a table summarizing the various model simulations to the supplementary information in order to provide greater detail.

Also, at or around L223: "The observations were averaged over the model grid-boxes and timestep." It would be great to be a bit more explicit about how the comparison was done - for example, was the model output also diagnosed and written out to a file on every timestep, or every few hours?

We have reworded the statement in Section 3 to be more explicit about the process and have also included more information on the plane-flight diagnostic in the supplementary materials

L112 "A standard bulk aerosol scheme": which one? Also please put into context the subsequent sentence "GEOS-chem also simulates sulfate aerosol…" – is this somehow a separate issue from the bulk aerosol scheme?

We have added an appropriate reference to the aerosol scheme used in this study and have reworded the paragraph to limit confusion.

Figure 4: It's rather unfortunate that the differences between the two schemes are greatest in areas where you have no measurements: central Africa and inland in China. This is pointed out in the conclusions, but perhaps Africa should be added to the list on line 612 – you could also point out that there do exist some datasets that might already help with resolving the large discrepancies there (DACCIWA, ORACLES, for example)?

We have added Africa to the list and have mentioned some relevant campaigns.

"The explicit aqueous uptake mechanism for the isoprene-derived SOA products also results in substantially larger global isoprene SOA burdens (0.31 Tg) when compared to the 'pureVBS' treatment of isoprene-derived SOA that simulates an annually averaged ISOA burden of 0.12 Tg" - -so was there an additional simulation performed with the aqueous uptake turned off? Can you be a bit more detailed about what differences this causes, maybe adding another row to Table 2 where isoprene SOA is split into aqueous and non-aqueous contributions?

The isoprene SOA in the complex scheme does not include any non-aqueous contribution and is an explicit scheme that does not include any reversible partitioning. The 'pure VBS' simulation models isoprene SOA using the VBS (no explicit mechanism) as in Pye et al. (2010), and was used in the paper in order to provide context for the complex scheme results. We have updated our model description to explicitly clarify this in order to limit any confusion and have also added a separate category to the model descriptions in the SI.

L295. It is stated in the abstract that the model skill is superior to previous model evaluations, and in this section at line 295 the model is compared to an ensemble from Tsigaridis et al 2014. However, the reasons why the model differs from the ensemble probably vary from model to model. For the GEOS-chem model, the authors already include some comments about how the current model differs from that in Heald et al 2011 at lines 427 and 438. Can the authors identify whether it is changes to the emissions inventories since the 2011 paper, or changes to the OA schemes, that are responsible for the differences? Also, perhaps it is worth saying why some of the campaigns from Heald et al 2011 were used in the current study, but not others (presumably this was just to avoid running the simulations for unfeasibly many years)?

While it is likely that the model improvement is largely due to the combination of changes in OA schemes and emissions, it is difficult to attribute model improvement between the different versions given the large number of changes to model code and inputs without running an extensive series of sensitivity experiments with the older code. This is thus regrettably beyond the scope of the work.

We selected a list of representative campaigns to conduct this study and, given the number of simulations required per campaign and our limited computational resources, we decided to focus on campaigns with AMS observations, within the last decade, and that were publicly-available when we started this project in 2017. Text to this effect has been added to Section 3.

L343: The regime analysis is interesting and very useful in the following interpretation, but needs some further explanation, or possibly further tuning of the classifications, because some features of Figure 5 are rather surprising. In Figure 5, many regions that must be at least relatively pristine compared to the eastern United States are categorized as anthropogenic (large portions of the North Atlantic and North Pacific ATOM flights, much of the Canadian Arctic) and perhaps this can explain the sentence "Median concentrations over anthropogenic regions are markedly lower than those over other sources"?

Another way to make this figure 5 less surprising might be to introduce separate categories for 'remote anthropogenic' and 'polluted anthropogenic' based on another mass threshold.

We acknowledge the reviewer's concern and have modified the paragraph to explicitly state that our classification of anthropogenic OA (and indeed all other categories) includes both 'fresh' and 'aged' regions which, particularly in the case of anthropogenic SOA, explains the lower median. The regime analysis is imperfect but is intended to provide broad classification and we have found that adding additional categories over the ones currently in the study can be overwhelming while adding little to the underlying classification that is based on a relative weighting as opposed to an absolute one. With regards to the North Pacific, we track much of that pollution to east Asian emissions from China and the surrounding countries, while the North Atlantic is influenced by both European and African emissions.

Then, it looks like most of the eastern USA is classified as "remote". Is "remote" being plotted on top of "anthropogenic" for example, so the high volume of data would cause misleading results where only the last plotted regime shows up? Or is the North Atlantic characterized as anthropogenic because the aerosol mass concentration can be quite high due to a lot of dust (and the North Pacific, potentially, due to volcanic sulfur). Could other aerosol types have been included in the 'aggregate OA mass concentration' threshold of 0.2mugsm3?

As the reviewer points out, the reason there appear to be a number of remote points over the eastern US is due to the density of observations, resulting in observations in the upper troposphere that are below 0.2 μg sm^{-3} (and thus, 'remote') being plotted over points lower in the troposphere. We have added a few lines to the paragraph in order to explicitly clarify this. The regime analysis has been conducted exclusively with OA concentrations and is thus not influenced by other aerosol types. The reason portions of the North Atlantic are classified as anthropogenic is because they do not meet the threshold for remote concentrations (0.2 μg sm^{-3}) and are composed of a minimum of 70% anthropogenic OA (from various continental sources)

The classification would presumably be quite different if the figure was remade using regime types from the complex scheme rather than the simple scheme. Perhaps this would be interesting to try, just to reproduce Figure 5 (no need to repeat the whole analysis!) It would overcome the shortcoming of the simple scheme already mentioned in the text that it tends to count (for example) anthropogenically influenced biogenic SOA as anthropogenic SOA.

In an attempt to address the reviewer's comment, we experimented with source regimes using the complex scheme, however, given the complexities involved in partitioning the POA it is difficult to separate the contribution from anthropogenic and fire sources without large structural changes to the code along with the addition of a number of new tracers (and repeating a suite of simulations).

Figures 7 and 8 show that in the remote/marine region, the two schemes also disagree radically on whether the aerosol is primary or secondary, above 2km altitude. This is well discussed in the first paragraph of the conclusion but also seems worthy of greater emphasis and discussion in the paper around line 505. It is remarkable how well both schemes reproduce observations despite this (at least in Figure 7 and in summer, and even the lack of variability noted at line 378 does not seem to be a large effect in Figure S2). It makes sense that semivolatile POA gets to high altitude more effectively than non-volatile POA, so it stands to reason that the complex scheme is doing well. So then it seems surprising that overall the model with complex POA and simple SOA, from fig S7, seems to underestimate OA in the remote region (negative NMB)- if I understand how the NMB is defined, it should overestimate it. Similarly, the reverse arrangement, with simple POA and complex SOA, should underestimate, but the NMB is positive. What does the altitude profile look like?

There are several ways to calculate NMB – please can the authors include an equation somewhere in the text to define it?

We agree that it is surprising that the simple and complex scheme broadly track each other given the large differences in OA contributions from the different sources. We have added a short discussion on this topic. We have also included an additional section on why we chose R^2 and NMB as representative metrics in the main text and have included the equations for how we calculate both metrics. The simple SOA is non-volatile and is thus less sensitive to the altitude profile than the complex SOA. This results in a larger complex SOA loading at higher altitudes and leads to a larger NMB.

In Figure 8, ATOM-2-W shows both models substantially overestimate SOA at high altitude, while ATOM-1-W is fine. This is explained in the text as a seasonal effect, L455. Does the overestimate square with the near-perfect agreement in Figure 7 remote/marine?

The overestimated ATom points are classified as Anthropogenic, not remote. This is why the overestimate is not present in the remote comparison.

I realise this is outside the scope of the current study, but do the authors intend to make use of a fuller range of capabilities of the ToF-AMS in tracking signatures of different aerosol sources – for example signatures of biomass burning (f60), SOA (f44) etc, relevant fragment ratios, etc, etc in future work? Or even PMF factors? I'm not an instrumentation expert, but my understanding is that the ToF-AMS can provide much richer information than simply OA, sulfate, and total

mass concentrations, and this could be used in future model evaluations to great effect. It is also one reason why the observation dataset is substantially improved relative to Heald et al 2011. I think this merits a comment in the conclusions alongside the comments about the importance of additional observational constraints from new campaigns, since the expense of new observations would be much easier to justify once the existing datasets have been fully exploited.

We wholeheartedly agree with the reviewer! Unfortunately, such tracers, PMF factors, and P-ToF size distributions are typically not provided in publicly-accessible datasets. We have added a statement in the conclusions addressing this point and stating that the standardized reporting of chemical signatures from AMS data could enable further model evaluation.

Figure 6, 10, and S2: the colors are confusing compared to the AMS conventions, please use red for sulfate and green for complex OA.

We apologize for the confusion; given our use of two OA schemes, we could not use standard 'AMS green' for organics, so decided to differentiate these throughout with red and blue. As a result, we cannot use red for sulfate. However, we agree that using green could be confusing and have changed the sulfate plots to purple so as to be clearly differentiated from the AMS color scheme.

In Table 3, the standard deviation is often greater than the mean and median, yet negative concentrations aren't possible. This is clearly a matter of opinion and a pretty minor point, but maybe presenting the interquartile range (or better still, the upper and lower quartiles separately) would be more instructive? Or a figure like figure S4, but just to represent variability in observations?

In order to prevent a skew in our analysis, we have not excluded negative observations from our dataset. We chose to use the mean and median as metrics to allow for ease of interpretation but have added a figure to the SI to represent the variability in the observations.

L524 I know it should be obvious but it may be worth saying "biogenic SOA yields for the simple scheme" as presumably this wasn't done for the complex scheme as the dependence is already present.

We have made the change to clarify the statement.

Response to Anonymous Referee #2

Use of ground measurements. It is not clear why the authors restrict their model evaluation to airborne measurements when there are also ground measurements available in the same areas (US, Europe) for the simulated periods. This is especially problematic because they conclude that the simple modeling scheme is especially attractive for health studies. They also suggest that based on the airborne measurements both schemes appear to overpredict OA in the lower

troposphere. This comparison (at least with the IMPROVE and EUCAARI measurements) should be added to the revised paper.

We agree that a comparison with ground observations would provide a more constrained understanding about exposure. However, this is not the focus of this study and we chose to limit our analysis to aircraft observations for the following reasons:

1. Ground networks are only available in a few locations (US and Europe)
2. These ground networks use different instrumentation; our goal was to use consistent AMS measurements.
3. We could have used globally distributed AMS observations, such as in Jimenez et al. (2009), however comparisons of global models with surface sites are more susceptible to representation errors and sub-grid meteorology that are both challenging to address. We specifically designed the study to focus on the regional constraints offered by airborne measurements around the world that sample OA under a range of conditions.
4. Health impacts are not the focus of this work (i.e. we do not focus on surface concentrations or exposures), therefore observational exploration throughout the full troposphere seemed best suited for exploring the OA budget.

We have modified the main text by adding more details explaining our rationale.

Treatment of POA. It is not clear how the POA emissions and the POA atmospheric chemistry are treated in the two models. Some major issues:

(a) Why is the POA emission rate (based on Table 2) in the simple model 21.8 Tg/yr and in the complex model 55.4 Tg/yr? Based on the paper there is a 27 percent increase of the emissions while these numbers suggest a 150 percent increase.

In the simple scheme, 50% of the POA is emitted as EPOA (Emitted Primary Organic Aerosol) and 50% is emitted as OPOA (Oxygenated Primary Organic Aerosol) to approximate the near-field aging of EPOA. Total OC emissions are 31.2 TgC. Thus, given the OC:OM ratios of 1.4 and 2.1 assumed for EPOA and OPOA respectively, total POA emissions in the simple scheme are 21.8 Tg EPOA and 32.8 Tg OPOA for a total annual POA emission of 54.6 Tg. In the complex scheme, all POA is emitted as gas-phase EPOG after scaling the same inventory used in the simple scheme by 27% to account for the extra gas-phase material. Total primary emissions in the Complex Scheme are thus solely from EPOG gas phase emissions and amount to 55.4 Tg. We agree that these details can be difficult to follow and have therefore added more information to the main text (and corrected the simple emissions from 54.3 Tg yr^{-1} to 54.6 Tg yr^{-1}). We have also included more information in the SI.

(b) What is the assumed saturation concentration of the POA in the complex model? What is its enthalpy of evaporation?

As described in Pye et al. (2010), EPOG saturation concentrations are 1646 and 20 μg m^{-3} at 300 K. As EPOG ages to OPOG, the volatility of the reaction products decreases by a

factor of 100 (Pye et al., 2010; Grieshop et al., 2009). An enthalpy of vaporization of 50 kJ mol^{-1} is assumed in this study. We have added these details in the SI with the appropriate references.

Anthropogenic SOA. How is this simulated in the complex model? Why is so much less than in the simple model? The production of SOA from IVOCs in the complex model is not described well. There is little information about how the IVOC emissions (shown in Table 1) have been estimated and the corresponding yields used. The sentence regarding the use of naphthalene as a proxy (lines 169-171) does not clarify this issue.

The anthropogenic SOA in the complex scheme is as described in Pye et al. (2010). To address the reviewer's questions, we have added more detailed information on the complex OA scheme (and the formation of SOA from IVOCs and aromatics) to the SI and have also expanded the discussion in the main text to provide greater clarity and address the discrepancy.

POA lifetime: Line 306. This is quite difficult to understand and it appears to be counterintuitive. The information about the POA treatment is limited. For example, the saturation concentrations of the two products used (lines 152-153) are not given. Also the conversion of the EPOG to the OPOG is not explained and the corresponding parameters for the reactions and volatilities are missing. Finally, there is no information about the removal of the corresponding organic vapors (e.g., assumed Henry's law coefficients). The authors should explain physically how a 27 percent increase in emissions (with some of them in the gas phase) leads to a more than 50 percent increase of the burden of particulate POA.

As with the previous points, we refer the reader to the original paper on this scheme (Pye et al., 2010) for a complete description. In light of the reviewer's comments, we have expanded the discussion in the main text and have included the information below in the SI:

EPOG saturation concentrations are 1646 and 20 μg m^{-3} at 300 K. As EPOG reacts with OH and ages to OPOG, the volatility of the reaction products decreases by a factor of 100. The reaction rate for POG to OPOG (K_{OH}) is 2 x 10^{-11} cm^3 $molec^{-1}$ s^{-1}

The 27% increase in emissions are all in the form of gas-phase POG (with a OM:OC of 1.4) that is hydrophobic and is advected higher in the troposphere before forming OA where it is less likely to be deposited. It is then aged to OPOG (with a OM:OC of 2.1). This sensitivity to temperature (and thus altitude) results in the formation of organic aerosol aloft, in a manner that the simple scheme cannot simulate due to its non-volatile representation, and leads to higher concentrations in the upper-troposphere where the aerosol experiences longer lifetimes.

The fraction of gas-phase OA precursors wet deposited is dictated by the liquid to gas ratio for a grid-box at any given timestep. For a soluble gas 'i', this ratio is calculated based on the following relationship:

$$\frac{C_{i,L}}{C_{i,G}} = K_i^* * L * R * T$$

where K_i* is the effective Henry's law constant that is calculated using the van't Hoff equation (Jacob et al., 2000), L is the cloud liquid water content, R is the ideal gas constant and T is the local temperature. Each organic gas-phase species has an associated Henry's law solubility constant (in M atm^{-1}), volatility constant (in K) and pH correction factor which is defined in the GEOS-Chem species database.

EPOG Henry's Law Solubility Constant = 9.5 M atm^{-1}

OPOG Henry's Law Solubility Constant = 1 x 10^5 M atm^{-1}

Lifetimes of OA components: A wide range of global average lifetimes (from 3 to 11.5 days) is predicted. This is rather surprising for particulate matter components that should have similar size distributions. A discussion of how removal is parameterized and an explanation of these unexpected differences among different components are needed.

We agree with the comment and were similarly surprised by the wide range in lifetimes. Closer inspection suggests that this is due to a few different factors. We have expanded our discussion in the main text and the SI to cover these points.

1. Spatial Distribution in Aerosol Types – Species emitted over marine / tropical regions experience a higher risk of being deposited via wet deposition than aerosol over more temperate regions.
2. Hydrophilic nature of the aerosol – EPOA is treated as hydrophobic, rainout is turned off and the rate constant for conversion of cloud condensate to precipitation is halved, leading to a longer lifetime against wet-deposition. Oxygenated OA (OPOA and SOA) are treated as hydrophilic and thus have shorter lifetimes.
3. Vertical Distribution – The complex scheme treats OA as semi-volatile. As a result, both POA and SOA species are often in the gas phase in the warmer parts of the troposphere and are less likely to be deposited. These gaseous vapors are advected to the upper troposphere where they then form OA aloft. These aerosol species then have a longer lifetime against deposition since they are less sensitive to meteorology in the lower troposphere.

We refer the readers to Wesely (1989), Zhang et al. (2001), Jacob et al. (2000), Liu et al. (2001) and Amos et al. (2012) for details on dry and wet deposition in GEOS-Chem and have included more details in the SI.

Uncertainty of measurements. The authors site a 34-38 percent uncertainty of the measurements that they use. However, this is not taken in the evaluation of the two models. Could the model errors and biases be due to the corresponding measurement errors? Could most of the R2 difference from unity just be due to these errors? These issues should be addressed and taken into account in the corresponding conclusions. For example, if one of the model was

perfect but the measurements had a 35 percent uncertainty what would be the R2 between measurements and predictions?

This is an interesting point. 33% of the modeled data-points fall within the observed uncertainty. We have added a statement to the conclusion that addresses this. If the model was perfect but you add noise (normally distributed with a mean scale factor of 1 and a SD of 0.14) to the observations, the R^2 is 0.97. Thus, measurement uncertainty is unlikely to be a major driving factor in the model-obs R^2.

Averaging times. The evaluation of any model does depend on the timescale investigated. This timescale appears to be 10 min. If this is the case, it should be mentioned in all graphs, tables but also in the text. An analysis at different timescales (say 1 hr and campaign average) could provide some additional insights. This would allow the authors to include all their measurements (avoid excluding the highest values).

We have added more explicit references to the 10 min timescale in the main text and referenced this in the figure captions. In addition, campaign average statistics are available in Table 2. We chose not to average over a more extended period given that the spatial variance in aircraft observations provides useful information that we prefer not to degrade.

Model performance statistics. The discussion is based on R2 and normalized mean bias (NMB). I think that the errors (both absolute and normalized) should be included in the analysis. For example, they appear to be quite useful in the discussion related to Figure 12.

The choice of metrics can be somewhat subjective and an initial draft of our study did include multiple metrics. However, we ultimately chose to limit ourselves to NMB and R^2 in order to maintain consistency and readability. Absolute differences and ratios are included in the SI (Figure S4). We found that the conclusions of our manuscript do not depend on the choice of metrics and have added a section to the paper explaining our choice of metrics along with their descriptions.

Role of enthalpy of evaporation. Given that a lot of the measurements were collected at relatively low temperatures the predicted partitioning of the semi-volatile OA components will depend on the assumed enthalpy of evaporation. It is not clear which values are used in the present work. The sensitivity of the conclusions of the paper to these assumed values should be discussed.

We assume an enthalpy of vaporization of 50 kJ mol^{-1} and have included that information in the main text and SI.

Underestimation of OA. Is it still appropriate to say (abstract and introduction) that models significantly underestimate observed OA concentrations in the troposphere?

The most recent studies including both models here tend to overestimate OA levels. Some additional discussion of the recent OA modeling work is needed here.

Certain recent studies with the GEOS-Chem model (such as Marais et al. 2016) have been shown to match the magnitude of SEUS observations, but since the scheme was developed and optimized for this region, this cannot be viewed as an independent test. The simple scheme as implemented here has not been previously evaluated in the literature (the older OA scheme in GEOS-Chem used different parametrizations) but previous evaluations of OA with GEOS-Chem have demonstrated a tendency to underestimate OA at the global scale (Heald et al., 2011; Spracklen et al., 2011; Hodzic et al., 2016). Our statement is intended to convey a general historical context (particularly in the GEOS-Chem model) as opposed to serving as a blanket statement for all regions.

Sources of bias. The complex model tends to overestimate OA levels. It is not entirely clear which attributes of this model (at least compared to the simple one) are contributing to this tendency for overestimation. Is it the isoprene SOA that is included in different ways in the two models? Something else? Some additional discussion is needed.

The discrepancy between the simple and complex scheme is the result of a number of factors and can be attributed to different reasons depending on the location. As Figure 11 shows, the complex model overestimates in many regions, but underestimates in others, and the reasons for these biases depend on the regional factors which are discussed in the main text. In general, Figure 4 shows that the burden in the complex scheme is higher generally because of more isoprene SOA and primary OA.

Sesquiterpenes. It is not clear how the models treats SOA from sesquiterpenes. In Figure 1 this pathway is missing. In line 168 they are mentioned as a source of SOA. The yields used are surprisingly low at least for the simple model: they are equal to those of the monoterpenes, despite the much larger size of these molecules. The yields used in the complex model are not clear. The same applies to their importance as SOA precursors in these simulations.

Thank you for pointing out this omission. In the simple scheme sesquiterpenes are assumed to have a 10% SOA yield. In the complex scheme, they are treated using the VBS framework (described in Pye et al. 2010) and have an average yield of 42% at 298K with a C_{OA} of 10 ug m^{-3}. In both cases, the resulting SOA is lumped with SOA from other terpenes (TSOA). We have clarified the description in the main text and added the relevant details to the SI.

Organonitrates. The treatment of organonitrates requires some additional explanation given that they are implicitly included in the SOA formed in the parameterizations of Pye et al. (2010). Do they represent additional SOA mass or do they describe a subset of the SOA predicted by the parameterizations used? Could this be contributing to the overestimations? Finally, there has

been considerable work quantifying the organonitrate PM levels in Europe (Kiendler-Scharr et al., GRL, 2016) during the simulated EURAARI period that is not used here.

The complex scheme uses an explicit mechanism to model the formation of organo-nitrates based on work by Fisher et al. (2016). The Pye et al. (2010) paper does not explicitly model SOA from this pathway, instead using lumped SOA yields within the VBS framework to model the SOA resulting from oxidation with NO_3. The simple scheme parametrization does not explicitly account for organo-nitrate formation. We have outlined the mechanisms used in this study in the Supplementary Information and also point the readers to the appropriate references for further detail.

Regarding new developments in model organo-nitrate treatment, the focus of this work is not specifically on organo-nitrates so we have not incorporated more recent developments in the field. We have added a reference to Kiendler-Scharr et al. (2016) in the discussion, suggesting that a more constrained treatment of organo-nitrates could improve model performance over Europe.

Model performance in Europe. The parameterizations used in both models have been based, to a large extent, on US field measurements. The relatively poor performance of both models in Europe during EUCAARI requires additional attention. The comparison with the ground sites would be quite helpful here. What is the source of the high predicted concentrations which are inconsistent with the measurements?

Both schemes largely under-predict OA concentrations over Europe, potentially due to an underestimate in terpene SOA. Unfortunately, to our knowledge there are no publicly accessible airborne AMS observations over Europe to further investigate this bias. We have expanded our discussion on this topic.

Model behavior during the winter. This is significant weakness of the paper given that similar modeling exercises suggest that the models have significant problems in the winter. The authors can use ground measurements to close this gap. They could also change the title of their paper to specify that this evaluation is only for the summer and spring.

Given the paucity of airborne AMS observations in the winter (with to our knowledge only one publicly accessible campaign during this season – WINTER 2015) and the computational constraints of running more simulations, as stated in our manuscript we do not feel that we can adequately characterize the full seasonal cycle. Introducing comparisons with ground observations over limited regions would skew our conclusions about wintertime OA, and would be inconsistent with the design of the study (see our response above). We have expanded on this aspect in the conclusions and have included a statement in the abstract in the interest of transparency and clarity.

Evaluation for CO and other gases. Given the importance of CO for the parameterization used in the simple model, an evaluation of the ability of the performance to reproduce measured CO levels is needed. A similar evaluation for isoprene (in the appropriate regions) would be helpful.

An evaluation of the model ability to reproduce gas-phase species was not the focus of this study and was deemed to be out of the scope of this analysis, particularly given that these observations were not available for all campaigns. We have provided global emissions numbers for CO, NOx, and isoprene, so that these can generally be compared to other studies.

Characterization of the two models. I found the characterization of the two models as simplex and complex rather misleading. Their differences are mainly in the processes that they simulate, the emissions that they use, and the parameters that they use. They are by no means a simplified version of the other. While I understand the need for names, I also think that the paper should include a table with the main differences in the two simulations. These differences should be the emissions (Table 1 is confusing right now), the processes simulated in one and not the other, the differences in the simulation of the same process (e.g., assumed effective yields for a given OA level), and the different parameters used. If the authors can attribute the differences in predictions of the two models to simplicity or complexity, this should be done carefully and should be properly supported.

Thank you for the suggestion. In order to provide clarity and limit any confusion we have added a table with the relevant details to the SI and also included a section in the main text explaining the difference in emissions.

Lines 42-43. This sentence is confusing.

We have modified the statement to limit confusion

Lines 73-74. The formation of SOA in some of these models was by no means instantaneous. The VOC precursors were required to react first.

While some types of SOA were formed via the reaction of VOC precursors, the studies we are referring to use a fixed yield approach to the formation of many types of SOA. We have modified the wording in order to ensure clarity.

Lines 131-132. The names of the species in the code are not needed here.

We include them because the use of EPOA and OPOA are not standard in the GEOS-Chem community when describing non-volatile OA, and we want to ensure that future users are clear about our definitions. Thus, in the interest of clarity, we prefer to retain this.

Lines 141-143. The use of the term yield is rather confusing. Does this mean for example for fires that the assumed SOAP emission is 1.3 percent of the emitted CO? Something else? In Figure 1 it appears that CO is producing SOA making this even more confusing.

We have modified the terminology to 'co-emission' in order to limit any confusion.

Lines 142-143. Please explain the biogenic sources discussed here. I am assuming that this means isoprene and the monoterpenes. Referring to Figure 1 could help.

We have expanded on the statement to provide more detail.

Lines 147-150. Please explain what do these tracers represent and how their use allows the independent adjustment of model parameters.

The default model only includes one SOAP and one SOAS tracer, making it impossible to differentiate the different sources. Our modified scheme separately tracers the SOAP and SOAS from fire, anthropogenic and biogenic sources in order to establish the relative contribution from each pathway.

Table 2. I find this table confusing. For example, the four POA emission rates do not add up to the total. It also mixes actual emission inputs with estimates from steady state calculations. May be the information could be clearer if it was replaced by two tables.

We have added a paragraph to the text to clarify some of the confusion about atmospherically formed vs directly emitted OA

Line 202: The 54.3 Tg/yr of POA emissions in the simple model cannot be found Table 2.

POA emissions (54.6 Tg yr^{-1}) are composed of direct EPOA + OPOA emissions but do not include OPOA steady state formation (which is included in the table). We have edited the main text to limit any confusion and corrected an error to change 54.3 Tg yr^{-1} to 54.6 Tg yr^{-1}.

Figure S1 should probably be moved in the main paper. If needed it can replace of the figures with the vertical profiles.

We have moved Figure S1 into the main text. It is now Figure 7.

The conclusion regarding the overestimation of the aqueous uptake of isoprene should be added to the abstract.

We have added a statement to the abstract.

An evaluation of global organic aerosol schemes using airborne observations

Sidhant J. Pai[1], Colette L. Heald[1,2], Jeffrey R. Pierce[3], Salvatore C. Farina[3], Eloise A. Marais[4], Jose L. Jimenez[5], Pedro Campuzano-Jost[5], Benjamin A. Nault[5], Ann M. Middlebrook[6], Hugh Coe[7], John E. Shilling[8], Roya Bahreini[9], Justin H. Dingle[9], Kennedy Vu[9]

[1]Department of Civil and Environmental Engineering, Massachusetts Institute of Technology, Cambridge, MA, 02139, USA
[2]Department of Earth, Atmospheric and Planetary Sciences, Massachusetts Institute of Technology, Cambridge, MA, 02139, USA
[3]Colorado State University, Department of Atmospheric Science, Fort Collins, CO, 80523, USA
[4]Department of Physics and Astronomy, University of Leicester, Leicester, LE1 7RH, UK.
[5]Department of Chemistry, and Cooperative Institute for Research in Environmental Sciences (CIRES), University of Colorado, Boulder, CO, 80309, USA
[6]NOAA Earth System Research Laboratory (ESRL) Chemical Sciences Division, 325 Broadway, Boulder, CO 80305, USA
[7]Centre for Atmospheric Science, School of Earth and Environmental Science, University of Manchester, Manchester, M13 9PL, UK
[8]Atmospheric Sciences and Global Change Division, Pacific Northwest National Laboratory, Richland, Washington, USA
[9]Department of Environmental Sciences, University of California, Riverside, CA 92521, USA

Correspondence to: Sidhant J. Pai (sidhantp@mit.edu) and Colette L. Heald (heald@mit.edu)

Abstract. Chemical transport models have historically struggled to accurately simulate the magnitude and variability of observed organic aerosol (OA), with previous studies demonstrating that models significantly underestimate observed concentrations in the troposphere. In this study, we explore two different model OA schemes within the standard GEOS-Chem chemical transport model and evaluate the simulations against a suite of 15 globally-distributed airborne campaigns from 2008-2017, primarily in the spring and summer seasons. These include the ATom, KORUS-AQ, GoAmazon, FRAPPE, SEAC4RS, SENEX, DC3, CalNex, OP3, EUCAARI, ARCTAS and ARCPAC campaigns and provide broad coverage over a diverse set of atmospheric-composition regimes – anthropogenic, biogenic, pyrogenic and remote. The schemes include significant differences in their treatment of the primary and secondary components of OA – a 'simple scheme' that models primary OA (POA) as non-volatile and takes a fixed-yield approach to secondary OA (SOA) formation, and a 'complex scheme' that simulates POA as semi-volatile and uses a more sophisticated volatility basis set approach for non-isoprene SOA, with an explicit aqueous uptake mechanism to model isoprene SOA. Despite these substantial differences, both the simple and complex schemes perform comparably across the aggregate dataset in their ability to capture the observed variability (with an R^2 of 0.41 and 0.44 respectively). The simple scheme displays greater skill in minimizing the overall model-bias (with an NMB of 0.04, compared to 0.30 for the complex scheme). Across both schemes, the model skill in reproducing observed OA is superior to previous model evaluations and approaches the fidelity of the sulfate simulation within the GEOS-Chem model. However, there are significant differences in model performance across different chemical source regimes,

classified here into 7 categories. Higher-resolution nested regional simulations indicate that model resolution is an important factor in capturing variability in highly-localized campaigns, while also demonstrating the importance of well-constrained emissions inventories and local meteorology, particularly over Asia. ~~A comparison of the POA loadings from the complex scheme with SOA loadings from the simple scheme (and vice versa).~~ Our analysis suggests that a semi-volatile treatment of POA is superior to a non-volatile treatment. It is also likely that the complex scheme parameterization overestimates biogenic SOA at the global scale. While this study identifies factors within the SOA schemes that likely contribute to OA model bias (such as a strong dependency of the bias in the complex scheme on relative humidity and sulfate concentrations), comparisons with the skill of the sulfate aerosol scheme in GEOS-Chem indicate the importance of other drivers of bias such as emissions, transport, and deposition that are exogenous to the OA chemical scheme.

1. Introduction

Aerosols in the atmosphere have significant climate impacts through radiative scattering and cloud formation (IPCC, 2013; Ramanathan et al., 2001). Exposure to these particles is also detrimental to human health and is associated with over 4 million premature deaths per year world-wide (Pope and Dockery, 2006; Cohen et al., 2017). Organic aerosol (OA) often accounts for a large portion of the total fine aerosol burden (Jimenez et al., 2009), a fraction that has been increasing over time, particularly in regions where sulfur dioxide controls have reduced anthropogenic sources of sulfate (Marais et al., 2017). Characterizing aerosol impacts on air quality and climate thus requires a comprehensive understanding of the lifecycle of organic aerosol in the atmosphere.

Organic aerosol that is emitted directly into the atmosphere from anthropogenic or natural sources is called primary organic aerosol (POA). A significant fraction of primary organic emissions have been shown to be semi-volatile, partitioning between the gas and particle phase depending on ambient temperature and background organic aerosol concentration (Grieshop et al., 2009; Lipsky and Robinson, 2006; Robinson et al., 2007; Shrivastava et al., 2006). As these compounds are dispersed through the atmosphere, they are oxidized (in both gas and particle phase) and typically form lower volatility products. In addition to the primary component, organic aerosol is also generated dynamically in the atmosphere from volatile organic compound (VOC) and intermediate volatility organic compound (IVOC) precursors that are both anthropogenic (e.g. benzene, toluene, xylene) and biogenic (e.g. isoprene, ~~and~~ monoterpenes, sesquiterpenes). These gas-phase precursors undergo multi-phase, multi-generational oxidation processes that result in a complex array of semi-volatile species that partition into organic aerosol under conducive conditions. This class of aerosol products is called secondary organic aerosols (SOA). Both POA and SOA are important drivers of climate and air quality, often influencing regions far removed from their original source locations (Kanakidou et al., 2005).

Primary organic aerosol has traditionally been modeled as non-volatile (e.g. Chung & Seinfeld, 2002), but recent studies have incorporated a semi-volatile treatment that allows the aerosol species to dynamically partition between the condensed-phase and gas-phase, while simultaneously undergoing gas-phase oxidation to form organic compounds of lower volatility (Donahue et al., 2006; Robinson et al., 2007; Huffman et al., 2009; Pye and Seinfeld, 2010). There has been a similar evolution in the methods to model the formation and chemical processing of SOA in

the atmosphere. Initial global modeling efforts often simulated SOA as a species that is directly ~~instantaneously~~ formed upon emission of various precursors based on a fixed yield from laboratory or field studies (Chin et al., 2002; Kim et al., 2015; Pandis et al., 1992; Park et al., 2003). Many earth system models continue to use this simple approach (Tsigaridis et al., 2014). The two-product absorptive reversible partitioning scheme was then developed to account for the semi-volatile nature of SOA, using lumped oxidation products from precursor VOCs (Odum et al., 1996; Pankow, 1994). Advances in computational resources have enabled recent studies to more effectively capture the volatility-distribution of organics, using a volatility basis set (VBS) of volatility-resolved semi-volatile surrogates that absorptively partition based on dry ambient OA concentrations (Donahue et al., 2006; Pye et al., 2010). There have also been more explicit chemical treatments of organic aerosol formation, such as those involving the implementation of a master chemical mechanism coupled with equilibrium absorptive-partitioning and reactive surface uptake mechanisms (Li et al., 2015; Xia et al., 2008) or the explicit description of irreversible aqueous OA formation pathways (Fisher et al., 2016; Lin et al., 2012; Marais et al., 2016).

The wide range of VOC precursors, the complexities of the various formation pathways, and the limited laboratory constraints on these processes make accurately modeling OA concentrations highly challenging. Previous model studies have identified large underestimates in the simulated OA when compared to observations (e.g. Heald et al., 2011; Volkamer et al., 2006). Over the past decade, the treatment of organic aerosol in chemical transport models has grown in complexity with models showing improved regional skill at simulating OA over areas like the southeast US (Marais et al., 2016; Budisulistiorini et al., 2017). However, studies that have evaluated OA model simulations against globally distributed measurements have demonstrated a consistent model inability to capture the magnitude and variability of observed OA concentrations (Heald et al., 2011; Tsigaridis et al., 2014). In particular, the evaluation by Heald et al. (2011) that used a two-product OA scheme revealed significant deficiencies in model skill and suggested that the GEOS-Chem model underestimated both the sources and sinks of OA at the global scale. The complex nature of OA formation and loss mechanisms in the atmosphere has thus made it difficult to constrain global models using a bottom-up approach, particularly given the uncertainties inherent in the various emission inventories and chemical mechanisms. Here, we use a top-down approach, leveraging a suite of 15 aircraft campaigns to evaluate the two different organic aerosol schemes implemented within the standard GEOS-Chem chemical transport model in order to assess their relative strengths and weaknesses over a wide range of chemical and spatial regimes.

2. Model Description

We use the chemical transport model GEOS-Chem (www.geos-chem.org) to simulate organic aerosol mass concentrations along the flight tracks of a suite of airborne campaigns described in Sect. 3. In order to contrast the different approaches to modeling organic aerosol and its precursors in the atmosphere, we perform a series of simulations from 2008 to 2017 using two distinct model schemes that vary based on their treatment of organic aerosol (see Sect. 2.1 and Table S1).

These simulations were performed with the GEOS-Chem model version 12.1.1 (https://doi.org/10.5281/zenodo.2249246) with a horizontal resolution of 2° x 2.5° and 47 vertical hybrid-sigma levels

that extend from the surface to the lower stratosphere. A series of nested simulations, over North America and Asia, were performed at a higher spatial resolution of 0.5° x 0.625° using boundary conditions from the 2° x 2.5° global run. The model is driven by the MERRA-2 assimilated meteorological product from the NASA Global Modeling and Assimilation Office (GMAO) with a transport time-step of 10 minutes as recommended by Philip et al. (2016). The model includes a coupled treatment of HO_x-NO_x-VOC-O_3 chemistry (Mao et al., 2013; Travis et al., 2016; Miller et al., 2017) with integrated Cl-Br-I chemistry (Sherwen et al., 2016) and uses a ~~standard~~ bulk aerosol scheme with fixed log-normal modes (Martin et al., 2003). ~~Ammonium and nitrate thermodynamics are described using the ISORROPIA II model (Fountoukis and Nenes, 2007).~~ GEOS-Chem ~~also~~ simulates sulfate aerosol (Park, 2004), sea-salt (Jaeglé et al., 2011), black carbon (Park et al., 2003) and mineral dust (Fairlie et al., 2007; Ridley et al., 2012). Ammonium and nitrate thermodynamics are described using the ISORROPIA II model (Fountoukis and Nenes, 2007). Deposition losses are dictated by aerosol and gas dry deposition to surfaces based on a resistor-in-series scheme (Wesely, 1989; Zhang et al., 2001) and wet deposition from scavenging by rainfall and moist convective cloud updrafts (Amos et al., 2012; Jacob et al., 2000; Liu et al., 2001). More details on the deposition schemes are provided in the SI.

2.1 Organic Aerosol Simulations

This study evaluates the two standard organic aerosol schemes within the GEOS-Chem model. The 'complex scheme' represents a more detailed, recently updated treatment of organic aerosol in the atmosphere based on numerous laboratory studies and an explicit chemical mechanism for the oxidation of isoprene. The 'simple scheme' is designed to serve as a computationally efficient alternative for approximating tropospheric OA concentrations without attempting to model the formation and fate of the various aerosol species mechanistically and without explicit thermodynamic partitioning. We note that the simple scheme was developed independently from the complex scheme and should not be regarded as a reduced version of the complex scheme. These schemes are described below and are graphically illustrated in Fig. 1.

The Simple scheme treats all organic aerosol as non-volatile. The POA consists of a hydrophobic 'emitted' component (EPOA) with an assumed organic mass-to-organic carbon (OM:OC) ratio of 1.4 and a hydrophilic 'oxygenated' component (OPOA) with an assumed OM:OC ratio of 2.1. Of the organic carbon emitted from primary sources, 50% is assumed to be hydrophilic (OPOA) to simulate the near-field oxidation of EPOA. The atmospheric aging of EPOA is modeled by its conversion to hydrophilic aerosol (OPOA) with an atmospheric lifetime of 1.15 days, with no explicit dependence on local oxidant levels (Chin et al., 2002; Cooke et al., 1999). The EPOA and OPOA species are represented within the GEOS-Chem model using the variable names 'OCPO' and 'OCPI' respectively. In addition, GEOS-Chem includes an online emission parameterization for sub-micron non-volatile marine primary organic aerosol (MPOA) as described in Gantt et al. (2015). The marine POA is emitted as hydrophobic (M-EPOA) and is aged in the atmosphere by its conversion to hydrophilic aerosol (M-OPOA), with the same 1.15-day lifetime. For the purpose of this study, the hydrophobic and hydrophilic components have been lumped together under the MPOA moniker.

The simple scheme uses a lumped SOA product (SOAS) with a molecular weight of 150 g mol^{-1} and an SOA precursor (SOAP) that is emitted from biogenic, pyrogenic and anthropogenic sources with fixed OA yields: 3% from isoprene

(Kim et al., 2015) and 10% from both monoterpenes and sesquiterpenes (Chin et al., 2002). SOA precursor emissions from combustion sources are estimated using CO emissions as a proxy, with a 1.3% scaled ~~SOAP~~ co-emission of SOAP~~yield~~ from fire and biofuel CO, and a 6.9% SOAP co-emission~~yield~~ from fossil fuel CO (Cubison et al., 2011; Hayes et al., 2015; Kim et al., 2015). For biogenic SOA from isoprene, monoterpenes and sesquiterpenes~~sources,~~ 50% is emitted directly as SOAS to account for the near-field formation of secondary organic aerosol. The SOAP converts to SOAS based on a first order rate constant with a lifetime of 1 day as it is transported through the troposphere (Fig. 1).~~.~~

For the purpose of this study, the default simple scheme in GEOS-Chem was modified to individually simulate 14 OA lumped model tracers from anthropogenic, biogenic, marine, and pyrogenic sources. These consisted of 6 POA tracers, 4 SOA tracers and 4 SOA precursor tracers, allowing for the independent adjustment of parameters such as emission rates, yields, chemical lifetimes and deposition rates, enabling a robust testing of various sensitivities, and OA source attributions.

The Complex scheme, based primarily on Pye et al. (2010) and Marais et al. (2016), is graphically described in Fig. 1. The primary organics are treated as semi-volatile and allowed to reversibly partition between aerosol (EPOA) and gas (EPOG) phase using a two-product reversible partitioning model while simultaneously undergoing oxidation with OH in the gas phase to form oxidized primary organic gases (OPOG) which, in turn, reversibly partition to oxidized primary organic aerosols (OPOA). Primary semi-volatile organic vapors that are oxidized to form lower volatility products are sometimes classified as secondary organic aerosol (Murphy et al., 2014). However, for the purpose of this study, we define SOA as being formed exclusively from volatile precursors, while classifying the OA resulting from the oxidation of primary organic compounds as OPOA, in order to be consistent with previous model studies using GEOS-Chem (Pye et al., 2010). Model EPOG emissions are based on the EPOA inventories used in the simple scheme and have been scaled up by 27% to account for semi-volatile organic matter emitted in the gas-phase (Pye et al., 2010; Schauer et al., 2001). As in the simple scheme, the EPOA and OPOA are assumed to have an OM:OC ratio of 1.4 and 2.1 respectively. The complex scheme also includes the non-volatile MPOA simulation as described above.

SOA formation from anthropogenic, pyrogenic and select biogenic precursors is based on the VBS outlined in Pye et al. (2010) that oxidizes gas-phase SOA precursors (with oxidants - OH, O_3) to form alkyl peroxy (RO_2) radicals that react with either HO_2 or NO. The SOA formed from these second-generation products depends on the NO_x regime – with high and low NO_x yields and partitioning coefficients based on experimental fits from laboratory studies. The resulting products are classified into two categories based on the origins of their precursors, Anthropogenic SOA (ASOA; formed from the oxidation of light aromatic compounds) and Terpene SOA (TSOA; formed from the oxidation of monoterpenes and sesquiterpenes) ~~(both monoterpene and sesquiterpene) SOA (TSOA),~~ that dynamically partition between the aerosol and gas phases based on their saturation vapor pressures and ambient aerosol concentrations. Aerosol formed from intermediate volatility organic compounds (IVOCs) is modelled using naphthalene as a proxy which, when oxidized, contributes to the ASOA lumped product. A comprehensive overview of the VBS scheme can be found in Pye et al., 2010.

The complex scheme builds on this VBS framework by incorporating aerosol formed irreversibly from the aqueous phase reactive uptake of isoprene (Marais et al., 2016) and the formation of organo-nitrates (Org-Nit) from both isoprene and monoterpene precursors (denoted in Fig. 1) based on work by Fisher et al. (2016). These mechanisms replace the 'pure-VBS' treatment of isoprene SOA (ISOA) and organic nitrates (formed from the oxidation of isoprene and monoterpenes by NO_3) from Pye et al. (2010). The total organic aerosol loadings in the complex scheme are thus comprised of the EPOA, OPOA, ASOA and TSOA species in addition to the various products resulting from the isoprene and monoterpene organo-nitrate oxidation pathways (organic nitrates from isoprene and monoterpene precursors, aerosol-phase glyoxal, methylglyoxal, isoprene epoxydiols (IEPOX), C_4 epoxides, organo-nitrate hydrolysis products, second-generation hydroxy-nitrates and low-volatility non-IEPOX products of isoprene hydroxy hydroperoxide oxidation), lumped here as ISOA and Org-Nit. ISOA and Org-Nit are generated exclusively through the aqueous uptake pathway and do not include any 'non-aqueous' OA. More information on the treatment of OA in the complex scheme can be found in the SI.

In order to conduct a comparison with a VBS treatment of isoprene SOA (as described in Pye et al., 2010), an analysis was also conducted with the isoprene SOA forming exclusively through the VBS (referred to here as 'pure VBS').

2.2 Emissions

Global annual mean emissions of key species for a single simulation year (2013) are shown in Table 1. The corresponding emissions (and atmospheric sources) for OA species are shown in Table 2. Year-specific pyrogenic emissions are simulated at a 3-hour resolution from the GFED4s satellite derived global fire emissions database (van der Werf et al., 2017). Global anthropogenic emissions follow the Community Emissions Data System (CEDS) inventory (Hoesly et al., 2018). Anthropogenic IVOC emissions are estimated using naphthalene as a proxy (see SI for more information), which is assumed to have the same spatial distribution as benzene and is scaled from the CEDS inventory using the same approach as Pye and Seinfeld (2010). These emissions are overwritten with regional inventories when available, such as the National Emissions Inventory (NEI 2011) for the US (as described by Travis et al., 2016), the Big Bend Regional Aerosol and Visibility Observational (BRAVO) inventory for Mexico (Kuhns et al., 2005), the Criteria Air Contaminants (CAC) inventory for Canada (https://www.canada.ca/en/environment-climate-change.html), the European Monitoring and Evaluation Programme (EMEP) inventory for Europe (http://www.emep.int/), the Diffuse and Inefficient Combustion Emissions (DICE) inventory for Africa (Marais and Wiedinmyer, 2016) and the MIX inventory for Asian emissions (Li et al., 2017). In addition to the anthropogenic and pyrogenic inventories listed above, nitrogen oxides are also emitted from lightning (Murray et al., 2012; Ott et al., 2010), soil (Hudman et al., 2012) and ship (Holmes et al., 2014) sources. Biogenic emissions for isoprene and terpene species in GEOS-Chem are based on the coupled ecosystem emissions model MEGAN (Model of Emissions of Gases and Aerosols from Nature) v2.1 (Guenther et al., 2012). All emissions are managed via the Harvard-NASA Emissions Component (HEMCO) module (Keller et al., 2014). We note that given the inter-annual variability in emissions, particularly from fires, the emissions for years other than 2013 may differ somewhat from the values shown in Table 1 and Table 2.

In the simple scheme, 50% of the primary OA is emitted as EPOA and 50% is emitted as OPOA to approximate the near-field aging of EPOA. Total OC emissions are 31.2 TgC. Given the OC:OM ratios of 1.4 and 2.1 assumed for EPOA and OPOA respectively, total POA emissions in the simple scheme are 21.8 Tg EPOA and 32.8 Tg OPOA for a total annual POA emission of 54.6 Tg. We note that OPOA emissions in the simple scheme are a subset of the sources listed in Table 2 since they do not include atmospheric formation through the oxidative aging of EPOA. In the complex scheme, all POA is emitted as gas-phase EPOG after scaling the same inventory used in the simple scheme by 27% to account for the extra gas-phase material. Total primary emissions in the Complex Scheme are thus exclusively from EPOG gas phase emissions and amount to 55.4 Tg yr^{-1}. Both schemes emit an additional 7.0 Tg yr^{-1} of OA from marine sources. The simple scheme also directly emits 71.7 Tg yr^{-1} of SOA (in the form of SOAS and SOAP), over half of which come from anthropogenic sources. The total OA source (POA + SOA; includes direct emissions and atmospheric formation) in both the complex and simple schemes (150.1 Tg yr^{-1} and 145.3 Tg yr^{-1} respectively; Table 2) is greater than the ensemble median OA source of around 100 Tg yr^{-1} calculated by Tsigaridis et al. (2014) across a set of various global models.

2.3 Model Evaluation

Two primary metrics have been used through this study evaluate model performance compared to ambient observations (see Sect. 3) – the coefficient of determination (R^2) and the normalized mean bias (NMB). The coefficient of determination is defined by the regression fit using Eq. (1) and can be interpreted as the proportion of the variance in the observational data that is accurately captured by the model. The normalized mean bias is calculated using Eq. (2). A positive NMB indicates that the model is biased high on average and vice versa.

$$Coefficient\ of\ Determination\ (R^2) = 1 - \frac{Residual\ Sum\ of\ Squares}{Total\ Sum\ of\ Squares} \quad (1)$$

$$Normalized\ Mean\ Bias\ (NMB) = \frac{\sum_1^n (Model - Observation)}{\sum_1^n (Observation)} \quad (2)$$

3. Description of Observations

For the purposes of evaluating the GEOS-Chem model, we focus on airborne data which provides regional 3D sampling and reduces the challenges associated with model representation error at single sites. We further define a set of observations that make use of a single measurement technique, were publicly-accessible, and that do not extend beyond the last decade. The resulting observations are from 15 aircraft campaigns conducted between 2008 and 2017 and cover a wide range of geographic locations and chemical regimes. Table 3 provides a brief overview of the various campaigns included here and Fig. 2 shows the spatial extent of the individual flight tracks. Aerosol concentrations were measured using Aerosol Mass Spectrometers (AMS) (Jayne et al., 2000; Canagaratna et al., 2007) with small variations in the instrumentation and aircraft inlet configurations between the different campaigns (as referenced in Table 3). The AMS measures sub-micron non-refractory dry aerosol mass and is estimated to have an uncertainty of 34-38%, depending on the species (Bahreini et al., 2009). All concentration measurements in this study have been converted to standard conditions of temperature and pressure (STP: 273 K, 1 atm), denoted as µg sm^{-3}. In addition to

organic aerosol mass loadings, concentrations of other species such as nitrogen oxides, carbon monoxide, isoprene, and sulfate are used in this study to validate chemical regimes (see Sect. 4.2). Table S2~~1~~ provides an overview of the instrumentation and associated primary investigators for the organic aerosol and trace gas observations. Environmental and meteorological measurements such as temperature and relative humidity are also used in the analysis.

Observations are gridded to the GEOS-Chem model resolution of 2° x 2.5° (or alternatively to 0.5° x 0.625° for comparisons with nested simulations) and are averaged over the model time-step of 10 minutes in cases where multiple observations were conducted within the span of a single timestep (see SI for more details on model sampling). In order to limit the impact of localized plumes, in particular from fires, we filter the observations to remove concentrations over the 97th percentile for each campaign, eliminating measurements that can often exceed 500 μg sm^{-3}. This enables a more fair comparison with the model by disregarding the impact of sub-grid features that cannot be reproduced by an Eulerian model (Rastigejev et al., 2010). Following the averaging process, we obtain a merged dataset of over 25,000 unique points, with a broad spatial extent (Fig. 2) covering a variety of chemical regimes representing anthropogenic, pyrogenic, biogenic, and remote environments. Despite the large temporal range of the observational dataset, most of the campaigns analyzed in this study were conducted during the spring and summer seasons, limiting the ability to perform a seasonal analysis.

Based on the proximity to emission sources and exposure to long-range pollutants, there is significant variation in the observed mean, medians and standard deviations across the different campaigns (Table 3; Fig. S1). The campaigns are also influenced by different OA sources depending on their sampling region. The EUCAARI campaign over western Europe (Morgan et al., 2010), KORUS-AQ over the Korean peninsula (Nault et al., 2018), CalNex over California (Ryerson et al., 2013) and DC3 (Barth et al., 2014) and FRAPPE over the central US (Dingle et al., 2016) sample over regions that are heavily influenced by anthropogenic emissions. In contrast, the GoAmazon campaigns during the wet and dry seasons (Martin et al., 2016; Shilling et al., 2018) over the Manaus region in the Amazon and the OP3 campaign (Hewitt et al., 2010) over equatorial forests in southeast Asia are heavily influenced by biogenic emissions, although the GoAmazon campaign in the dry season is also strongly influenced by biomass burning. Additionally, data from both seasons of the GoAmazon campaign are influenced by anthropogenic urban outflow from Manaus (Shilling et al., 2018). Campaigns like SENEX (Warneke et al., 2016) and SEAC4RS (Toon et al., 2016) that conducted measurements over the southeast US are influenced by both anthropogenic and biogenic emissions while the ARCPAC campaign (Brock et al., 2011) during the spring and the ARCTAS (Jacob et al., 2010) campaign during the spring and summer over the northern latitudes are strongly influenced by pyrogenic emissions from forest fires (particularly during the summer) and aged anthropogenic and biogenic emissions over the Arctic region. The KORUS-AQ campaign also includes a short deployment over California. However, for the purpose of this study, we restrict observations from this campaign to those over the Korean peninsula. Lastly, the dataset includes measurements from the ATom-1 and ATom-2 campaigns (Wofsy et al., 2018). We divide the ATom campaigns into two datasets using a land-mask in order to separate the observations of remote, well-mixed air masses over the Atlantic and the Pacific from near-source measurements over North America.

Figure 3 demonstrates that organic aerosol accounts for a significant portion (52% on average) of the total non-refractory aerosol mass loadings measured by AMS across all of the campaigns. The GoAmazon measurements during the dry season have the highest contribution of OA to the total submicron aerosol loading (77%) while the ARCTAS campaign during the spring has the lowest OA contribution of any campaign (31%).

4. Results and Discussion

4.1 Simulated OA Budget

Figure 4 shows the global annual-mean simulated surface OA concentrations and global annual-mean burdens using the simple and complex schemes for the year 2013 (burden numbers are provided in Table 2). The complex scheme simulates a larger annual-mean OA burden than the simple scheme (2.37 Tg compared to 1.94 Tg). This is largely due to the scaled emissions of the primary organic gases in the complex scheme (greater by a factor of 27%) as well as the semi-volatile treatment of the EPOA/EPOG and OPOA/OPOG species that substantially extends their tropospheric residence time, due to the longer lifetime of the gas-phase component in the boundary layer. As a result, the complex scheme simulates a larger POA burden (EPOA + OPOA + MPOA) of 1.46 Tg, compared to 0.92 Tg POA in the simple scheme. The majority (91.4%) of the POA in the complex scheme consists of oxidized POA and oxidized MPOA (M-OPOA) that, given its aged and chemically processed nature, is often indistinguishable from secondary organic aerosol with typical AMS measurements (Jimenez et al., 2009). Consequently, 94.7% of the global OA burden in the complex scheme is oxygenated organic aerosol (OOA = OPOA + M-OPOA + SOA; Table 2). Similarly, 91.7% of the total POA burden and 96.1% of the total OA burden are oxygenated in the simple scheme.

Both the complex and simple schemes simulate comparable global SOA burdens (0.91 Tg and 1.02 Tg respectively). However, the complex scheme produces more isoprene-derived SOA (ISOA) and biogenic organo-nitrates (Org-Nit) than the simple scheme (Fig. 4d), particularly over areas with elevated isoprene and anthropogenic sulfate concentrations (such as the southeast US and southeast Asia) since the ISOA formation is acid-catalyzed. The explicit aqueous uptake mechanism for the isoprene-derived SOA products also results in substantially larger global isoprene SOA burdens (0.31 Tg) when compared to the 'pure-VBS' treatment of isoprene-derived SOA that simulates an annually averaged ISOA burden of 0.12 Tg. This is consistent with other comparisons that have shown the VBS treatment in GEOS-Chem under-predicts observed ISOA concentrations compared to the complex treatment (Jo et al., 2019). Despite the different treatments, both the complex and simple schemes have similar terpene-derived SOA (TSOA) burdens at 0.19 Tg and 0.18 Tg, respectively (Table 2).

Anthropogenic SOA (ASOA) is a particularly important global OA source in the simple scheme, accounting for almost a third of the total OA burden. The simple scheme, with its near-field formation of SOA proportional to anthropogenic CO emissions, simulates a substantially larger ASOA burden than the complex scheme (0.63 Tg vs 0.10 Tg; Table 2), particularly over industrialized regions in Asia (Fig. 4c). Previous studies that have constrained global SOA burdens using observed mass loadings have proposed a missing model SOA source over anthropogenic regions (Spracklen et al., 2011), as have recent regional studies (Schroder et al., 2018; Shah et al., 2019). The simple scheme appears to capture a greater fraction of this missing burden. However, we note that ASOA yields in the simple scheme are based

on a lumped parameterization over the Los Angeles basin (Hayes et al., 2015) and might not be representative of global yields across different chemical regimes. The global ASOA burden of 0.63 Tg is 4 times greater than the ASOA burden proposed by Spracklen et al. 2011, but well within the 'anthropogenically controlled' SOA burden proposed by the same study. This suggests that the simple parametrization in its current form might unintentionally represent some anthropogenically-controlled biogenic SOA. Additionally, while the simple scheme includes separate SOA yield parameters for fossil fuel and biofuel combustion, the emissions inventories used in this study do not always explicitly differentiate between the two sources. As a consequence, biofuel is often lumped together with fossil fuel CO, potentially leading to an overestimate in ASOA yields from biofuel emissions.

Pye and Seinfeld (2010) performed a similar analysis of tropospheric OA burdens using a semi-volatile POA treatment and a 'pure-VBS' treatment of SOA (i.e. all SOA treated in the VBS, including isoprene) with the GEOS-Chem model (v8.01.04). Their model simulated 0.03 Tg EPOA, 0.81 Tg OPOA and 0.80 Tg SOA, compared to 0.11Tg EPOA, 1.27 Tg OPOA and 0.91 Tg SOA for the complex scheme and 0.06 Tg EPOA. 0.78 Tg OPOA and 1.02 Tg SOA for the simple scheme in this study. When compared to an analysis of organic aerosol loadings from 31 different chemical transport and general circulation models (Tsigaridis et al., 2014), the primary OA burden from the complex scheme (EPOA + MPOA + OPOA) is substantially higher than most of the models surveyed, while the SOA burden falls below the mean but above the median of the distribution. The simple scheme, with a much smaller POA burden, is approximately on par with the Tsigaridis et al. (2014) ensemble mean. The simple SOA burden is roughly equivalent to the Tsigaridis et al. model mean (but significantly greater than the median) for global SOA loadings.

Aerosol lifetimes are calculated using the ratio between the mass burden and the physical loss rates due to dry and wet deposition (Table 2). POA in the complex scheme has an average lifetime to physical loss of 6.1 days (τ_{EPOA} ~ 11.5 days, τ_{OPOA} ~ 6.3 days, τ_{MPOA} ~ 3.0 days) in the atmosphere while SOA has a lifetime of 5.3 days on average (τ_{ASOA} ~ 7.9 days, τ_{TSOA} ~ 5.3 days, τ_{ISOA} ~ 5.1 days, $\tau_{ORG\text{-}NIT}$ ~ 4.9 days). POA in the simple scheme has an average global lifetime of 4.6 days (τ_{EPOA} ~ 7.8 days, τ_{OPOA} ~ 4.6 days, τ_{MPOA} ~ 3.0 days), while the parameterized SOA species have an average lifetime of 5.2 days (τ_{ASOA} ~ 5.6 days, τ_{TSOA} ~ 4.3 days, τ_{ISOA} ~ 4.7 days). POA lifetimes in both the complex and simple schemes are similar to the simulated POA lifetimes from Tsigaridis et al. (2014) who calculated an ensemble mean POA lifetime of approximately 5 days. SOA lifetimes from this study are lower than the ensemble-mean of 8 days calculated by Tsigaridis et al. (2014). The range in aerosol lifetimes can be attributed to several different factors. The hydrophobic nature of EPOA leads to longer lifetimes against wet-deposition since the particles are unaffected by rainout. The spatial distribution of the different aerosol types also plays an important role in determining their lifetimes, with species emitted over marine / tropical regions experiencing a higher likelihood of being deposited via wet deposition than aerosol over drier regions. Surface land types also affect dry deposition velocities, impacting aerosol lifetimes. ~~Additionally~~In addition, there is a marked difference in lifetimes between the semi-volatile species in the complex scheme and non-volatile species in the simple scheme. Due to the temperature dependent partitioning, the semi-volatile aerosol species are often in the gas-phase in the warmer parts of the troposphere and are advected to higher altitudes before they partition to aerosol. The non-volatile species do not simulate this process and are more likely to be deposited before they can be transported to higher altitudes.

4.2 Regime Analysis

We use the observations from the 15 field campaigns described in Sect. 3 as a single coherent dataset. Given the wide range of chemical regimes sampled by the various field campaigns, a method for classifying the observations is needed to better inform the model-measurement comparisons. While the chemical composition of the observed OA can provide some insight into source types or aging, a comprehensive classification is not possible using only the observations, requiring that we rely on the model for such a segmentation. In this analysis, we use the relative dominance of the different OA species within the GEOS-Chem simple scheme simulation to classify the measurements into different regimes (described in Table S3~~2~~ in Supplementary Information). The sorting algorithm weights the relative importance of the three OA source types – Anthropogenic (A), Biogenic (B), and Pyrogenic (F), based on their relative contribution by mass to the total OA loading in the model. Any data point with a source contribution greater than 70% of the total organic mass loading is categorized as being dominated by that source (such as A for Anthropogenic). Although this threshold limit is somewhat arbitrary, an analysis of different threshold values between 60%-80% shows that the resulting classifications are not particularly sensitive to changes within this range. Data points without a single dominant source but with two large sources, contributing greater than 85% of the total OA mass, are classified into a second type of regime category (such as AB for Anthropogenic/Biogenic) and points without any dominant OA source types are classified into the mixed regime category (AFB). Points with an aggregate OA mass concentration below 0.2 μg sm^{-3} across the three source types are classified as 'Remote / Marine'. Points where MPOA contributes over 50% of the mass are also categorized under the 'Remote / Marine' regime.

While we expect these model-based categories to adequately reflect source influences (i.e. biogenic emissions over the Amazon vs. anthropogenic emissions over Asia), the relative mass contributions simulated by the model are subject to large uncertainties in OA formation and lifetime. As noted in Sect. 3, sampling conditions over the regions can vary significantly from the model treatment (such as the sampling of the Manaus anthropogenic plume or biomass burning plumes during the 'biogenic' GoAmazon campaign). Due to the coarse model resolution, the regime segmentation described above is incapable of accurately categorizing some of these data points. We therefore compare the relative concentrations of observed NO_x, CO and isoprene to independently validate the segmentation approach. For instance, mean observed NO_x values over the Anthropogenic regime approach 1 ppb, compared to 0.36 ppb over the AB regime and 0.17 ppb over the Biogenic regime, consistent with the expected chemical signature over these regions. Similarly, averaged isoprene observations over the biogenic regime are over 20 times greater than average measurements over the Anthropogenic regime.

Median concentrations over anthropogenic regions are markedly lower than those over other sources. Fire influenced regions display the highest variability, consistent with the expected source profile. Table S1 provides an overview of the observational data-sets used for this validation. An overview of the resulting segmentation, validation, and regime categories is provided in Table S2. Figure 5 provides a spatial representation of the regime categorization for all the flight data. We note that a large proportion of the observations from the GoAmazon and OP3 campaigns are densely co-located over the Amazon and Borneo and are thus difficult to discern in the figure. We also note that the 'remote' points over the south-east US represent observations in the upper troposphere and are plotted over points in the lower

troposphere making them difficult to distinguish. While the regime analysis provides useful insight into the primary sources of OA over the region, the classifications are intended to be broad and do not, for instance, distinguish between fresh and aged aerosol contributions from the same source. For example, a number of points over the northern Atlantic and Pacific oceans that are classified as anthropogenic because they are composed of a minimum of 70% anthropogenic OA from continental sources and are high enough in concentration to not be classified as 'remote'.

4.3 Evaluation of Model Simulations against Airborne Measurements

Here we evaluate the two model schemes against the suite of airborne observations described in Sect. 3. Despite the substantial differences described in Sect. 2.1, both schemes reproduce the broad distribution (Fig. 6a) of OA observations. While the schemes exhibit slight offsets in their peaks near the lower end of the distribution, there is no evidence of a large systematic skew compared to observations, suggesting that there is not an obvious mode of formation or loss of OA that the model fails to capture. Differences between the two model distributions are also relatively small and both exhibit fairly comparable skill. The simple scheme is less biased than the complex scheme on average with median OA values of 0.81 μg sm^{-3} and 0.86 μg sm^{-3} respectively, compared to the observational median of 0.68 μg sm^{-3}. An analysis of the model-observation distributions for the individual campaigns (see Fig. 7~~S1~~) demonstrates that both model schemes appear to overestimate OA mass at the low and high ends of the distribution for several campaigns (as seen in the case of KORUS, GOAMA-W and OP3), while underestimating organic aerosol loadings in the middle of the distribution, suggesting a potential mischaracterization of aerosol sources and lifetimes over these regions. This might also be the result of the coarse model resolution in regions with a high spatial variance in source strengths. Both model schemes underestimate the lowest concentrations and overestimate the highest concentrations over the ocean (ATOM1-W and ATOM2-W). However, Fig. 6a suggests that these are not pervasive issues with the OA simulation at the global scale. We note, however, that this could be due to an averaging effect. Figure 6b shows the same comparison for sulfate, as a benchmark for a species that is generally well simulated by the GEOS-Chem model (Fisher et al., 2011; Heald et al., 2011; Kim et al., 2015). While the comparison suggests that there continues to be further scope for improvement within the OA chemical schemes, the model simulations are approaching the skill of the sulfate simulation both in terms of bias (the sulfate simulation normalized mean bias of 0.20 is similar to the model OA bias outlined above) and captured variability (with an R^2 of 0.62 for the model sulfate scheme relative to the observations, compared to an R^2 of 0.41 and 0.44 for the simple and complex OA schemes respectively). This suggests the potential importance of other drivers of variability common to both sulfate and organic aerosol, such as emissions and transport, in controlling aerosol concentrations.

Figure 8~~7~~ shows that both the complex and simple schemes exhibit substantial skill in capturing the vertical OA profile across the aggregate dataset, with a vertical R^2 of 0.97 and 0.95 across the complex and simple schemes respectively. Despite significant differences in the treatment of OA formation and atmospheric processing (and thus the source of simulated OA), both schemes appear to have similar skill in reproducing the observed vertical profile across the individual regimes with the exception of the Remote regime (driven largely by ATOM1-W and ATOM2-W) where both schemes struggle somewhat to reproduce the variability in the observed vertical profile (Fig. S2). This result is not surprising given the low concentrations and the potential for uncertainties in transport and chemical processing to

be exacerbated in the remote regime. Overall, the schemes display similar skill at capturing the vertical variability across the different regimes, highlighting that much of this variability is likely driven by the prescribed transport and vertical mixing and is independent of the OA chemical scheme.

When compared in aggregate, the simple scheme is less biased in the lower troposphere, while the complex scheme is less biased in the upper troposphere (Fig. 8~~7~~; Fig. S2). This could be due to the partitioning mechanism in the complex scheme that is able to model semi-volatile OPOA and SOA with greater sophistication using the VBS framework. There are also various regime-specific differences in model performance. For instance, the complex scheme significantly overestimates OA in the lower troposphere over fire-influenced regions, likely due to the 27% increase in primary OA emissions to account for the dynamic partitioning between gas and aerosol phase POA. However, both the complex and simple schemes underestimate OA loadings in the mid-troposphere over these same regions. This bias may be due to fire injection from large fires into the free troposphere, particularly over boreal regions (Turquety et al., 2007) that is not captured by the model (all emissions from fires are assumed to be in the boundary layer). This shortcoming is also evident over regions influenced by both anthropogenic and fire emissions (AF Regime). Figure 8~~7~~ also demonstrates that lower tropospheric concentrations cannot be reproduced over oceans without the inclusion of a marine source of POA, although the comparisons suggest that the marine POA source may be a factor of ~2 too high. While the model appears to capture the vertical profile of OA in anthropogenic regions reasonably well (Fig. 8~~7~~), there are regional differences (Fig. 9~~8~~), with large model underestimates of OA in the lower troposphere over California (CalNex), the central US (DC3) and Europe (EUCAARI) and large over-estimates over Korea and parts of the Pacific influenced by outflow from Asia (Fig. 9~~8~~; Fig. S3). These differences are consistent across both the simple and complex schemes, highlighting the importance of accurate anthropogenic emission inventories. In regions influenced by both anthropogenic and biogenic emissions (AB Regime) the complex scheme is less biased than the simple scheme, which underestimates the observed concentrations. This difference in bias is likely due to the more sophisticated treatment of isoprene-derived SOA yields (through the aqueous uptake and organic nitrate formation mechanisms) in the complex scheme. The NO_x-dependent yields of isoprene and ~~mono~~terpene-derived SOA in the complex scheme might also be a source of increased model skill, given that organic nitrates and oxidized isoprene products account for a dominant fraction of the total modelled OA in the complex scheme over these regions. The relative skill of the complex scheme is unsurprising given that the vast majority of the AB Regime is over the southeast US, for which the complex scheme was developed and validated. However, the model skill over the AB regime may be fortuitous, given that recent studies have demonstrated a significant fraction of the observed OA over the southeast US is generated from monoterpene precursors, rather than isoprene (Xu et al., 2018; Zhang et al., 2018). This potentially suggests that monoterpene SOA yields over the southeast US are low in the model. This may also contribute to the underestimate of OA observed during EUCAARI, which is influenced by the forests of Northern Europe (Fig. 9~~8~~; Fig. S3). Recent work has also demonstrated that organo-nitrates contribute a significant fraction of the total OA mass over certain parts of Europe (Kiendler-Scharr et al., 2016), potentially indicating a model underestimate in organo-nitrate formation over the region. -In contrast to its skill over the US, the complex scheme displays a large positive bias over biogenic (B) regions (such as the Amazon), primarily driven by an overestimate in terpene SOA, potentially suggesting that the scheme may not accurately capture global biogenic SOA burdens and

needs to be better constrained. The overestimate of OA in both schemes in the boundary layer over the Amazon and Borneo is accompanied by an under-estimate in the upper-troposphere (Fig. 98), potentially indicating overly-rapid model SOA formation or a failure to capture vertical mixing in the region.

We note that while the observations used in this study have a large spatial range, they are temporally limited and might not be representative of the mean state. Atypical meteorological conditions during the different campaigns may contribute significantly to the model-observation bias. For example, the EUCAARI campaign was characterized by a westward flow across Germany and southern UK (Morgan et al., 2010), capped by a strong inversion that limited vertical mixing. Similarly, differences in sampling priorities might impact the chemical composition of the observations in a manner that deviates from climatology. For instance, the GoAmazon campaign was partially oriented toward sampling anthropogenic outflow from the city of Manaus (Shilling et al., 2018), impacting the OA measurements in a manner that the model is ill-equipped to reproduce. However, despite the various gaps in model fidelity, this analysis suggests that both schemes are relatively skilled at capturing the observed magnitude and vertical variability across the different regimes. A previous comparison of observed vertical profiles by Heald et al. (2011) concluded that the 2-product SOA with non-volatile POA model used in earlier versions of GEOS-Chem required additional sinks and sources in order to match observations, suggesting the need for photochemical sinks from photolysis and fragmentation pathways. Figure 87 indicates no obvious need for large additional sinks for either scheme in aggregate, although specific regions may benefit from a more sophisticated treatment of SOA formation and loss.

An analysis of the coefficients of determination (R^2) and the normalized mean biases (NMB) across the different regimes (Fig. 109) and campaigns (Fig. 110) indicates that the complex scheme marginally outperforms the simple scheme across the aggregate dataset in its ability to reproduce the observed OA variability (with an R^2 of 0.44 compared to an R^2 of 0.41 for the simple scheme), with small differences in performance over the different regimes. The simple scheme is more skilled at minimizing bias over the aggregate dataset and most source regimes, but is biased low over the AB and AFB regimes. Figure S3 provides a spatial context to the model-measurement comparisons discussed here. The result that both the complex and simple schemes slightly over-estimate OA in the aggregate dataset is distinct from the conclusion drawn by Heald et al. (2011) who demonstrated a consistent model underestimate of OA over most regions. In this study, median modelled concentrations are within 1 $\mu g\ sm^{-3}$ of the observations for 14 out of the 17 datasets analyzed with both schemes. Figure S4 provides distributions of the ratio and bias between the observed and modelled organic aerosol concentrations for both model schemes across the different campaigns.

When compared to the simple scheme, the complex scheme does a superior job at minimizing the bias over much of the US. However, there continues to be an underestimate in OA loadings in both schemes (Fig. 98; Fig. S3). The bias is likely driven by a variety of factors that need to be explored on a regional basis. For instance, a previous model analysis of FRAPPE observations over Colorado suggested that an underestimate of anthropogenic emissions from the oil and gas sector contributed to an underestimate of ASOA in the region (Bahreini et al., 2018). Both schemes over-estimate OA loadings in the northern latitudes (over parts of Alaska and Canada), likely due to an overestimate in POA from fires (Fig. 98; Fig. 110; Fig. S2; Fig. S3). The complex scheme is also biased high over the Amazon

rainforest, due to the large mass loadings of terpene SOA and various isoprene and monoterpene-derived organo-nitrates. Conversely, the simple scheme assumes an identical SOA yield from both monoterpenes and sesquiterpenes, likely degrading its skill. Both schemes are biased low over Europe but high over the Korean peninsula, both anthropogenically influenced regions, potentially arising from the different regional inventories (EMEP and MIX) used by the model. Both schemes overestimate the OA concentrations observed during the winter ATom-2 deployment (Fig. 9~~8~~; Fig. 1~~10~~) driven largely by an overestimate in anthropogenic OA, particularly in the North Pacific (Fig. S3); a similar bias is not apparent in the summertime ATom-1 deployment, suggesting a potential seasonal overestimate in anthropogenic emissions in Asia that may warrant further study. In comparison to the complex scheme, simulations conducted using a 'pure-VBS' treatment of SOA were significantly less skilled at capturing OA variability and minimizing model bias over the aggregate dataset, demonstrating the value of an explicit description of isoprene SOA over the non-mechanistic VBS treatment.

4.4 Exploring the model-measurement differences in OA

There are many factors that contribute to the model performance over individual campaigns or regions and investigating the specific drivers of regional differences is not the goal of this work. However, here we explore general features of the model-measurement comparisons to identify issues that may inform the development of future model OA schemes.

There is a large spread in the model-observation bias both within and across the individual campaigns. A comparison of OA metrics (such as R^2 and NMB) with the corresponding model sulfate simulations for the same campaigns demonstrates a similar variance (Fig. 1~~10~~). This suggests that the lack of model skill over certain campaigns could be due to physical processes, such as transport and deposition, that impact both OA and sulfate species and are independent of the chemical scheme utilized.

A comparison between the simulated and observed coefficients of variation (CV; defined as the ratio of the standard deviation to the mean) for the different campaigns indicates that both the complex and simple schemes are relatively skilled at capturing the range of observations within the individual campaigns, with the CV from the simple scheme and the complex scheme both showing a high degree of correlation when compared to the observed CV (R^2 of 0.7; Fig. 1~~2~~~~1~~). The CV provides a measure of statistical dispersion. Figure 1~~2~~~~1~~ highlights how localized campaigns such as GoAmazon and FRAPPE have low CVs. Both schemes demonstrate a lack of ability to accurately capture intra-campaign variability (described above by the campaign R^2 in Fig. 1~~10~~). The coarse model resolution and the resulting inability to resolve sub-grid concentration and emission gradients is likely an important barrier to model skill, particularly across more localized campaigns (with low CVs) with smaller dynamic ranges and/or spatial extents, like OP3, KORUS-AQ and FRAPPE. To explore this, additional simulations (not shown) were conducted using a nested 0.5° x 0.625° grid with the simple scheme (while maintaining all other model parameters) over North America for the FRAPPE campaign, and over Asia for the KORUS-AQ and OP3 campaigns. The nested simulations performed significantly better at capturing the observed variability in OA for FRAPPE (with a change in R^2 from 0.19 to 0.34). However, the nested KORUS-AQ simulations resulted in a decrease in model skill, with a change in R^2 from 0.37 to 0.25. This result suggests that uncertainties in emission inventories and meteorology over Asia may degrade higher-

resolution comparisons, consistent with recent work demonstrating deficiencies in emission inventories in the region (Goldberg et al., 2018). The nested simulations also did nothing to improve model fidelity for the OP3 campaign over Borneo (with a change in R^2 from 0.49 to 0.48). Biogenic emissions and chemical conditions are likely relatively uniform over this region, and therefore a higher resolution simulation does not lead to a distinct improvement in the simulation.

To compare the underlying source signatures for the ambient OA concentrations over different regimes, we analyze the relationship between OA and CO concentrations across both the model schemes and the observational data-set (Fig. S5). Generally, the model underestimates the observed OA:CO slope, but captures the relative difference in OA:CO slopes observed in different environments. The two schemes are broadly consistent, and the model skill in reproducing this relationship is not notably better or worse over most regimes or environments, providing little insight into model scheme deficiencies. However, there is a notable difference between the observed and modelled OA:CO slope over the anthropogenic regime (though it is not consistent over all regions), potentially warranting further exploration of regional anthropogenic OA yields within the simple scheme.

Model-bias is also evaluated as a function of a suite of observed parameters (Relative Humidity, Temperature NO_x, sulfate, isoprene, CO) to identify any salient relationships (Fig. S6). We find that the model-observation bias in the complex scheme displays a robust positive correlation with the observed relative humidity and sulfate concentrations (Fig. 1~~3~~2). This suggests that the aqueous uptake of isoprene oxidation products in the complex scheme is overestimated in conditions of high humidity and high acidity, and that further work is needed to constrain this formation pathway under a range of ambient environmental conditions. It also suggests that large additional pathways of aqueous SOA formation are unlikely to be missing from the model.

The simple and complex schemes differ significantly in their treatment of primary organic aerosol. The simple scheme simulates POA using two non-volatile primary species while the complex scheme uses two semi-volatile primary species that partition between the gas and aerosol phase. This is an important difference, because aerosol partitioning in the semi-volatile species is sensitive to ambient temperature and organic aerosol concentration, influencing concentrations far away from the original source. Given the differences in POA treatment, an analysis of model skill (in terms of its ability to minimize bias and capture observational variability) was conducted by considering the effects of combining EPOA and OPOA loadings from the complex scheme with SOA loadings from the simple scheme (and vice versa). With an R^2 of 0.46 and an NMB of 0.03, this model configuration (complex scheme POA with simple scheme SOA) outperformed both the simple and complex schemes over the aggregate dataset in its ability to capture the observed variability and minimize observational bias, supporting the need to explicitly model the semi-volatile nature of POA (Fig. S7). We note that this analysis assumes a parameterized enthalpy of vaporization of 50 kJ mol^{-1} to estimate saturation vapor pressures for semi-volatile partitioning in the complex scheme, an assumption that needs to be more rigorously examined in field and modeling studies.

Based on the results from the simple scheme, an offline analysis was conducted to optimize the various model parameters by running a multi-variate linear regression in combination with a gradient descent optimizer that used a weighted cost-function to maximize the coefficient of determination and minimize the normalized mean bias. This

was done across multiple parameter classes (such as emission rates and yields) in order to ascertain a set of optimized model parameters. The optimized parameters improved the model coefficient of determination by only up to 5% in most cases. This is perhaps unsurprising given that this simplistic analysis assumes that simulated OA concentrations are linearly correlated with changes in emissions and yields, an assumption that is not truly representative of the model treatment which includes non-linear effects such as wet deposition loss. More work is required to optimize these parameter classes using an online analysis.

We also incorporated a rudimentary NO_x and sulfate dependency into the biogenic SOA yields for the simple scheme, using offline monthly-averaged NO_x and sulfate concentrations from a full-chemistry GEOS-Chem simulation for the year 2013. Isoprene-derived SOA was modelled as having a negative NO_x dependency, ranging from a 3% yield in low-NOx conditions to a 2.25% yield at high-NO_x. Monoterpene SOA was also modelled as having a negative NO_x dependency – ranging from a 10% yield under low-NO_x conditions to a 7.5% yield under high-NO_x conditions. Sesquiterpene SOA yields were simulated as having a positive NOx dependence, ranging from 10% under low-NOx conditions to 20% under high-NOx conditions. These yields were determined based on an analysis of relevant literature (e.g. Kroll et al., 2006; Ng et al., 2007) coupled with various offline optimizations from this study. ISOA was also modelled as having a positive SO_4 dependence (from a yield of 1.5% in clean conditions to a high of 4.5% in extremely polluted conditions with high sulfate) based on previous work (Marais et al., 2016) that demonstrated the importance of the acid-catalyzed SOA formation pathway for isoprene.

The NOx-dependent parameterization did not meaningfully improve model skill. However, the sulfate parametrization improved model performance by a few percentage points, bringing the aggregate R^2 to within 0.01 of the complex scheme, demonstrating the potential to further improve model performance. The analysis also points to the limitations of the simple scheme in its current form. For instance, OA yields have also been shown to be highly variable by region and source, particularly in the case of fires (Jolleys et al., 2014), a facet that is not currently captured within the simple scheme. Chemical processing lifetimes are also highly dependent on the ambient regime, with observational studies finding that OA in urban environments (e.g. Jimenez et al., 2009) is often oxidized at timescales that are significantly faster than the 1.15 days assumed in the simple scheme. Our rudimentary optimization of the simple scheme with a sulfate dependency demonstrates the potential to further improve model performance, although additional work is needed to conduct a more rigorous optimization of the various model parameters.

5. Conclusions

In this study, we use a suite of observations that represent a variety of spatial and chemical regimes to undertake a comprehensive evaluation of the two standard organic aerosol schemes in the GEOS-Chem chemical transport model, both with very different treatments of OA. The simple scheme, which uses non-volatile tracers to model primary organic aerosol, simulates a total annual POA burden that is approximately two-thirds of the comparable burden simulated by the complex scheme that treats POA as semi-volatile. While the total SOA burdens are similar, the simple scheme simulates an anthropogenic SOA burden that is over 6 times greater than the complex scheme. Conversely, the complex scheme simulates a global burden of biogenic SOA that is roughly 2.5 times greater than the comparable

burden in the simple scheme, largely due to higher isoprene SOA and organo-nitrate mass loadings. Due to the lack of well-differentiated fossil-fuel and biofuel emissions, the simple parameterization likely overestimates ASOA from biofuel sources. We note that the simple ASOA parameterization as applied in this study might also capture some 610 'anthropogenically controlled' SOA formed from biogenic VOC precursors, potentially accounting for some of the disparities noted above. More work is needed to constrain these yields across different chemical regimes at a global scale.

Despite the substantial difference in the complexity of these OA schemes and the relative magnitudes of their sources, differences in their ability to capture observed airborne OA concentrations from around the world are modest. The 615 simple scheme appears to slightly out-perform the more sophisticated complex scheme in terms of its ability to minimize bias over the aggregate dataset while the complex scheme is slightly more skilled in its ability to capture the observed variability. When compared spatially to the simple scheme, the complex treatment is less biased over the southeast US and certain regions in North America and Europe, while displaying reduced skill in pyrogenic regimes over the northern latitudes and biogenic regimes in the Amazon, where it produces large overestimates. When 620 comparing vertical profiles, both schemes overestimate OA loadings in the lower troposphere. However, the complex scheme is more skilled at capturing the mid-tropospheric burden, likely due to the more sophisticated semi-volatile treatment of primary OA. Both schemes underestimate mid-tropospheric OA loadings over fire influenced campaigns, pointing to the potential importance of fire injection into the free troposphere in those regions, which was not modeled in this study. The overestimate of OA in the tropical boundary layer and the underestimate aloft similarly indicates 625 model failure to capture the chemical lifetimes of biogenic SOA formation, or points to deficiencies in its ability to capture vertical mixing in these regions. Our analysis of nested simulations over North America and Asia also points to the importance of constraining regional emissions and local meteorology over Asia in order to improve model fidelity. As a result of our analysis, we recommend that (1) POA be modelled as semi-volatile, (2) fire POA emissions not be scaled up by 27% in the complex scheme and (3) marine POA be included in the simulation of marine- 630 influenced regions. Further explorations of fire injection heights of aerosols (e.g. Zhu et al., 2018) and anthropogenic emissions of OA precursors, particularly in Asia, are needed. However, despite these deficiencies, both model schemes generally capture the magnitude of the observed OA. This is particularly true, given the 38% uncertainty associated with the AMS OA observations; 33% of the modeled data-points fall within this observed uncertainty, demonstrating significant progress since the first airborne analysis of OA simulated in the GEOS-Chem model, which revealed up to 635 an order of magnitude biases (Heald et al., 2005).

The surprising result that both the simple and complex schemes perform comparably across the aggregate data-set challenges our expectations that a more complex and mechanistic description of OA should outperform a highly parameterized scheme. This may suggest that accurately capturing the source influence (i.e. emissions of OA and its precursors) is a more crucial limitation on current model skill than the specific details pertaining to OA formation. 640 Alternatively, it may suggest that there remain substantial deficiencies in our understanding of the mechanistic formation of OA, as represented in the complex scheme (for example, associated with the oxidation of aromatics). The VBS oxidation of monoterpenes and sesquiterpenes in the complex scheme uses NO_x dependent yields to determine the formation of second generation oxidation products. However, these yields are uncertain and recent

studies have suggested the importance of accounting for interactions between multi-generational oxidation products when determining these yields, demonstrating that such interactions can significantly depress SOA formation under ambient conditions (McFiggans et al., 2019). Recent work has also demonstrated the importance of RO_2 autoxidation pathways in the formation of SOA (e.g. Crounse et al., 2013; D'Ambro et al., 2017; Pye et al., 2019). A more sophisticated, explicit treatment that accounts for these oxidation product interactions under different chemical regimes could thus improve model fidelity (but with an associated computational cost). Additionally, the underlying mechanisms (and related uptake coefficients) behind the treatment of isoprene in the complex scheme were developed and validated primarily using data from campaigns over the southeast US; more work is needed to constrain these coefficients under different chemical regimes outside this region. Finally, the lack of model fidelity could also indicate the importance of better constraining the physical processes inherent to both schemes, such as transport and deposition, or point to the salience of photochemical loss, atmospheric aging and fragmentation loss which are not represented in either scheme (Heald et al., 2011; Hodzic et al., 2016). In addition to these factors, the observational comparison with model sulfate suggests that the large drivers of unexplained model variability might be exogenous to the OA chemical scheme.

At the global scale, the computational advantages and relative skill of the simple scheme make it an attractive tool for use in health and climate studies. Our analysis demonstrates that this computational benefit is accompanied by a relatively limited decline in model skill. However, caution should be exercised when applying such a scheme that fails to incorporate the mechanistic responses necessary to ensure predictive skill. There is thus a need to improve upon both the simple parameterized approach as well as the more sophisticated mechanistic scheme in order to further our understanding of organic aerosol in the atmosphere.

This study highlights the critical need to develop new methods to translate experimental studies on the formation and fate of OA into global models, in order to identify the key processes that are required to reproduce observed atmospheric OA concentrations. The study also indicates the importance of additional observational constraints to benchmark and improve model fidelity. The AMS observations offer a rich mass-differentiated dataset that could be further leveraged using factor ratios and clustering analyses to inform future model evaluations. Standardized reporting of AMS data during future campaigns could enable further model evaluation using a more comprehensive range of the instrument's capabilities. In addition o~~O~~bservations of organic aerosol would be particularly useful in understudied regions such as India, China, ~~and~~ Central Asia and Africa. ~~Existing datasets~~Recent campaigns over these regions (such as the 2016 DACCIWA, 2018 ORACLES and 2016 SWAAMI campaigns) could also be leveraged to study the relevant chemistry. Due to the relative paucity of airborne AMS observations, this study does not include an analysis of seasonal trends. Additional aircraft campaigns over the fall and winter seasons (such as the 2015 WINTER campaign over the north-eastern US) could enable a more comprehensive intra-annual analysis which could provide insight into seasonal sources. There is also a need for more field observations at a regional-scale, as opposed to localized sampling, in order to better constrain and improve the treatment of organic aerosol in large-scale regional and global models. Finally, this analysis, while a comprehensive model evaluation of OA, is limited to two schemes within one model. An on-going, meticulous evaluation of new OA model schemes against globally distributed datasets is paramount to the advancement of the simulation of the air quality and climate impacts of aerosols.

6. Author Contributions

CLH designed the study. SJP modified the code, performed the simulations and led the analysis. JRP, SCF, and EAM contributed to the GEOS-Chem organic aerosol simulation. JLJ, PC, BAN, AMM, HC, JES, RB, JHD, KV provided organic aerosol measurements used in the analysis. SJP and CLH wrote the paper with input from the co-authors and acknowledged individuals below.

7. Competing Interests

The authors declare that they have no conflict of interest

8. Acknowledgements

This work was supported by the National Science Foundation (AGS-1564495). The authors would like to acknowledge Katherine R. Travis, Jesse H. Kroll, Jeffrey L. Collett, Jr. and Taehyoung Lee for useful discussions and inputs. We also acknowledge the following investigators who provided measurements of NO_x, CO, and isoprene: Andrew J. Weinheimer, Armin Wisthaler, Bruce C. Daube, Carsten Warneke, Chelsea R. Thompson, David J. Knapp, Denise D. Montzka, Donald R. Blake, Eric A. Kort, Eric C. Apel, Frank M. Flocke, Glen Sachse, Glenn S. Diskin, Ilana B. Pollack, Jeffrey Peischl, John E. Shilling, John S. Holloway, Joost A. de Gouw, Lisa Kaser, Markus Müller, Martin Graus, Philipp Eichler, Rebecca S. Hornbrook, Roisin Commane, Sally E. Pusede, Stephen R. Springston, Steven C. Wofsy, Teresa L. Campos, Thomas B. Ryerson, Tomas Mikoviny. RB was supported by the Colorado Department of Public Health and Environment. JES was supported by the U.S. Department of Energy Office of Biological and Environmental Research as part of the ARM and ASR programs. The Pacific Northwest National Laboratory is operated for DOE by Battelle Memorial Institute under contract DE-AC05-76RL01830. JRP was supported by the U.S. NSF(AGS-1559607) and the NOAA 31(NA17OAR430001). Aerosol measurements from the EUCAARI and OP3 campaigns was collected under NERC grants NE/D013690/1, NE/D004624/1 and NE/E01108X/1. The CU-Boulder group was supported by NASA (NNX15AH33, NNX15AT96G, and 80NSSC18K0630), EPA STAR (83587701-0), and DOE (DE-SC0016559). This manuscript has not been reviewed by the EPA, and thus no endorsement should be inferred. PTR-MS measurements during DC3 and KORUS-AQ were supported by the Austrian Federal Ministry for Transport, Innovation and Technology through the Austrian Space Applications Programme (ASAP) of the Austrian Research Promotion Agency (FFG). GoAmazon data was obtained from the Atmospheric Radiation Measurement (ARM) user facility (doi: 10.5439/1346559), a U.S. Department of Energy (DOE) Office of Science user facility managed by the Office of Biological and Environmental Research.

9. References

Amos, H. M., Jacob, D. J., Holmes, C. D., Fisher, J. A., Wang, Q., Yantosca, R. M., Corbitt, E. S., Galarneau, E., Rutter, A. P., Gustin, M. S., Steffen, A., Schauer, J. J., Graydon, J. A., Louis, V. L. St., Talbot, R. W., Edgerton, E. S., Zhang, Y. and Sunderland, E. M.: Gas-particle partitioning of atmospheric Hg(II) and its effect on global mercury deposition, Atmospheric Chem. Phys., 12, 591–603, doi:10.5194/acp-12-591-2012, 2012.

Bahreini, R., Ervens, B., Middlebrook, A. M., Warneke, C., de Gouw, J. A., DeCarlo, P. F., Jimenez, J. L., Brock, C. A., Neuman, J. A., Ryerson, T. B., Stark, H., Atlas, E., Brioude, J., Fried, A., Holloway, J. S., Peischl, J., Richter, D., Walega, J., Weibring, P., Wollny, A. G. and Fehsenfeld, F. C.: Organic aerosol formation in urban and industrial plumes near Houston and Dallas, Texas, J. Geophys. Res., 114, doi:10.1029/2008JD011493, 2009.

Bahreini, R., Ahmadov, R., McKeen, S. A., Vu, K. T., Dingle, J. H., Apel, E. C., Blake, D. R., Blake, N., Campos, T. L., Cantrell, C., Flocke, F., Fried, A., Gilman, J. B., Hills, A. J., Hornbrook, R. S., Huey, G., Kaser, L., Lerner, B. M., Mauldin, R. L., Meinardi, S., Montzka, D. D., Richter, D., Schroeder, J. R., Stell, M., Tanner, D., Walega, J., Weibring, P. and Weinheimer, A.: Sources and characteristics of summertime organic aerosol in the Colorado Front Range: perspective from measurements and WRF-Chem modeling, Atmospheric Chem. Phys., 18(11), 8293–8312, doi:https://doi.org/10.5194/acp-18-8293-2018, 2018.

Barth, M. C., Cantrell, C. A., Brune, W. H., Rutledge, S. A., Crawford, J. H., Huntrieser, H., Carey, L. D., MacGorman, D., Weisman, M., Pickering, K. E., Bruning, E., Anderson, B., Apel, E., Biggerstaff, M., Campos, T., Campuzano-Jost, P., Cohen, R., Crounse, J., Day, D. A., Diskin, G., Flocke, F., Fried, A., Garland, C., Heikes, B., Honomichl, S., Hornbrook, R., Huey, L. G., Jimenez, J. L., Lang, T., Lichtenstern, M., Mikoviny, T., Nault, B., O'Sullivan, D., Pan, L. L., Peischl, J., Pollack, I., Richter, D., Riemer, D., Ryerson, T., Schlager, H., St. Clair, J., Walega, J., Weibring, P., Weinheimer, A., Wennberg, P., Wisthaler, A., Wooldridge, P. J. and Ziegler, C.: The Deep Convective Clouds and Chemistry (DC3) Field Campaign, Bull. Am. Meteorol. Soc., 96(8), 1281–1309, doi:10.1175/BAMS-D-13-00290.1, 2014.

Brock, C. A., Cozic, J., Bahreini, R., Froyd, K. D., Middlebrook, A. M., McComiskey, A., Brioude, J., Cooper, O. R., Stohl, A., Aikin, K. C., Gouw, J. A. de, Fahey, D. W., Ferrare, R. A., Gao, R.-S., Gore, W., Holloway, J. S., Hübler, G., Jefferson, A., Lack, D. A., Lance, S., Moore, R. H., Murphy, D. M., Nenes, A., Novelli, P. C., Nowak, J. B., Ogren, J. A., Peischl, J., Pierce, R. B., Pilewskie, P., Quinn, P. K., Ryerson, T. B., Schmidt, K. S., Schwarz, J. P., Sodemann, H., Spackman, J. R., Stark, H., Thomson, D. S., Thornberry, T., Veres, P., Watts, L. A., Warneke, C. and Wollny, A. G.: Characteristics, sources, and transport of aerosols measured in spring 2008 during the aerosol, radiation, and cloud processes affecting Arctic Climate (ARCPAC) Project, Atmospheric Chem. Phys., 11(6), 2423–2453, doi:https://doi.org/10.5194/acp-11-2423-2011, 2011.

Budisulistiorini, S. H., Nenes, A., Carlton, A. G., Surratt, J. D., McNeill, V. F. and Pye, H. O. T.: Simulating Aqueous-Phase Isoprene-Epoxydiol (IEPOX) Secondary Organic Aerosol Production During the 2013 Southern Oxidant and Aerosol Study (SOAS), Environ. Sci. Technol., 51(9), 5026–5034, doi:10.1021/acs.est.6b05750, 2017.

Canagaratna, M. R., Jayne, J. T., Jimenez, J. L., Allan, J. D., Alfarra, M. R., Zhang, Q., Onasch, T. B., Drewnick, F., Coe, H., Middlebrook, A., Delia, A., Williams, L. R., Trimborn, A. M., Northway, M. J., DeCarlo, P. F., Kolb, C. E., Davidovits, P. and Worsnop, D. R.: Chemical and microphysical characterization of ambient aerosols with the aerodyne aerosol mass spectrometer, Mass Spectrom. Rev., 26(2), 185–222, doi:10.1002/mas.20115, 2007.

Chin, M., Ginoux, P., Kinne, S., Torres, O., Holben, B. N., Duncan, B. N., Martin, R. V., Logan, J. A., Higurashi, A. and Nakajima, T.: Tropospheric Aerosol Optical Thickness from the GOCART Model and Comparisons with Satellite and Sun Photometer Measurements, J. Atmospheric Sci., 59(3), 461–483, doi:10.1175/1520-0469(2002)059<0461:TAOTFT>2.0.CO;2, 2002.

Chung, S. H. and Seinfeld, J. H.: Global distribution and climate forcing of carbonaceous aerosols, J. Geophys. Res., 107(D19), doi:10.1029/2001JD001397, 2002.

Cohen, A. J., Brauer, M., Burnett, R., Anderson, H. R., Frostad, J., Estep, K., Balakrishnan, K., Brunekreef, B., Dandona, L., Dandona, R., Feigin, V., Freedman, G., Hubbell, B., Jobling, A., Kan, H., Knibbs, L., Liu, Y., Martin, R., Morawska, L., Pope, C. A., Shin, H., Straif, K., Shaddick, G., Thomas, M., Dingenen, R. van, Donkelaar, A. van, Vos, T., Murray, C. J. L. and Forouzanfar, M. H.: Estimates and 25-year trends of the global burden of disease attributable to ambient air pollution: an analysis of data from the Global Burden of Diseases Study 2015, The Lancet, 389(10082), 1907–1918, doi:10.1016/S0140-6736(17)30505-6, 2017.

Cooke, W. F., Liousse, C., Cachier, H. and Feichter, J.: Construction of a 1° × 1° fossil fuel emission data set for carbonaceous aerosol and implementation and radiative impact in the ECHAM4 model, J. Geophys. Res. Atmospheres, 104(D18), 22137–22162, doi:10.1029/1999JD900187, 1999.

Crounse, J. D., Nielsen, L. B., Jørgensen, S., Kjaergaard, H. G. and Wennberg, P. O.: Autoxidation of Organic Compounds in the Atmosphere, J. Phys. Chem. Lett., 4(20), 3513–3520, doi:10.1021/jz4019207, 2013.

Cubison, M. J., Ortega, A. M., Hayes, P. L., Farmer, D. K., Day, D., Lechner, M. J., Brune, W. H., Apel, E., Diskin, G. S., Fisher, J. A., Fuelberg, H. E., Hecobian, A., Knapp, D. J., Mikoviny, T., Riemer, D., Sachse, G. W., Sessions, W., Weber, R. J., Weinheimer, A. J., Wisthaler, A. and Jimenez, J. L.: Effects of aging on organic aerosol from open biomass burning smoke in aircraft and laboratory studies, Atmospheric Chem. Phys., 11(23), 12049–12064, doi:10.5194/acp-11-12049-2011, 2011.

D'Ambro, E. L., Møller, K. H., Lopez-Hilfiker, F. D., Schobesberger, S., Liu, J., Shilling, J. E., Lee, B. H., Kjaergaard, H. G. and Thornton, J. A.: Isomerization of Second-Generation Isoprene Peroxy Radicals: Epoxide Formation and Implications for Secondary Organic Aerosol Yields, Environ. Sci. Technol., 51(9), 4978–4987, doi:10.1021/acs.est.7b00460, 2017.

Dingle, J. H., Vu, K., Bahreini, R., Apel, E. C., Campos, T. L., Flocke, F., Fried, A., Herndon, S., Hills, A. J., Hornbrook, R. S., Huey, G., Kaser, L., Montzka, D. D., Nowak, J. B., Reeves, M., Richter, D., Roscioli, J. R., Shertz, S., Stell, M., Tanner, D., Tyndall, G., Walega, J., Weibring, P. and Weinheimer, A.: Aerosol optical extinction during the Front Range Air Pollution and Photochemistry Éxperiment (FRAPPÉ) 2014 summertime field campaign, Colorado, USA, Atmospheric Chem. Phys., 16(17), 11207–11217, doi:10.5194/acp-16-11207-2016, 2016.

Donahue, N. M., Robinson, A. L., Stanier, C. O. and Pandis, S. N.: Coupled Partitioning, Dilution, and Chemical Aging of Semivolatile Organics, Environ. Sci. Technol., 40(8), 2635–2643, doi:10.1021/es052297c, 2006.

Fairlie, D. T., Jacob, D. J. and Park, R. J.: The impact of transpacific transport of mineral dust in the United States, Atmos. Environ., 41(6), 1251–1266, doi:10.1016/j.atmosenv.2006.09.048, 2007.

Fisher, J. A., Jacob, D. J., Wang, Q., Bahreini, R., Carouge, C. C., Cubison, M. J., Dibb, J. E., Diehl, T., Jimenez, J. L., Leibensperger, E. M., Lu, Z., Meinders, M. B. J., Pye, H. O. T., Quinn, P. K., Sharma, S., Streets, D. G., van Donkelaar, A. and Yantosca, R. M.: Sources, distribution, and acidity of sulfate–ammonium aerosol in the Arctic in winter–spring, Atmos. Environ., 45(39), 7301–7318, doi:10.1016/j.atmosenv.2011.08.030, 2011.

Fisher, J. A., Jacob, D. J., Travis, K. R., Kim, P. S., Marais, E. A., Chan Miller, C., Yu, K., Zhu, L., Yantosca, R. M., Sulprizio, M. P., Mao, J., Wennberg, P. O., Crounse, J. D., Teng, A. P., Nguyen, T. B., Clair, J. M. S., Cohen, R. C., Romer, P., Nault, B. A., Wooldridge, P. J., Jimenez, J. L., Campuzano-Jost, P., Day, D. A., Hu, W., Shepson, P. B., Xiong, F., Blake, D. R., Goldstein, A. H., Misztal, P. K., Hanisco, T. F., Wolfe, G. M., Ryerson, T. B., Wisthaler, A. and Mikoviny, T.: Organic nitrate chemistry and its implications for nitrogen budgets in an isoprene- and monoterpene-rich atmosphere: constraints from aircraft (SEAC^{4}RS) and ground-based (SOAS) observations in the Southeast US, Atmospheric Chem. Phys., 16(9), 5969–5991, doi:https://doi.org/10.5194/acp-16-5969-2016, 2016.

Fountoukis, C. and Nenes, A.: ISORROPIA II: a computationally efficient thermodynamic equilibrium model for K+–Ca2+–Mg2+–NH4+–Na+–SO24−–NO−3 –Cl−–H2O aerosols, Atmospheric Chem. Phys., 7, 4639–4659, doi:https://doi.org/10.5194/acp-7-4639-2007, 2007.

Gantt, B., Johnson, M. S., Crippa, M., Prévôt, A. S. H. and Meskhidze, N.: Implementing marine organic aerosols into the GEOS-Chem model, Geosci. Model Dev., 8(3), 619–629, doi:10.5194/gmd-8-619-2015, 2015.

Goldberg, D. L., Saide, P. E., Lamsal, L. N., de Foy, B., Lu, Z., Woo, J.-H., Kim, Y., Kim, J., Gao, M., Carmichael, G. and Streets, D. G.: A top-down assessment using OMI NO2 suggests an underestimate in the NOx emissions inventory in Seoul, South Korea during KORUS-AQ, Atmospheric Chem. Phys. Discuss., 1–25, doi:10.5194/acp-2018-678, 2018.

Grieshop, A. P., Logue, J. M., Donahue, N. M. and Robinson, A. L.: Laboratory investigation of photochemical oxidation of organic aerosol from wood fires 1: measurement and simulation of organic aerosol evolution, Atmospheric Chem. Phys., 9(4), 1263–1277, doi:https://doi.org/10.5194/acp-9-1263-2009, 2009.

Guenther, A. B., Jiang, X., Heald, C. L., Sakulyanontvittaya, T., Duhl, T., Emmons, L. K. and Wang, X.: The Model of Emissions of Gases and Aerosols from Nature version 2.1 (MEGAN2.1): an extended and updated framework for modeling biogenic emissions, Geosci. Model Dev., 5(6), 1471–1492, doi:10.5194/gmd-5-1471-2012, 2012.

Hayes, P. L., Carlton, A. G., Baker, K. R., Ahmadov, R., Washenfelder, R. A., Alvarez, S., Rappenglück, B., Gilman, J. B., Kuster, W. C., de Gouw, J. A., Zotter, P., Prévôt, A. S. H., Szidat, S., Kleindienst, T. E., Offenberg, J. H., Ma, P. K. and Jimenez, J. L.: Modeling the formation and aging of secondary organic aerosols in Los Angeles during CalNex 2010, Atmospheric Chem. Phys., 15(10), 5773–5801, doi:10.5194/acp-15-5773-2015, 2015.

Heald, C. L., Jacob, D. J., Park, R. J., Russell, L. M., Huebert, B. J., Seinfeld, J. H., Liao, H. and Weber, R. J.: A large organic aerosol source in the free troposphere missing from current models, Geophys. Res. Lett., 32(18), doi:10.1029/2005GL023831, 2005.

Heald, C. L., Coe, H., Jimenez, J. L., Weber, R. J., Bahreini, R., Middlebrook, A. M., Russell, L. M., Jolleys, M., Fu, T.-M., Allan, J. D., Bower, K. N., Capes, G., Crosier, J., Morgan, W. T., Robinson, N. H., Williams, P. I., Cubison, M. J., DeCarlo, P. F. and Dunlea, E. J.: Exploring the vertical profile of atmospheric organic aerosol: comparing 17 aircraft field campaigns with a global model, Atmospheric Chem. Phys., 11(24), 12673–12696, doi:10.5194/acp-11-12673-2011, 2011.

Hewitt, C. N., Lee, J. D., MacKenzie, A. R., Barkley, M. P., Carslaw, N., Carver, G. D., Chappell, N. A., Coe, H., Collier, C., Commane, R., Davies, F., Davison, B., DiCarlo, P., Marco, C. F. D., Dorsey, J. R., Edwards, P. M., Evans, M. J., Fowler, D., Furneaux, K. L., Gallagher, M., Guenther, A., Heard, D. E., Helfter, C., Hopkins, J., Ingham, T., Irwin, M., Jones, C., Karunaharan, A., Langford, B., Lewis, A. C., Lim, S. F., MacDonald, S. M., Mahajan, A. S., Malpass, S., McFiggans, G., Mills, G., Misztal, P., Moller, S., Monks, P. S., Nemitz, E., Nicolas-Perea, V., Oetjen, H., Oram, D. E., Palmer, P. I., Phillips, G. J., Pike, R., Plane, J. M. C., Pugh, T., Pyle, J. A., Reeves, C. E., Robinson, N. H., Stewart, D., Stone, D., Whalley, L. K. and Yang, X.: Corrigendum to "Overview: oxidant and particle photochemical processes above a south-east Asian tropical rainforest (the OP3 project): introduction, rationale, location characteristics and tools" published in Atmos. Chem. Phys., 10, 169–199, 2010, Atmospheric Chem. Phys., 10(2), 563–563, doi:https://doi.org/10.5194/acp-10-563-2010, 2010.

Hodzic, A., Kasibhatla, P. S., Jo, D. S., Cappa, C. D., Jimenez, J. L., Madronich, S. and Park, R. J.: Rethinking the global secondary organic aerosol (SOA) budget: stronger production, faster removal, shorter lifetime, Atmospheric Chem. Phys., 16(12), 7917–7941, doi:https://doi.org/10.5194/acp-16-7917-2016, 2016.

Hoesly, R. M., Smith, S. J., Feng, L., Klimont, Z., Janssens-Maenhout, G., Pitkanen, T., Seibert, J. J., Vu, L., Andres, R. J., Bolt, R. M., Bond, T. C., Dawidowski, L., Kholod, N., Kurokawa, J., Li, M., Liu, L., Lu, Z., Moura, M. C. P., O'Rourke, P. R. and Zhang, Q.: Historical (1750–2014) anthropogenic emissions of reactive gases and aerosols from the Community Emissions Data System (CEDS), Geosci. Model Dev., 11(1), 369–408, doi:https://doi.org/10.5194/gmd-11-369-2018, 2018.

Holmes, C. D., Prather, M. J. and Vinken, G. C. M.: The climate impact of ship NO_x emissions: an improved estimate accounting for plume chemistry, Atmospheric Chem. Phys., 14(13), 6801–6812, doi:https://doi.org/10.5194/acp-14-6801-2014, 2014.

Hudman, R. C., Moore, N. E., Mebust, A. K., Martin, R. V., Russell, A. R., Valin, L. C. and Cohen, R. C.: Steps towards a mechanistic model of global soil nitric oxide emissions: implementation and space based-constraints, Atmospheric Chem. Phys., 12(16), 7779–7795, doi:https://doi.org/10.5194/acp-12-7779-2012, 2012.

Huffman, J. A., Docherty, K. S., Mohr, C., Cubison, M. J., Ulbrich, I. M., Ziemann, P. J., Onasch, T. B. and Jimenez, J. L.: Chemically-Resolved Volatility Measurements of Organic Aerosol from Different Sources, Environ. Sci. Technol., 43(14), 5351–5357, doi:10.1021/es803539d, 2009.

IPCC: Climate Change 2013: The Physical Science Basis. Contribution of Working Group I to the Fifth Assessment Report of the Intergovernmental Panel on Climate Change, Cambridge University Press, Cambridge, United Kingdom and New York, NY, USA. [online] Available from: https://www.ipcc.ch/site/assets/uploads/2018/02/WG1AR5_all_final.pdf (Accessed 11 February 2019), 2013.

Jacob, D. J., Liu, H., Mari, C. and Yantosca, R. M.: Harvard wet deposition scheme for GMI, , 6, 2000.

Jacob, D. J., Crawford, J. H., Maring, H., Clarke, A. D., Dibb, J. E., Emmons, L. K., Ferrare, R. A., Hostetler, C. A., Russell, P. B., Singh, H. B., Thompson, A. M., Shaw, G. E., McCauley, E., Pederson, J. R. and Fisher, J. A.: The Arctic Research of the Composition of the Troposphere from Aircraft and Satellites (ARCTAS) mission: design, execution, and first results, Atmospheric Chem. Phys., 10(11), 5191–5212, doi:https://doi.org/10.5194/acp-10-5191-2010, 2010.

Jaeglé, L., Quinn, P. K., Bates, T. S., Alexander, B. and Lin, J.-T.: Global distribution of sea salt aerosols: new constraints from in situ and remote sensing observations, Atmospheric Chem. Phys., 11(7), 3137–3157, doi:10.5194/acp-11-3137-2011, 2011.

Jayne, J. T., Leard, D. C., Zhang, X., Davidovits, P., Smith, K. A., Kolb, C. E. and Worsnop, D. R.: Development of an Aerosol Mass Spectrometer for Size and Composition Analysis of Submicron Particles, Aerosol Sci. Technol., 33(1–2), 49–70, doi:10.1080/027868200410840, 2000.

Jimenez, J. L., Canagaratna, M. R., Donahue, N. M., Prevot, A. S. H., Zhang, Q., Kroll, J. H., DeCarlo, P. F., Allan, J. D., Coe, H., Ng, N. L., Aiken, A. C., Docherty, K. S., Ulbrich, I. M., Grieshop, A. P., Robinson, A. L., Duplissy, J., Smith, J. D., Wilson, K. R., Lanz, V. A., Hueglin, C., Sun, Y. L., Tian, J., Laaksonen, A., Raatikainen, T., Rautiainen, J., Vaattovaara, P., Ehn, M., Kulmala, M., Tomlinson, J. M., Collins, D. R., Cubison, M. J., E, Dunlea, J., Huffman, J. A., Onasch, T. B., Alfarra, M. R., Williams, P. I., Bower, K., Kondo, Y., Schneider, J., Drewnick, F., Borrmann, S., Weimer, S., Demerjian, K., Salcedo, D., Cottrell, L., Griffin, R., Takami, A., Miyoshi, T., Hatakeyama, S., Shimono, A., Sun, J. Y., Zhang, Y. M., Dzepina, K., Kimmel, J. R., Sueper, D., Jayne, J. T., Herndon, S. C., Trimborn, A. M., Williams, L. R., Wood, E. C., Middlebrook, A. M., Kolb, C. E., Baltensperger, U. and Worsnop, D. R.: Evolution of Organic Aerosols in the Atmosphere, Science, 326(5959), 1525–1529, doi:10.1126/science.1180353, 2009.

Jo, D. S., Hodzic, A., Emmons, L. K., Marais, E. A., Peng, Z., Nault, B. A., Hu, W., Campuzano-Jost, P. and Jimenez, J. L.: A simplified parameterization of isoprene-epoxydiol-derived secondary organic aerosol (IEPOX-SOA) for global chemistry and climate models, Geosci. Model Dev. Discuss., 1–36, doi:10.5194/gmd-2019-9, 2019.

Jolleys, M. D., Coe, H., McFiggans, G., McMeeking, G. R., Lee, T., Kreidenweis, S. M., Collett, J. L. and Sullivan, A. P.: Organic aerosol emission ratios from the laboratory combustion of biomass fuels: BBOA emission ratios in chamber studies, J. Geophys. Res. Atmospheres, 119(22), 12,850-12,871, doi:10.1002/2014JD021589, 2014.

Kanakidou, M., Seinfeld, J. H., Pandis, S. N., Barnes, I., Dentener, F. J., Facchini, M. C., Dingenen, R. V., Ervens, B., Nenes, A., Nielsen, C. J., Swietlicki, E., Putaud, J. P., Balkanski, Y., Fuzzi, S., Horth, J., Moortgat, G. K., Winterhalter, R., Myhre, C. E. L., Tsigaridis, K., Vignati, E., Stephanou, E. G. and Wilson, J.: Organic aerosol and global climate modelling: a review, Atmospheric Chem. Phys., 5(4), 1053–1123, doi:https://doi.org/10.5194/acp-5-1053-2005, 2005.

Keller, C. A., Long, M. S., Yantosca, R. M., Da Silva, A. M., Pawson, S. and Jacob, D. J.: HEMCO v1.0: a versatile, ESMF-compliant component for calculating emissions in atmospheric models, Geosci. Model Dev., 7(4), 1409–1417, doi:https://doi.org/10.5194/gmd-7-1409-2014, 2014.

Kiendler-Scharr, A., Mensah, A. A., Friese, E., Topping, D., Nemitz, E., Prevot, A. S. H., Äijälä, M., Allan, J., Canonaco, F., Canagaratna, M., Carbone, S., Crippa, M., Osto, M. D., Day, D. A., Carlo, P. D., Marco, C. F. D., Elbern, H., Eriksson, A., Freney, E., Hao, L., Herrmann, H., Hildebrandt, L., Hillamo, R., Jimenez, J. L., Laaksonen, A., McFiggans, G., Mohr, C., O'Dowd, C., Otjes, R., Ovadnevaite, J., Pandis, S. N., Poulain, L., Schlag, P., Sellegri, K., Swietlicki, E., Tiitta, P., Vermeulen, A., Wahner, A., Worsnop, D. and Wu, H.-C.: Ubiquity of organic nitrates

from nighttime chemistry in the European submicron aerosol, Geophys. Res. Lett., 43(14), 7735–7744, doi:10.1002/2016GL069239, 2016.

Kim, P. S., Jacob, D. J., Fisher, J. A., Travis, K., Yu, K., Zhu, L., Yantosca, R. M., Sulprizio, M. P., Jimenez, J. L., Campuzano-Jost, P., Froyd, K. D., Liao, J., Hair, J. W., Fenn, M. A., Butler, C. F., Wagner, N. L., Gordon, T. D., Welti, A., Wennberg, P. O., Crounse, J. D., St. Clair, J. M., Teng, A. P., Millet, D. B., Schwarz, J. P., Markovic, M. Z. and Perring, A. E.: Sources, seasonality, and trends of southeast US aerosol: an integrated analysis of surface, aircraft, and satellite observations with the GEOS-Chem chemical transport model, Atmospheric Chem. Phys., 15(18), 10411–10433, doi:10.5194/acp-15-10411-2015, 2015.

Kroll, J. H., Ng, N. L., Murphy, S. M., Flagan, R. C. and Seinfeld, J. H.: Secondary Organic Aerosol Formation from Isoprene Photooxidation, Environ. Sci. Technol., 40(6), 1869–1877, doi:10.1021/es0524301, 2006.

Kuhns, H., Knipping, E. M. and Vukovich, J. M.: Development of a United States–Mexico Emissions Inventory for the Big Bend Regional Aerosol and Visibility Observational (BRAVO) Study, J. Air Waste Manag. Assoc., 55(5), 677–692, doi:10.1080/10473289.2005.10464648, 2005.

Li, J., Cleveland, M., Ziemba, L. D., Griffin, R. J., Barsanti, K. C., Pankow, J. F. and Ying, Q.: Modeling regional secondary organic aerosol using the Master Chemical Mechanism, Atmos. Environ., 102, 52–61, doi:10.1016/j.atmosenv.2014.11.054, 2015.

Li, M., Zhang, Q., Kurokawa, J., Woo, J.-H., He, K., Lu, Z., Ohara, T., Song, Y., Streets, D. G., Carmichael, G. R., Cheng, Y., Hong, C., Huo, H., Jiang, X., Kang, S., Liu, F., Su, H. and Zheng, B.: MIX: a mosaic Asian anthropogenic emission inventory under the international collaboration framework of the MICS-Asia and HTAP, Atmospheric Chem. Phys., 17(2), 935–963, doi:10.5194/acp-17-935-2017, 2017.

Lin, G., Penner, J. E., Sillman, S., Taraborrelli, D. and Lelieveld, J.: Global modeling of SOA formation from dicarbonyls, epoxides, organic nitrates and peroxides, Atmospheric Chem. Phys., 12(10), 4743–4774, doi:10.5194/acp-12-4743-2012, 2012.

Lipsky, E. M. and Robinson, A. L.: Effects of Dilution on Fine Particle Mass and Partitioning of Semivolatile Organics in Diesel Exhaust and Wood Smoke, Environ. Sci. Technol., 40(1), 155–162, doi:10.1021/es050319p, 2006.

Liu, H., Jacob, D. J., Bey, I. and Yantosca, R. M.: Constraints from ^{210}Pb and ^{7}Be on wet deposition and transport in a global three-dimensional chemical tracer model driven by assimilated meteorological fields, J. Geophys. Res. Atmospheres, 106(D11), 12109–12128, doi:10.1029/2000JD900839, 2001.

Mao, J., Paulot, F., Jacob, D. J., Cohen, R. C., Crounse, J. D., Wennberg, P. O., Keller, C. A., Hudman, R. C., Barkley, M. P. and Horowitz, L. W.: Ozone and organic nitrates over the eastern United States: Sensitivity to isoprene chemistry: OZONE AND ORGANIC NITRATES OVER EAST U.S., J. Geophys. Res. Atmospheres, 118(19), 11,256-11,268, doi:10.1002/jgrd.50817, 2013.

Marais, E. A. and Wiedinmyer, C.: Air Quality Impact of Diffuse and Inefficient Combustion Emissions in Africa (DICE-Africa), Environ. Sci. Technol., 50(19), 10739–10745, doi:10.1021/acs.est.6b02602, 2016.

Marais, E. A., Jacob, D. J., Jimenez, J. L., Campuzano-Jost, P., Day, D. A., Hu, W., Krechmer, J., Zhu, L., Kim, P. S., Miller, C. C., Fisher, J. A., Travis, K., Yu, K., Hanisco, T. F., Wolfe, G. M., Arkinson, H. L., Pye, H. O. T., Froyd, K. D., Liao, J. and McNeill, V. F.: Aqueous-phase mechanism for secondary organic aerosol formation from isoprene: application to the southeast United States and co-benefit of SO₂ emission controls, Atmospheric Chem. Phys., 16(3), 1603–1618, doi:10.5194/acp-16-1603-2016, 2016.

Marais, E. A., Jacob, D. J., Turner, J. R. and Mickley, L. J.: Evidence of 1991–2013 decrease of biogenic secondary organic aerosol in response to SO_2 emission controls, Environ. Res. Lett., 12(5), 054018, doi:10.1088/1748-9326/aa69c8, 2017.

Martin, R. V., Jacob, D. J., Yantosca, R. M., Chin, M. and Ginoux, P.: Global and regional decreases in tropospheric oxidants from photochemical effects of aerosols: PHOTOCHEMICAL EFFECTS OF AEROSOLS, J. Geophys. Res. Atmospheres, 108(D3), n/a-n/a, doi:10.1029/2002JD002622, 2003.

Martin, S. T., Artaxo, P., Machado, L. a. T., Manzi, A. O., Souza, R. a. F., Schumacher, C., Wang, J., Andreae, M. O., Barbosa, H. M. J., Fan, J., Fisch, G., Goldstein, A. H., Guenther, A., Jimenez, J. L., Pöschl, U., Silva Dias, M. A., Smith, J. N. and Wendisch, M.: Introduction: Observations and Modeling of the Green Ocean Amazon (GoAmazon2014/5), Atmospheric Chem. Phys., 16(8), 4785–4797, doi:https://doi.org/10.5194/acp-16-4785-2016, 2016.

McFiggans, G., Mentel, T. F., Wildt, J., Pullinen, I., Kang, S., Kleist, E., Schmitt, S., Springer, M., Tillmann, R., Wu, C., Zhao, D., Hallquist, M., Faxon, C., Le Breton, M., Hallquist, Å. M., Simpson, D., Bergström, R., Jenkin, M. E., Ehn, M., Thornton, J. A., Alfarra, M. R., Bannan, T. J., Percival, C. J., Priestley, M., Topping, D. and Kiendler-Scharr, A.: Secondary organic aerosol reduced by mixture of atmospheric vapours, Nature, 565(7741), 587–593, doi:10.1038/s41586-018-0871-y, 2019.

Miller, C. C., Jacob, D. J., Marais, E. A., Yu, K., Travis, K. R., Kim, P. S., Fisher, J. A., Zhu, L., Wolfe, G. M., Hanisco, T. F., Keutsch, F. N., Kaiser, J., Min, K.-E., Brown, S. S., Washenfelder, R. A., González Abad, G. and Chance, K.: Glyoxal yield from isoprene oxidation and relation to formaldehyde: chemical mechanism, constraints from SENEX aircraft observations, and interpretation of OMI satellite data, Atmospheric Chem. Phys., 17(14), 8725–8738, doi:10.5194/acp-17-8725-2017, 2017.

Morgan, W. T., Allan, J. D., Bower, K. N., Highwood, E. J., Liu, D., McMeeking, G. R., Northway, M. J., Williams, P. I., Krejci, R. and Coe, H.: Airborne measurements of the spatial distribution of aerosol chemical composition across Europe and evolution of the organic fraction, Atmospheric Chem. Phys., 10, 4065–4083, doi:https://doi.org/10.5194/acp-10-4065-2010, 2010.

Murphy, B. N., Donahue, N. M., Robinson, A. L. and Pandis, S. N.: A naming convention for atmospheric organic aerosol, Atmospheric Chem. Phys., 14(11), 5825–5839, doi:10.5194/acp-14-5825-2014, 2014.

Murray, L. T., Jacob, D. J., Logan, J. A., Hudman, R. C. and Koshak, W. J.: Optimized regional and interannual variability of lightning in a global chemical transport model constrained by LIS/OTD satellite data: IAV OF LIGHTNING CONSTRAINED BY LIS/OTD, J. Geophys. Res. Atmospheres, 117(D20), doi:10.1029/2012JD017934, 2012.

Nault, B. A., Campuzano-Jost, P., Day, D. A., Schroder, J. C., Anderson, B., Beyersdorf, A. J., Blake, D. R., Brune, W. H., Choi, Y., Corr, C. A., de Gouw, J. A., Dibb, J., DiGangi, J. P., Diskin, G. S., Fried, A., Huey, L. G., Kim, M. J., Knote, C. J., Lamb, K. D., Lee, T., Park, T., Pusede, S. E., Scheuer, E., Thornhill, K. L., Woo, J.-H. and Jimenez, J. L.: Secondary organic aerosol production from local emissions dominates the organic aerosol budget over Seoul, South Korea, during KORUS-AQ, Atmospheric Chem. Phys., 18(24), 17769–17800, doi:10.5194/acp-18-17769-2018, 2018.

Ng, N. L., Chhabra, P. S., Chan, A. W. H., Surratt, J. D., Kroll, J. H., Kwan, A. J., McCabe, D. C., Wennberg, P. O., Sorooshian, A., Murphy, S. M., Dalleska, N. F., Flagan, R. C. and Seinfeld, J. H.: Effect of NOx level on secondary organic aerosol (SOA) formation from the photooxidation of terpenes, Atmospheric Chem. Phys., 7, 5159–5174, doi:https://doi.org/10.5194/acp-7-5159-2007, 2007.

Odum, J. R., Hoffmann, T., Bowman, F., Collins, D., Flagan, R. C. and Seinfeld, J. H.: Gas/Particle Partitioning and Secondary Organic Aerosol Yields, Environ. Sci. Technol., 30(8), 2580–2585, doi:10.1021/es950943+, 1996.

Ott, L. E., Pickering, K. E., Stenchikov, G. L., Allen, D. J., DeCaria, A. J., Ridley, B., Lin, R.-F., Lang, S. and Tao, W.-K.: Production of lightning NO_x and its vertical distribution calculated from three-dimensional cloud-scale chemical transport model simulations, J. Geophys. Res., 115(D4), doi:10.1029/2009JD011880, 2010.

Pandis, S. N., Harley, R. A., Cass, G. R. and Seinfeld, J. H.: Secondary organic aerosol formation and transport, Atmospheric Environ. Part Gen. Top., 26(13), 2269–2282, doi:10.1016/0960-1686(92)90358-R, 1992.

Pankow, J. F.: An absorption model of the gas/aerosol partitioning involved in the formation of secondary organic aerosol, Atmos. Environ., 28(2), 189–193, doi:10.1016/1352-2310(94)90094-9, 1994.

Park, R. J.: Natural and transboundary pollution influences on sulfate-nitrate-ammonium aerosols in the United States: Implications for policy, J. Geophys. Res., 109(D15), doi:10.1029/2003JD004473, 2004.

Park, R. J., Jacob, D. J., Martin, R. V. and Chin, M.: Sources of carbonaceous aerosols over the United States and implications for natural visibility, J. Geophys. Res., 108(D12), doi:10.1029/2002JD003190, 2003.

Philip, S., Martin, R. V. and Keller, C. A.: Sensitivity of chemistry-transport model simulations to the duration of chemical and transport operators: a case study with GEOS-Chem v10-01, Geosci. Model Dev., 9(5), 1683–1695, doi:https://doi.org/10.5194/gmd-9-1683-2016, 2016.

Pope, C. A. and Dockery, D. W.: Health Effects of Fine Particulate Air Pollution: Lines that Connect, J. Air Waste Manag. Assoc., 56(6), 709–742, doi:10.1080/10473289.2006.10464485, 2006.

Pye, H. O. T. and Seinfeld, J. H.: A global perspective on aerosol from low-volatility organic compounds, Atmospheric Chem. Phys., 10, 4377–4401, doi:https://doi.org/10.5194/acp-10-4377-2010, 2010.

Pye, H. O. T., Chan, A. W. H., Barkley, M. P. and Seinfeld, J. H.: Global modeling of organic aerosol: the importance of reactive nitrogen (NO_x and NO_3), Atmospheric Chem. Phys., 10(22), 11261–11276, doi:10.5194/acp-10-11261-2010, 2010.

Pye, H. O. T., D'Ambro, E. L., Lee, B. H., Schobesberger, S., Takeuchi, M., Zhao, Y., Lopez-Hilfiker, F., Liu, J., Shilling, J. E., Xing, J., Mathur, R., Middlebrook, A. M., Liao, J., Welti, A., Graus, M., Warneke, C., de Gouw, J. A., Holloway, J. S., Ryerson, T. B., Pollack, I. B. and Thornton, J. A.: Anthropogenic enhancements to production of highly oxygenated molecules from autoxidation, Proc. Natl. Acad. Sci., 201810774, doi:10.1073/pnas.1810774116, 2019.

Ramanathan, V., Crutzen, P. J., Kiehl, J. T. and Rosenfeld, D.: Aerosols, Climate, and the Hydrological Cycle, Science, 294(5549), 2119–2124, doi:10.1126/science.1064034, 2001.

Rastigejev, Y., Park, R., Brenner, M. P. and Jacob, D. J.: Resolving intercontinental pollution plumes in global models of atmospheric transport, J. Geophys. Res., 115(D2), doi:10.1029/2009JD012568, 2010.

Ridley, D. A., Heald, C. L. and Ford, B.: North African dust export and deposition: A satellite and model perspective., J. Geophys. Res. Atmospheres, 117(D2), doi:10.1029/2011JD016794, 2012.

Robinson, A. L., Donahue, N. M., Shrivastava, M. K., Weitkamp, E. A., Sage, A. M., Grieshop, A. P., Lane, T. E., Pierce, J. R. and Pandis, S. N.: Rethinking Organic Aerosols: Semivolatile Emissions and Photochemical Aging, Science, 315(5816), 1259–1262, doi:10.1126/science.1133061, 2007.

Ryerson, T. B., Andrews, A. E., Angevine, W. M., Bates, T. S., Brock, C. A., Cairns, B., Cohen, R. C., Cooper, O. R., de Gouw, J. A., Fehsenfeld, F. C., Ferrare, R. A., Fischer, M. L., Flagan, R. C., Goldstein, A. H., Hair, J. W., Hardesty, R. M., Hostetler, C. A., Jimenez, J. L., Langford, A. O., McCauley, E., McKeen, S. A., Molina, L. T., Nenes, A., Oltmans, S. J., Parrish, D. D., Pederson, J. R., Pierce, R. B., Prather, K., Quinn, P. K., Seinfeld, J. H., Senff, C. J., Sorooshian, A., Stutz, J., Surratt, J. D., Trainer, M., Volkamer, R., Williams, E. J. and Wofsy, S. C.: The 2010 California Research at the Nexus of Air Quality and Climate Change (CalNex) field study, J. Geophys. Res. Atmospheres, 118(11), 5830–5866, doi:10.1002/jgrd.50331, 2013.

Schauer, J. J., Kleeman, M. J., Cass, G. R. and Simoneit, B. R. T.: Measurement of Emissions from Air Pollution Sources. 3. C1−C29 Organic Compounds from Fireplace Combustion of Wood, Environ. Sci. Technol., 35(9), 1716–1728, doi:10.1021/es001331e, 2001.

Schroder, J. C., Campuzano-Jost, P., Day, D. A., Shah, V., Larson, K., Sommers, J. M., Sullivan, A. P., Campos, T., Reeves, J. M., Hills, A., Hornbrook, R. S., Blake, N. J., Scheuer, E., Guo, H., Fibiger, D. L., McDuffie, E. E., Hayes, P. L., Weber, R. J., Dibb, J. E., Apel, E. C., Jaeglé, L., Brown, S. S., Thornton, J. A. and Jimenez, J. L.: Sources and Secondary Production of Organic Aerosols in the Northeastern United States during WINTER, J. Geophys. Res. Atmospheres, doi:10.1029/2018JD028475, 2018.

Shah, V., Jaeglé, L., Jimenez, J. L., Schroder, J. C., Campuzano-Jost, P., Campos, T. L., Reeves, J. M., Stell, M., Brown, S. S., Lee, B. H., Lopez-Hilfiker, F. D. and Thornton, J. A.: Widespread Pollution From Secondary Sources of Organic Aerosols During Winter in the Northeastern United States, Geophys. Res. Lett., 0(0), doi:10.1029/2018GL081530, 2019.

Sherwen, T., Schmidt, J. A., Evans, M. J., Carpenter, L. J., Großmann, K., Eastham, S. D., Jacob, D. J., Dix, B., Koenig, T. K., Sinreich, R., Ortega, I., Volkamer, R., Saiz-Lopez, A., Prados-Roman, C., Mahajan, A. S. and Ordóñez, C.: Global impacts of tropospheric halogens (Cl, Br, I) on oxidants and composition in GEOS-Chem, Atmospheric Chem. Phys., 16(18), 12239–12271, doi:10.5194/acp-16-12239-2016, 2016.

Shilling, J. E., Pekour, M. S., Fortner, E. C., Artaxo, P., de Sá, S., Hubbe, J. M., Longo, K. M., Machado, L. A. T., Martin, S. T., Springston, S. R., Tomlinson, J. and Wang, J.: Aircraft observations of the chemical composition and aging of aerosol in the Manaus urban plume during GoAmazon 2014/5, Atmospheric Chem. Phys., 18(14), 10773–10797, doi:10.5194/acp-18-10773-2018, 2018.

Shrivastava, M. K., Lipsky, E. M., Stanier, C. O. and Robinson, A. L.: Modeling Semivolatile Organic Aerosol Mass Emissions from Combustion Systems, Environ. Sci. Technol., 40(8), 2671–2677, doi:10.1021/es0522231, 2006.

Spracklen, D. V., Jimenez, J. L., Carslaw, K. S., Worsnop, D. R., Evans, M. J., Mann, G. W., Zhang, Q., Canagaratna, M. R., Allan, J., Coe, H., McFiggans, G., Rap, A. and Forster, P.: Aerosol mass spectrometer constraint on the global secondary organic aerosol budget, Atmospheric Chem. Phys., 11(23), 12109–12136, doi:10.5194/acp-11-12109-2011, 2011.

Toon, O. B., Maring, H., Dibb, J., Ferrare, R., Jacob, D. J., Jensen, E. J., Luo, Z. J., Mace, G. G., Pan, L. L., Pfister, L., Rosenlof, K. H., Redemann, J., Reid, J. S., Singh, H. B., Thompson, A. M., Yokelson, R., Minnis, P., Chen, G., Jucks, K. W. and Pszenny, A.: Planning, implementation, and scientific goals of the Studies of Emissions and Atmospheric Composition, Clouds and Climate Coupling by Regional Surveys (SEAC ^{4} RS) field mission: Planning SEAC4RS, J. Geophys. Res. Atmospheres, 121(9), 4967–5009, doi:10.1002/2015JD024297, 2016.

Travis, K. R., Jacob, D. J., Fisher, J. A., Kim, P. S., Marais, E. A., Zhu, L., Yu, K., Miller, C. C., Yantosca, R. M., Sulprizio, M. P., Thompson, A. M., Wennberg, P. O., Crounse, J. D., St. Clair, J. M., Cohen, R. C., Laughner, J. L., Dibb, J. E., Hall, S. R., Ullmann, K., Wolfe, G. M., Pollack, I. B., Peischl, J., Neuman, J. A. and Zhou, X.: Why do models overestimate surface ozone in the Southeast United States?, Atmospheric Chem. Phys., 16(21), 13561–13577, doi:10.5194/acp-16-13561-2016, 2016.

Tsigaridis, K., Daskalakis, N., Kanakidou, M., Adams, P. J., Artaxo, P., Bahadur, R., Balkanski, Y., Bauer, S. E., Bellouin, N., Benedetti, A., Bergman, T., Berntsen, T. K., Beukes, J. P., Bian, H., Carslaw, K. S., Chin, M., Curci, G., Diehl, T., Easter, R. C., Ghan, S. J., Gong, S. L., Hodzic, A., Hoyle, C. R., Iversen, T., Jathar, S., Jimenez, J. L., Kaiser, J. W., Kirkevåg, A., Koch, D., Kokkola, H., Lee, Y. H., Lin, G., Liu, X., Luo, G., Ma, X., Mann, G. W., Mihalopoulos, N., Morcrette, J.-J., Müller, J.-F., Myhre, G., Myriokefalitakis, S., Ng, N. L., O'Donnell, D., Penner, J. E., Pozzoli, L., Pringle, K. J., Russell, L. M., Schulz, M., Sciare, J., Seland, ø., Shindell, D. T., Sillman, S., Skeie, R. B., Spracklen, D., Stavrakou, T., Steenrod, S. D., Takemura, T., Tiitta, P., Tilmes, S., Tost, H., van Noije, T., van Zyl, P. G., von Salzen, K., Yu, F., Wang, Z., Wang, Z., Zaveri, R. A., Zhang, H., Zhang, K., Zhang, Q. and Zhang, X.: The AeroCom evaluation and intercomparison of organic aerosol in global models, Atmospheric Chem. Phys., 14(19), 10845–10895, doi:10.5194/acp-14-10845-2014, 2014.

Turquety, S., Logan, J. A., Jacob, D. J., Hudman, R. C., Leung, F. Y., Heald, C. L., Yantosca, R. M., Wu, S., Emmons, L. K., Edwards, D. P. and Sachse, G. W.: Inventory of boreal fire emissions for North America in 2004: Importance of peat burning and pyroconvective injection, J. Geophys. Res. Atmospheres, 112(D12), doi:10.1029/2006JD007281, 2007.

Volkamer, R., Jimenez, J. L., Martini, F. S., Dzepina, K., Zhang, Q., Salcedo, D., Molina, L. T., Worsnop, D. R. and Molina, M. J.: Secondary organic aerosol formation from anthropogenic air pollution: Rapid and higher than expected, Geophys. Res. Lett., 33(17), doi:10.1029/2006GL026899, 2006.

Warneke, C., Trainer, M., de Gouw, J. A., Parrish, D. D., Fahey, D. W., Ravishankara, A. R., Middlebrook, A. M., Brock, C. A., Roberts, J. M., Brown, S. S., Neuman, J. A., Lerner, B. M., Lack, D., Law, D., Hübler, G., Pollack, I., Sjostedt, S., Ryerson, T. B., Gilman, J. B., Liao, J., Holloway, J., Peischl, J., Nowak, J. B., Aikin, K., Min, K.-E., Washenfelder, R. A., Graus, M. G., Richardson, M., Markovic, M. Z., Wagner, N. L., Welti, A., Veres, P. R., Edwards, P., Schwarz, J. P., Gordon, T., Dube, W. P., McKeen, S., Brioude, J., Ahmadov, R., Bougiatioti, A., Lin, J. J., Nenes, A., Wolfe, G. M., Hanisco, T. F., Lee, B. H., Lopez-Hilfiker, F. D., Thornton, J. A., Keutsch, F. N., Kaiser, J., Mao, J. and Hatch, C.: Instrumentation and Measurement Strategy for the NOAA SENEX Aircraft Campaign as Part of the Southeast Atmosphere Study 2013, Atmospheric Meas. Tech., 9(7), 3063–3093, doi:10.5194/amt-9-3063-2016, 2016.

van der Werf, G. R., Randerson, J. T., Giglio, L., Leeuwen, T. T. van, Chen, Y., Rogers, B. M., Mu, M., Marle, M. J. E. van, Morton, D. C., Collatz, G. J., Yokelson, R. J. and Kasibhatla, P. S.: Global fire emissions estimates during 1997–2016, Earth Syst. Sci. Data, 9(2), 697–720, doi:https://doi.org/10.5194/essd-9-697-2017, 2017.

Wesely, M. L.: Parameterization of surface resistances to gaseous dry deposition in regional-scale numerical models, Atmospheric Environ. 1967, 23(6), 1293–1304, doi:10.1016/0004-6981(89)90153-4, 1989.

Wofsy, S. C., Afshar, S., Allen, H. M., Apel, E., Asher, E. C., Barletta, B., Bent, J., Bian, H., Biggs, B. C., Blake, D. R., Blake, N., Bourgeois, I., Brock, C. A., Brune, W. H., Budney, J. W., Bui, T. P., Butler, A., Campuzano-Jost, P., Chang, C. S., Chin, M., Commane, R., Correa, G., Crounse, J. D., Cullis, P. D., Daube, B. C., Day, D. A., Dean-Day, J. M., Dibb, J. E., Digangi, J. P., Diskin, G. S., Dollner, M., Elkins, J. W., Erdesz, F., Fiore, A. M., Flynn, C. M., Froyd, K., Gesler, D. W., Hall, S. R., Hanisco, T. F., Hannun, R. A., Hills, A. J., Hintsa, E. J., Hoffman, A., Hornbrook, R. S., Huey, L. G., Hughes, S., Jimenez, J. L., Johnson, B. J., Katich, J. M., Keeling, R. F., Kim, M. J., Kupc, A., Lait, L. R., Lamarque, J.-F., Liu, J., Mckain, K., Mclaughlin, R. J., Meinardi, S., Miller, D. O., Montzka, S. A., Moore, F. L., Morgan, E. J., Murphy, D. M., Murray, L. T., Nault, B. A., Neuman, J. A., Newman, P. A., Nicely, J. M., Pan, X., Paplawsky, W., Peischl, J., Prather, M. J., Price, D. J., Ray, E., Reeves, J. M., Richardson, M., Rollins, A. W., Rosenlof, K. H., Ryerson, T. B., Scheuer, E., Schill, G. P., Schroder, J. C., Schwarz, J. P., St. Clair, J. M., Steenrod, S. D., Stephens, B. B., Strode, S. A., Sweeney, C., Tanner, D., Teng, A. P., Thames, A. B., Thompson, C. R., Ullmann, K., Veres, P. R., Vizenor, N., Wagner, N. L., Watt, A., Weber, R., Weinzierl, B., et al.: ATom: Merged Atmospheric Chemistry, Trace Gases, and Aerosols, ORNL DAAC, doi:https://doi.org/10.3334/ORNLDAAC/1581, 2018.

Xia, A. G., Michelangeli, D. V. and Makar, P. A.: Box model studies of the secondary organic aerosol formation under different HC/NOx conditions using the subset of the Master Chemical Mechanism for α-pinene oxidation, J. Geophys. Res. Atmospheres, 113(D10), doi:10.1029/2007JD008726, 2008.

Xu, L., Pye, H. O. T., He, J., Chen, Y., Murphy, B. N. and Ng, N. L.: Experimental and model estimates of the contributions from biogenic monoterpenes and sesquiterpenes to secondary organic aerosol in the southeastern United States, Atmospheric Chem. Phys., 18(17), 12613–12637, doi:10.5194/acp-18-12613-2018, 2018.

Zhang, H., Yee, L. D., Lee, B. H., Curtis, M. P., Worton, D. R., Isaacman-VanWertz, G., Offenberg, J. H., Lewandowski, M., Kleindienst, T. E., Beaver, M. R., Holder, A. L., Lonneman, W. A., Docherty, K. S., Jaoui, M., Pye, H. O. T., Hu, W., Day, D. A., Campuzano-Jost, P., Jimenez, J. L., Guo, H., Weber, R. J., Gouw, J. de, Koss, A. R., Edgerton, E. S., Brune, W., Mohr, C., Lopez-Hilfiker, F. D., Lutz, A., Kreisberg, N. M., Spielman, S. R., Hering, S. V., Wilson, K. R., Thornton, J. A. and Goldstein, A. H.: Monoterpenes are the largest source of summertime organic aerosol in the southeastern United States, Proc. Natl. Acad. Sci., 115(9), 2038–2043, doi:10.1073/pnas.1717513115, 2018.

Zhang, L., Gong, S., Padro, J. and Barrie, L.: A size-segregated particle dry deposition scheme for an atmospheric aerosol module, Atmos. Environ., 35(3), 549–560, doi:10.1016/S1352-2310(00)00326-5, 2001.

Zhu, L., Val Martin, M., Gatti, L. V., Kahn, R., Hecobian, A. and Fischer, E. V.: Development and implementation of a new biomass burning emissions injection height scheme (BBEIH v1.0) for the GEOS-Chem model (v9-01-01), Geosci. Model Dev., 11(10), 4103–4116, doi:10.5194/gmd-11-4103-2018, 2018.

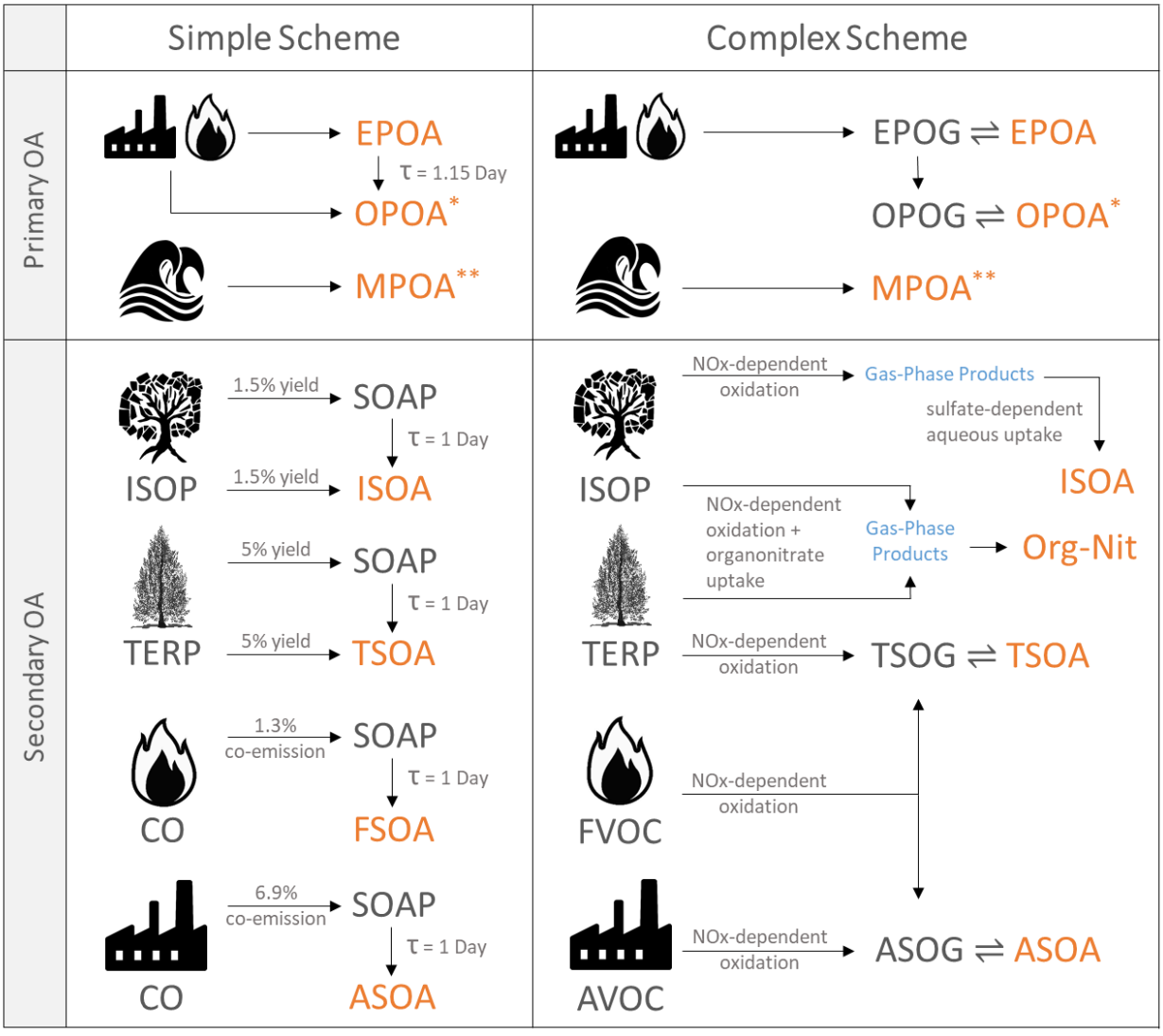

Figure 1 – A graphical overview of the two organic aerosol model schemes in GEOS-Chem. TERP denotes monoterpenes and sesquiterpenes. Pyrogenic VOCs (FVOC) denote the various volatile and semi-volatile organic compounds emitted from fires while anthropogenic VOCs (AVOC) are comprised of benzene, toluene, xylene and various intermediate-volatility organic compounds that are modelled using naphthalene as a proxy. OPOA* is sometimes classified as secondary organic aerosol from SVOCs. MPOA denotes lumped marine POA consisting of both fresh (M-EPOA) and oxidized (M-OPOA) components. Species in orange contribute to OA. See Sect. 2.1 text for details.**

Species	Annual Global Emissions (Tg year $^{-1}$)
Total Aromatics	**25.6**
- Anthropogenic	23.5
- Pyrogenic	2.1
IVOCs	**5.43**
Isoprene	**385.3**
Terpenes	**153.6**
Total CO	**891.2**
- Anthropogenic	593.0
- Pyrogenic	298.2
Total NO_x	**111.7**
- Anthropogenic	70.7
- Pyrogenic	12.1
- Lightning	12.7
- Soil and Fertilizer	16.2

Table 1. Global annual mean emissions of SOA precursors and relevant species used in the GEOS-Chem simulation for the year 2013.

	Complex					Simple				
	Source (Tg yr^{-1})	Burden (Tg)	Lifetime (days)	Dry Dep. (Tg yr^{-1})	Wet Dep. (Tg yr^{-1})	Source (Tg yr^{-1})	Burden (Tg)	Lifetime (days)	Dry Dep. (Tg yr^{-1})	Wet Dep. (Tg yr^{-1})
Total POA	**87.3**†	**1.46**	**6.1**	**14.7**	**72.6**	**73.8**†	**0.92**	**4.6**	**13.2**	**60.6**
- Emitted POA	55.4††	0.11	11.5	2.1	1.4	21.8	0.06	7.8	1.4	1.4
- Marine EPOA	7.0	0.02	4.3	0.9	0.8	7.0	0.02	4.3	0.9	0.8
- Oxygenated POA*	74.1†	1.27	6.3	10.2	63.9	61.3†	0.78	4.6	9.4	51.9
- Marine OPOA*	8.0†	0.06	2.8	1.5	6.5	8.0†	0.06	2.8	1.5	6.5
Total SOA	**62.9**†	**0.91**	**5.3**	**7.3**	**55.6**	**71.7**	**1.02**	**5.2**	**9.4**	**62.2**
- Anthropogenic SOA	4.6†	0.10	7.9	0.6	4.0	41.0	0.63	5.6	6.2	34.8
- Terpene SOA	13.1†	0.19	5.3	1.5	11.6	15.2	0.18	4.3	1.6	13.6
- Isoprene SOA	22.2†	0.31	5.1	2.3	19.9	11.6	0.15	4.7	1.1	10.4
- Organic Nitrates	23.0†	0.31	4.9	2.9	20.1	-	-	-	-	-
- Pyrogenic SOA	-	-	-	-	-	3.9	0.06	5.7	0.5	3.4
Total OOA**	**145.0**†	**2.24**	**5.6**	**19.0**	**126.0**	**140.9**†	**1.86**	**4.8**	**20.3**	**120.6**
Total OA	**150.1**†	**2.37**	**5.8**	**21.9**	**128.2**	**145.3**†	**1.94**	**4.9**	**22.6**	**122.8**

*SVOCs from primary sources that are oxidized in the atmosphere, sometimes classified as SOA

**OOA (Oxygenated Organic Aerosol) = OPOA + M-OPOA + SOA

†Calculated based on a steady-state assumption with depositional losses in order to account for atmospheric formation.

††Primary organic emissions in the complex scheme are in gas phase (EPOG) while primary organic emissions in the simple scheme are in the form of non-volatile particulate. An OM:OC ratio of 1.4 is assumed for the EPOG and EPOA species while an OM:OC ratio of 2.1 is assumed for the OPOA species.

Table 2. Annual mean simulated global source, burden, lifetime (against physical deposition) and wet and dry deposition rates for the individual OA species averaged over 2013 for the complex and simple schemes.

Campaign	Dates (UTC)	Region	Abbreviation	Measurement Technique	Mean / Median / SD
ARCPAC (Brock et al., 2011)	2008 Spring (03/29 - 04/24)	Arctic / North America	-	C-ToF-AMS	1.9 / 0.9 / 2.1
ARCTAS (Jacob et al., 2010)	2008 Spring (04/01 – 04/20)	Arctic / North America	ARCTAS-SP	HR-ToF-AMS	0.7 / 0.4 / 0.9
ARCTAS (Jacob et al., 2010)	2008 Summer (06/18 – 07/13)	Arctic / North America	ARCTAS-SU	HR-ToF-AMS	3.2 / 0.9 / 5.1
EUCAARI (Morgan et al., 2010)	2008 Spring (05/06 - 05/22)	North West Europe	-	C-ToF-AMS	2.5 / 2.4 / 2.0
OP3 (Hewitt et al., 2010)	2008 Summer (07/10 - 07/20)	Borneo	-	C-ToF-AMS	0.4 / 0.1 / 0.5
CalNex (Ryerson et al., 2013)	2010 Spring and Summer (04/30 – 06/22)	South West US	-	C-ToF-AMS	1.3 / 0.8 / 1.4
DC3 (Barth et al., 2014)	2012 Spring and Summer (05/18 - 06/23)	Central US	-	HR-ToF-AMS	2.5 / 1.4 / 2.4
SENEX (Warneke et al., 2016)	2013 Summer (06/03 – 07/10)	South East US	-	C-ToF-AMS	5.3 / 4.7 / 3.7
SEAC4RS (Toon et al., 2016)	2013 Summer and Fall (08/06 – 09/24)	South East / West US	-	HR-ToF-AMS	3.2 / 0.6 / 4.6
GoAmazon (Shilling et al., 2018)	2014 Wet Season (02/22 – 03/23)	Amazon	GOAMA-W	HR-ToF-AMS	1.0 / 0.9 / 0.6
FRAPPE (Dingle et al., 2016)	2014 Summer (07/26 – 08/19)	Central US	-	C-ToF-mAMS	2.7 / 2.5 / 1.4
GoAmazon (Shilling et al., 2018)	2014 Dry Season (09/06 – 10/04)	Amazon	GOAMA-D	HR-ToF-AMS	4.6 / 4.6 / 1.8
KORUS-AQ (Nault et al., 2018)	2016 Spring and Summer (05/03 – 06/10)	South Korea	KORUS	HR-ToF-AMS	4.8 / 2.4 / 5.5
ATom (Wofsy et al., 2018)	2016 Summer (07/29 – 08/20)	Remote Ocean North America	ATOM1-W ATOM1-L	HR-ToF-AMS	0.1 / 0.1 / 0.2 0.5 / 0.2 / 0.8
ATom (Wofsy et al., 2018)	2017 Spring (01/26 – 02/21)	Remote Ocean North America	ATOM2-W ATOM2-L	HR-ToF-AMS	0.1 / 0.1 / 0.1 0.1 / 0.1 / 0.1
Aggregate					2.4 / 0.7 / 3.6

Table 3. Aircraft measurements of organic aerosol used in this analysis. The statistical metrics for OA provided above (Mean / Median / Standard Deviation) are based on filtered data for each campaign (as discussed in the text) and are in units of μg m^{-3}

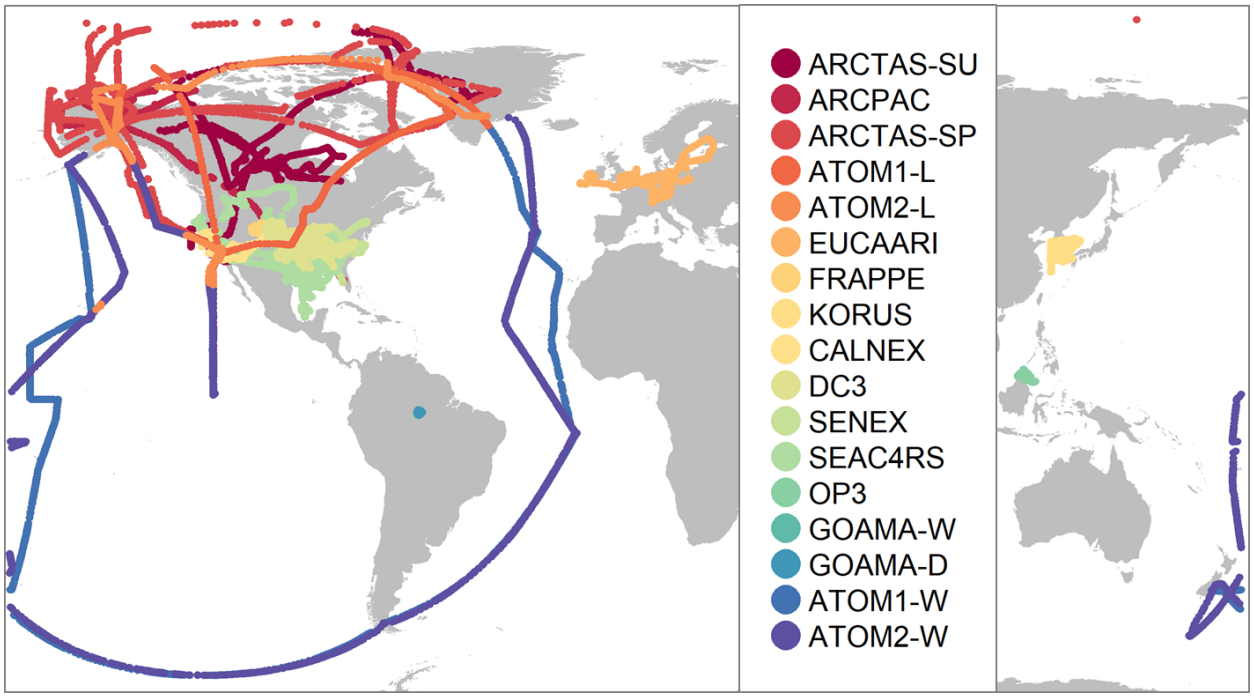

Figure 2. Location of flight tracks for the airborne field campaigns.

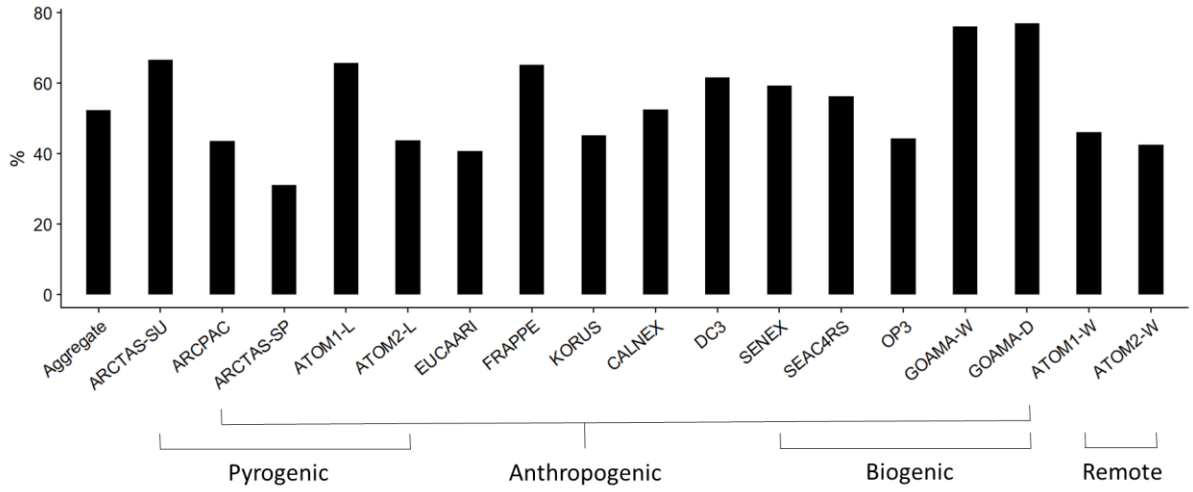

Figure 3. The percentage contribution of organic aerosol by mass to the total observed non-refractory mass concentrations measured by the AMS, organized by campaign. This includes aerosol mass from organic aerosol, sulfate, nitrate and ammonium. Campaigns are broadly organized based largely on model characterized source influence. However, as noted in the text, this characterization is often not indicative of the true sampling profile. For instance, the GoAmazon campaigns sampled heavily from fire and anthropogenic sources in addition to being strongly influenced by biogenic sources.

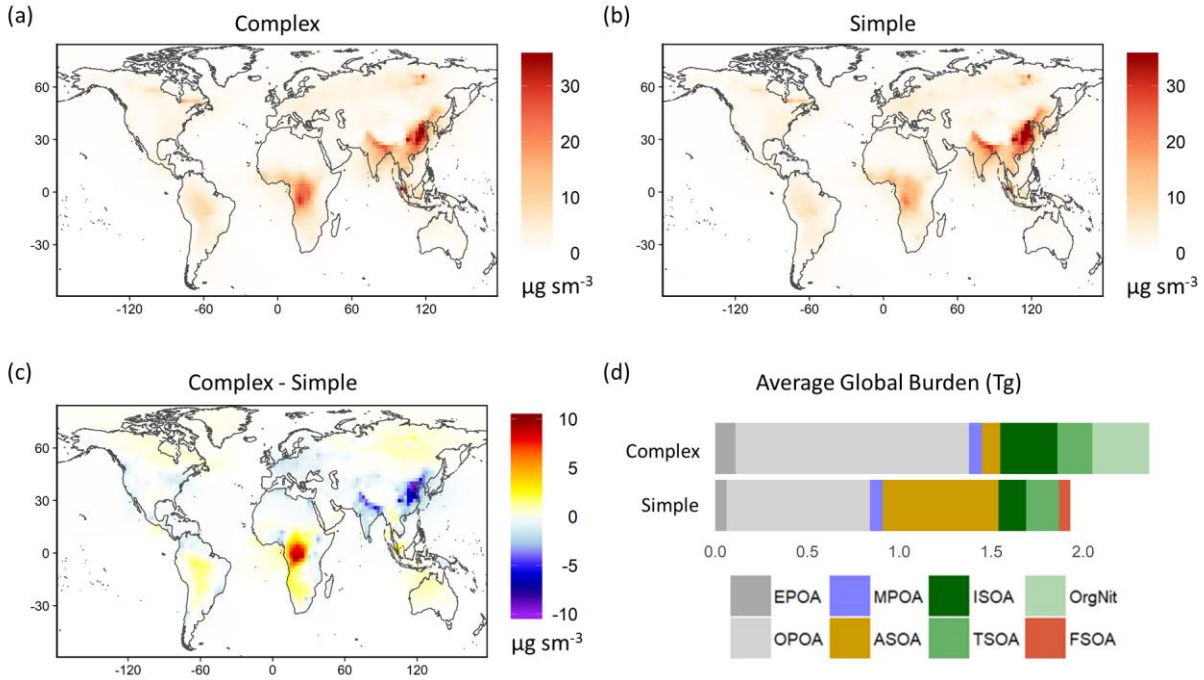

Figure 4. Global map of simulated OA surface concentrations in 2013 for the (a) complex and (b) simple schemes; Panel (c) illustrates the difference in OA surface loadings between the complex and simple schemes. Panel (d) displays the total global burden for the individual OA species from both schemes averaged over 2013. Refer to Sect. 3 for details on model sampling and averaging.

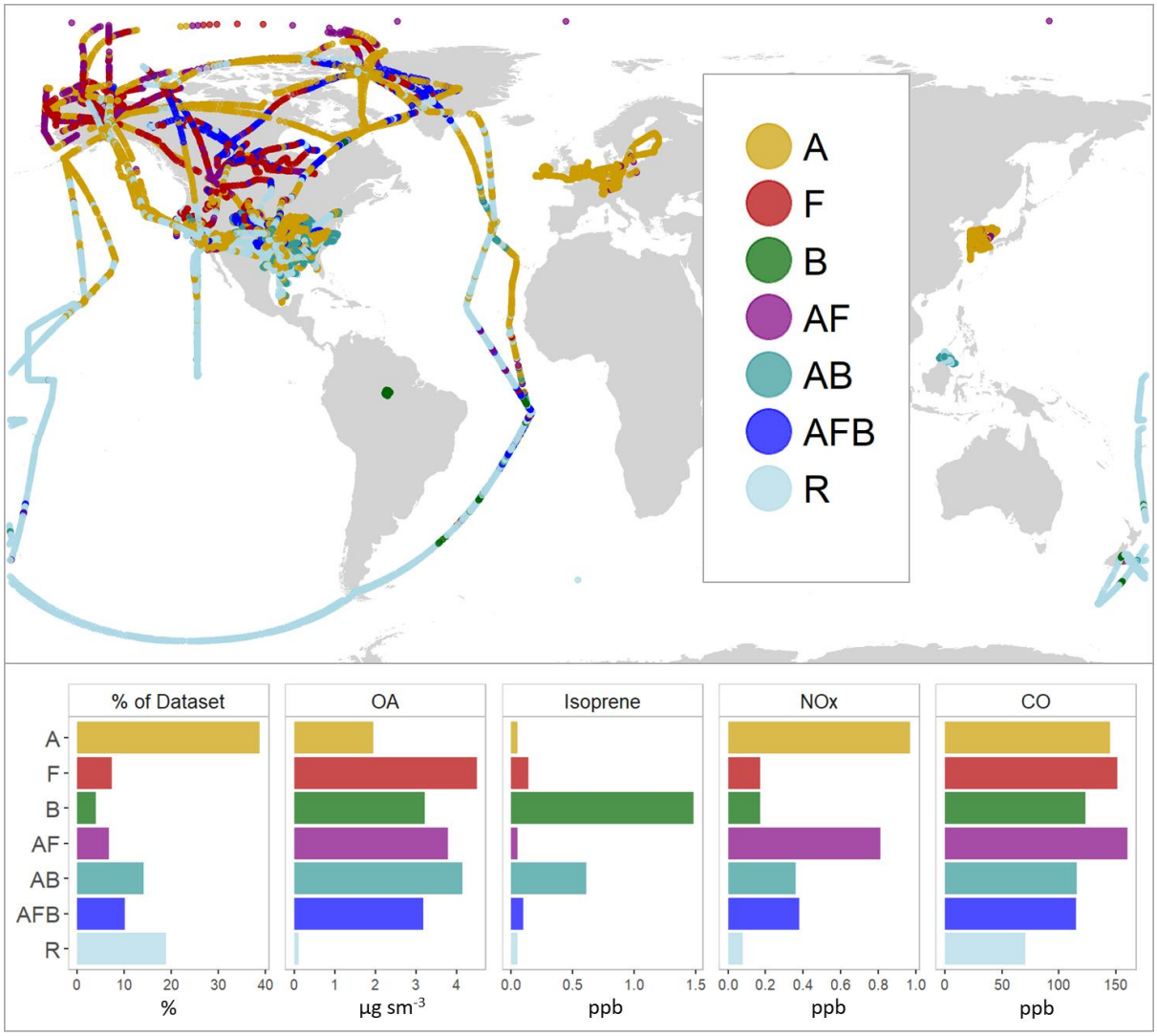

Figure 5. Flight tracks colored by regime type (top). The bar plots (bottom) compare observed mean values for various species across the different regimes. Mean values for OA are in units of µg sm^{-3}. Mean values of isoprene, nitrogen oxides and carbon monoxide are in units of parts per billion (ppb). The Regimes are as follows – Anthropogenic (A), Pyrogenic (F), Biogenic (B), Anthropogenic + Pyrogenic (AF), Anthropogenic + Biogenic (AB), Mixed (AFB) and Remote / Marine (R). Refer to Sect. 3 for details on model sampling and averaging.

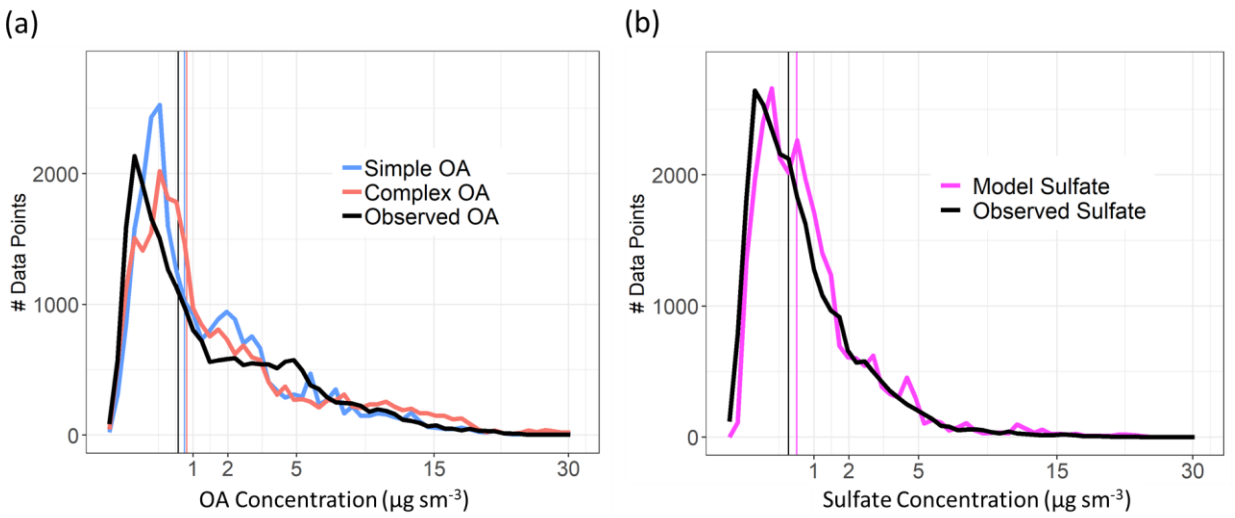

Figure 6. (a) Distribution plots of OA mass concentrations for the simple scheme (blue), complex scheme (red) and AMS observations (black). The x-axis has been transformed using a square-root function. Vertical lines represent median values for the different distributions. (b) Distribution plots of sulfate mass concentrations for the model (purple) and AMS observations (black). Refer to Sect. 3 for details on model sampling and averaging.

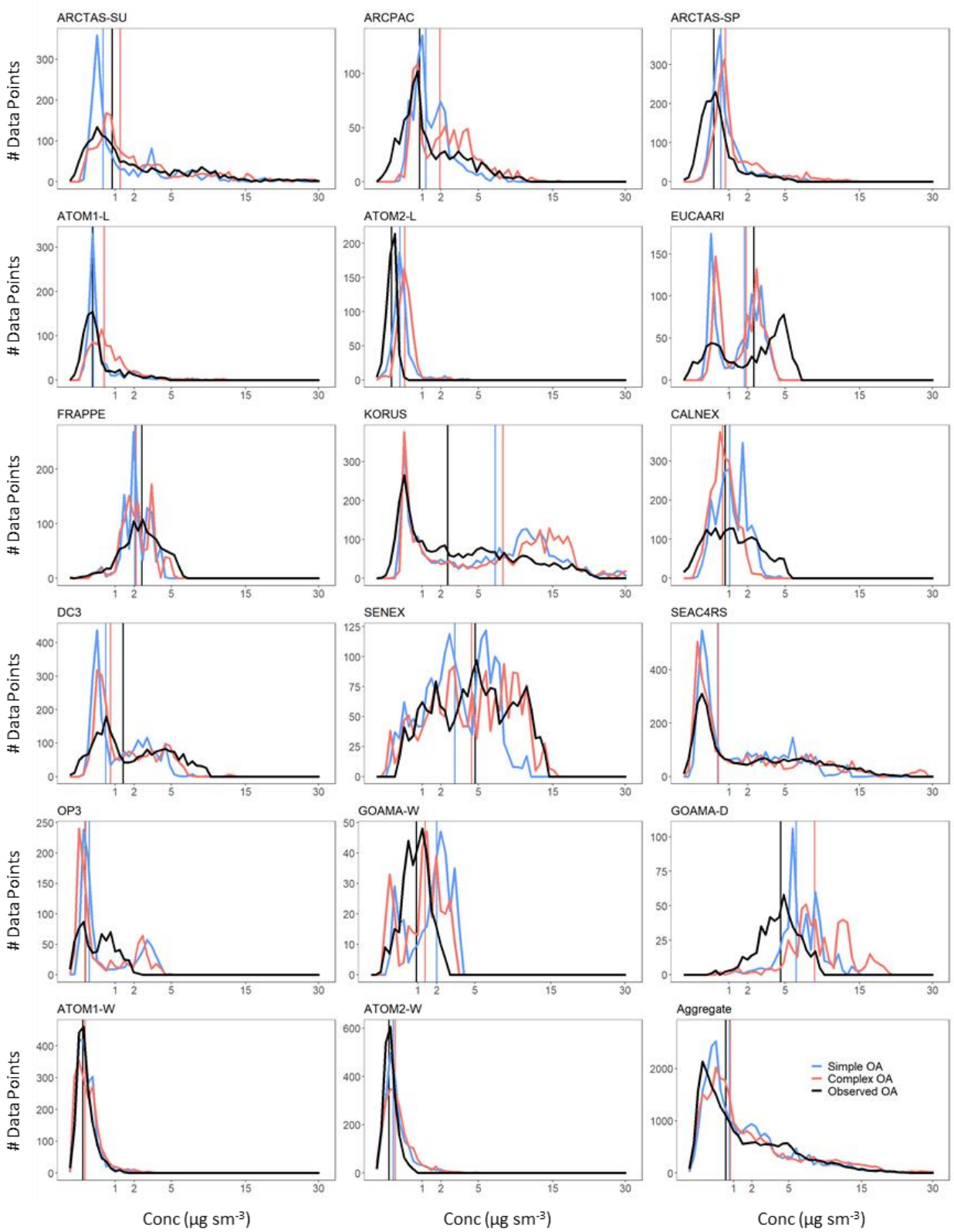

Figure 7. Superimposed distributions from the simple (blue) and complex (red) schemes with the observations in black for the different campaigns. Vertical lines represent median values for the different distributions.

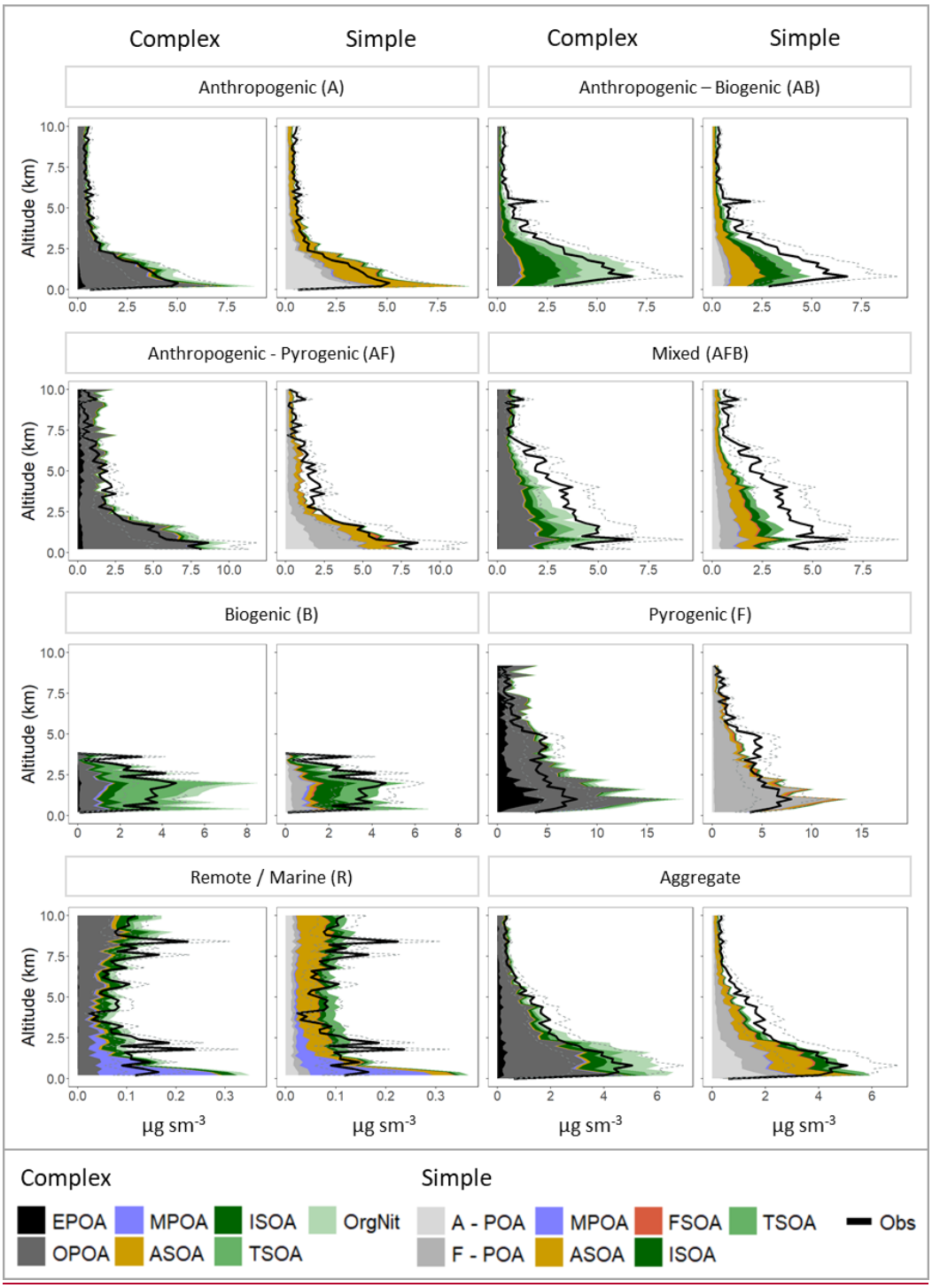

Figure 8~~7~~. Mean vertical profiles (in kilometers) comparing the observed (black) and simulated (colored) OA mass concentrations classified into the different regimes. The dashed lines represent the uncertainty in the observed OA mass loadings. The profiles are binned at 200m intervals. For the simple scheme, A-POA represents anthropogenic POA and F-POA represents pyrogenic POA. Refer to text for other OA categories and details on model sampling.

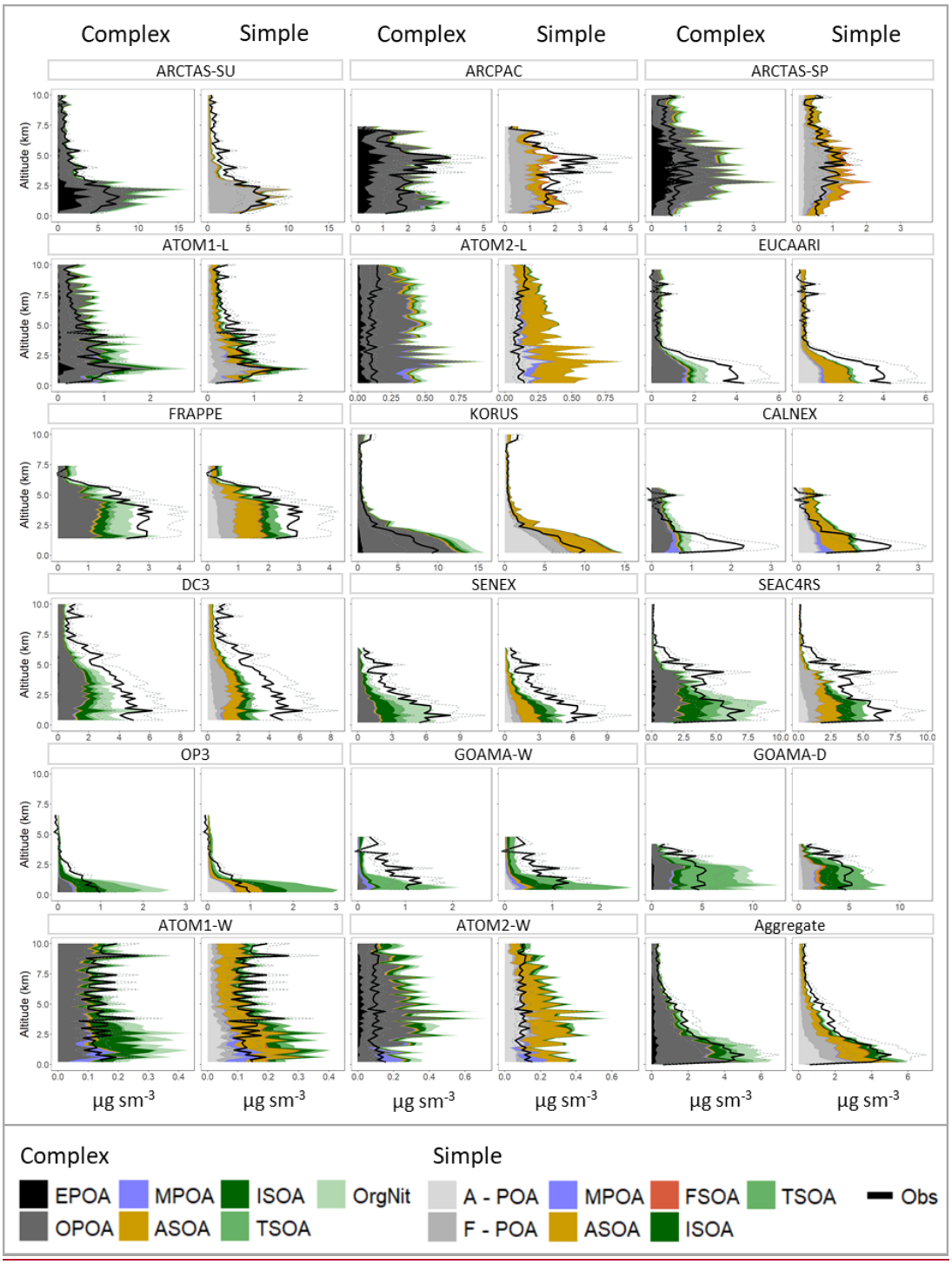

Figure 9~~8~~. Mean vertical profiles (in kilometers) comparing the observed (black) and simulated (colored) OA mass concentrations across the different campaigns. The dashed lines represent the uncertainty in the observed OA mass loadings. The profiles are binned at 200m intervals. For the simple scheme, A-POA represents anthropogenic POA and F-POA represents pyrogenic POA. Refer to text for other OA categories and details on model sampling.

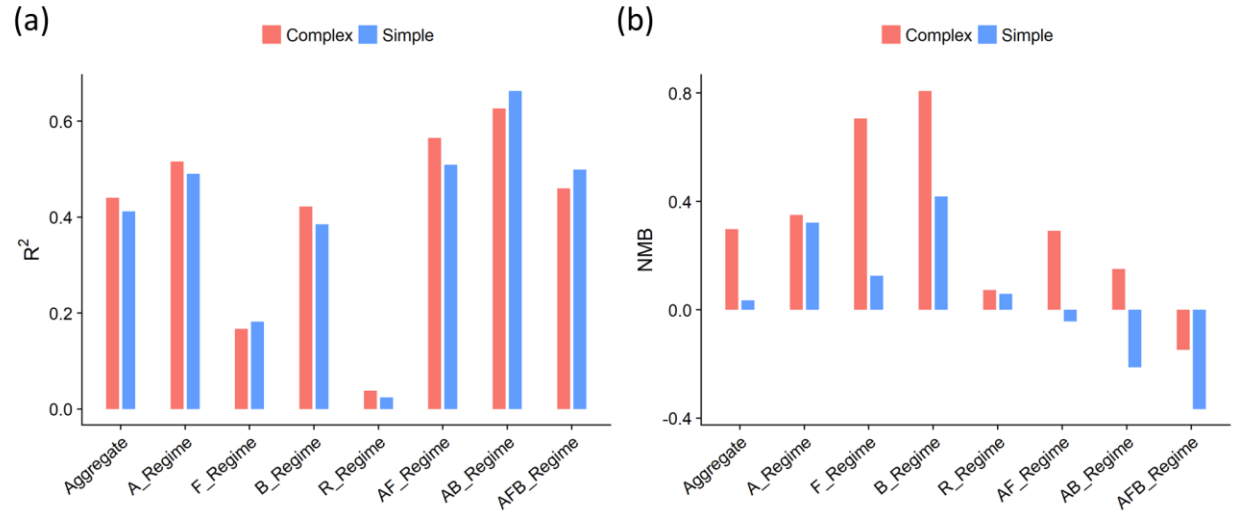

Figure 10.9 Statistical evaluation of the OA model skill for the complex (red) and simple (blue) scheme against observations shown as (a) the coefficients of determination (R^2) and (b) the normalized mean bias (NMB) across the segmented regimes. A positive normalized mean bias indicates that the model over predicts OA loadings.

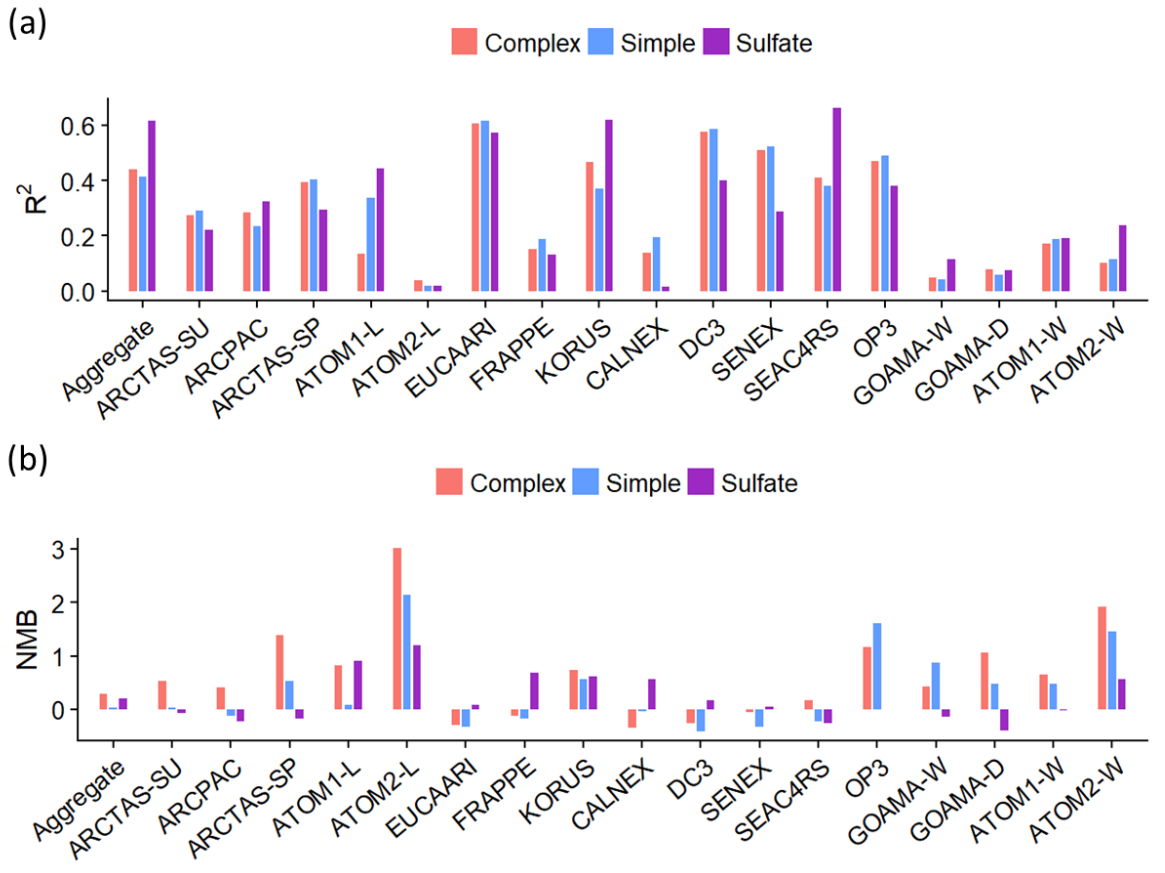

Figure 10. —Statistical evaluation of the model skill against observations shown as (a) the coefficients of determination (R^2) and (b) the normalized mean bias (NMB) across the individual field campaigns. The OA complex (red) and simple (blue) schemes are compared to the sulfate simulation (purple).

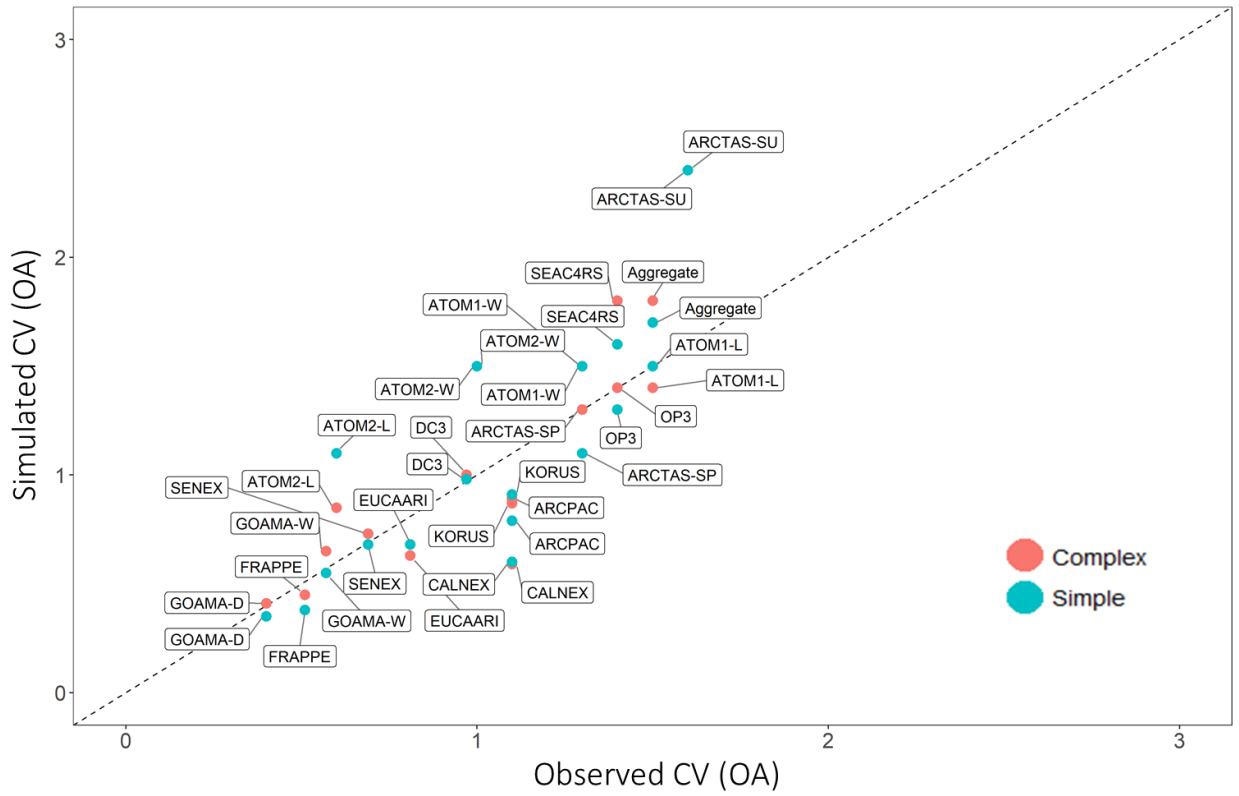

Figure 12.1 — A comparison of the simulated (GEOS-Chem) coefficient of variation (CV, the ratio of the standard deviation to the mean) for complex (red) and simple (blue) OA schemes against the observed CV for each airborne campaign. The one-to-one line is shown as a dashed black line.

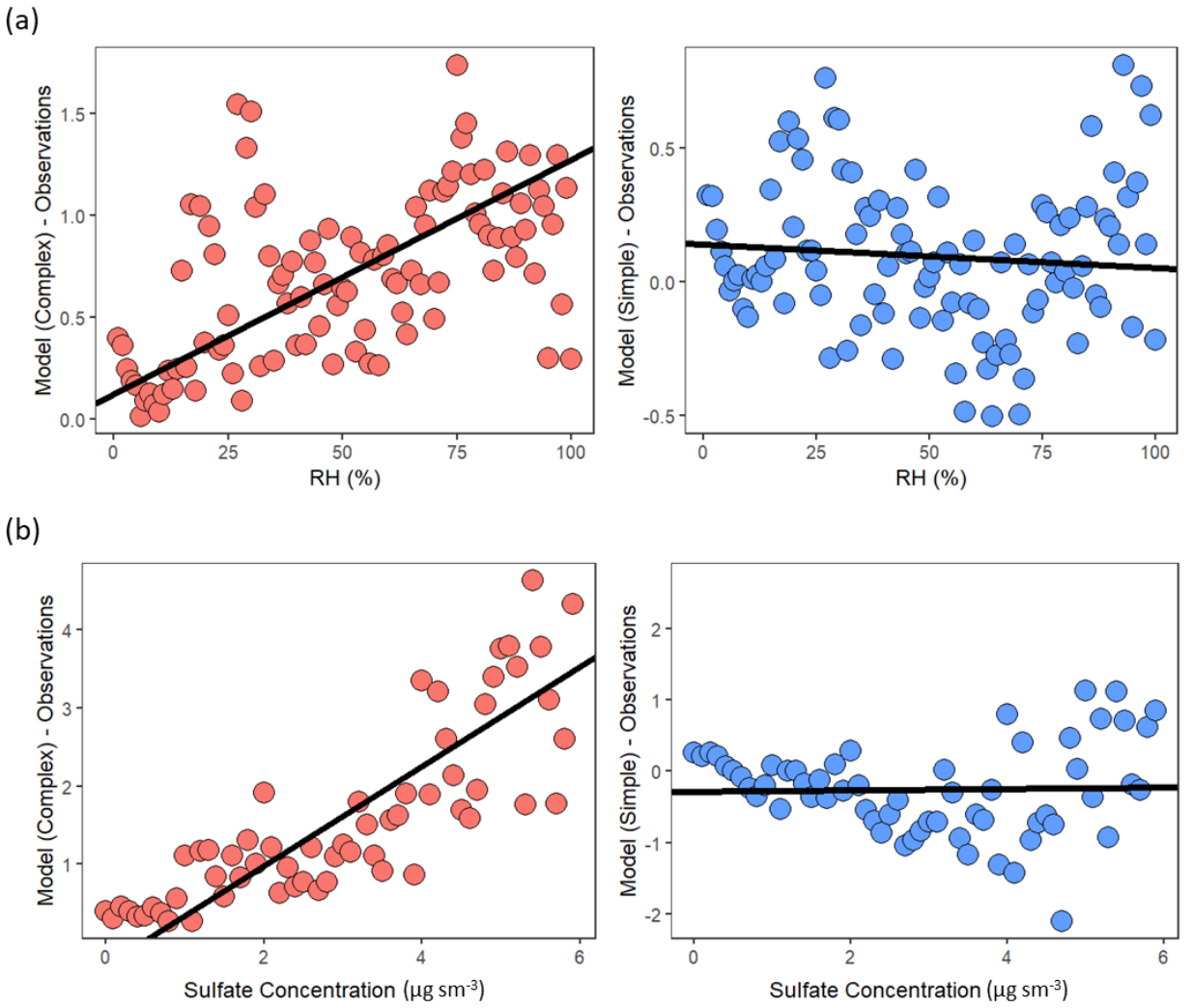

Figure 132. A comparison of model-observation OA bias and observed a) relative humidity and b) sulfate mass concentrations for the complex (red) and simple (blue) schemes across the aggregate dataset (observations are binned by intervals of 1% for RH and 0.1 µg sm^{-3} for sulfate). The best fit line is shown in black.

Supplementary Materials

An evaluation of global organic aerosol schemes using airborne observations

Sidhant J. Pai, Colette L. Heald, Jeffrey R. Pierce, Eloise A. Marais, Salvatore C. Farina, Jose L. Jimenez, Pedro Campuzano-Jost, Benjamin A. Nault, Ann M. Middlebrook, Hugh Coe, John E. Shilling, Roya Bahreini, Justin H. Dingle, Kennedy Vu

Simulation	Simulation Periods	Lumped Organic Aerosol Tracers	POA Treatment	SOA Treatment
Simple Scheme	2007/03/01 – 2008/08/01 2009/11/01 – 2010/07/01 2011/12/01 – 2012/07/01 2012/06/01 – 2014/01/01 2013/09/01 – 2014/02/01 2014/02/01 – 2014/11/01 2015/11/01 – 2016/09/01 2016/08/01 – 2017/03/01	• EPOA and OPOA (Non-volatile) • SOA • M-EPOA and M-OPOA	Non-volatile POA. 50% is emitted as fresh hydrophobic OA (EPOA) and 50% is emitted directly as aged hydrophilic OA (OPOA). EPOA is aged to OPOA in the atmosphere with a fixed lifetime of 1 day.	Non-volatile SOA. Emitted with the following emission factors: • 1.5% SOA precursor (SOAP) and 1.5% SOA from isoprene • 5% SOAP and 5% SOA from monoterpenes and sesquiterpenes, • 1.3% SOAP from CO emissions from fire sources • 6.9% of CO emissions from anthropogenic combustion sources. SOAP converts to SOA with a fixed lifetime of 1.15 days. The modified scheme individually simulates SOAP and SOA from each source. The default simple scheme lumps SOAP and SOA from all sources.
Modified Simple Scheme		• A-EPOA, A-OPOA and ASOA (Non-volatile anthropogenic OA) • F-EPOA, F-OPOA and FSOA (Non-volatile pyrogenic OA) • M-EPOA and M-OPOA (Non-volatile marine POA) • ISOA (Non-volatile isoprene SOA) • TSOA (Non-volatile terpene SOA)		
Pure VBS Scheme		• EPOA and OPOA • ASOA (VBS anthropogenic SOA) • ISOA (VBS isoprene SOA) • TSOA (VBS terpene SOA) • M-EPOA and M-OPOA (Non-volatile marine POA)	Semi-volatile. 49% is emitted as $EPOG_1$ with a saturation concentration (C*) of 1646 μg m^{-3} and 51% is emitted as $EPOG_2$ with C* of 20 μg m^{-3}. $EPOG_1$ and $EPOG_2$ reversibly partition to $EPOA_1$ and $EPOA_2$. $EPOG_1$ and $EPOG_2$ are aged in gas-phase via reaction with OH radical to $OPOG_1$ and $OPOG_2$ with C* of 16.46 μg m^{-3} and 0.2 μg m^{-3} respectively.	Gas-phase SOA precursors (aromatics, IVOCs, terpenes and isoprene) are oxidized with oxidants OH, O_3 to form alkyl peroxy (RO_2) radicals that react with either HO_2 or NO depending on the NOx regime. The resulting products are classified based on the origins of their precursors into Anthropogenic SOA (ASOA), Isoprene SOA (ISOA) and Terpene SOA (TSOA), that dynamically partition between the aerosol and gas phases based on their saturation vapor pressures and ambient aerosol concentrations. Aerosol formed from intermediate volatility organic compounds (IVOCs) is modelled using naphthalene as a proxy which, when oxidized, contributes to the ASOA lumped product.
Complex Scheme		• EPOA and OPOA (Semi-volatile) • ASOA (VBS anthropogenic SOA) • ISOA (Aqueous isoprene SOA) • TSOA (VBS terpene SOA) • OrgNit (Organic Nitrates) • M-EPOA and M-OPOA (Non-volatile marine POA)		The Complex scheme builds on VBS framework but replaces VBS isoprene SOA with isoprene-derived OA formed irreversibly from the aqueous phase reactive uptake of isoprene oxidation products. It also includes an explicit formation mechanism for organo-nitrates from isoprene and monoterpene oxidation pathways.

Table S1. A brief description of the various simulations presented in this study

S1. Model Sampling with the 'Planeflight Diagnostic'

Latitude, longitude and timestamp information was extracted from the aircraft campaign data and used in conjunction with the default GEOS-Chem 'Planeflight Diagnostic' to sample the appropriate model gridbox at the appropriate spatial and temporal spot. Model transport timestep was set for 10 minute intervals and chemistry timestep was set at 20 minutes. Diagnostic output from the planeflight sampling was averaged in cases where multiple observations were conducted within the span of a single model timestep within a certain gridbox.

S2. Organic Aerosol in the Complex Scheme

S2.1 Absorptive Partitioning

The complex scheme simulates both primary and secondary OA as semi-volatile using an absorptive partitioning model (Chung and Seinfeld, 2002; Pye et al., 2010), with each class of organic compound (i) associated with a saturation vapor pressure (C_i^*) that determines the fraction of the tracer in both gas and aerosol phase using the following relationship:

$$C_i^* = \frac{[G_i][M_o]}{[A_i]} \quad \text{(S1)}$$

$$[M_o] = \sum [A_i] \quad \text{(S2)}$$

Where [Gi] and [Ai] are the concentrations of the semi-volatile i in the gas and aerosol phase respectively and [Mo] is the concentration of the particle-phase absorptive material into which the semi-volatile i can partition. The saturation vapor pressure is temperature dependent and is dynamically calculated using the following equation:

$$\frac{C_i^*(T_2)}{C_i^*(T_1)} = \frac{T_2}{T_1} \exp\left(\frac{\Delta H_i}{R}\left(\frac{1}{T_2} - \frac{1}{T_1}\right)\right) \quad \text{(S3)}$$

An enthalpy of vaporization of 50 kJ mol^{-1} is assumed to estimate C* over a range of ambient temperatures.

S2.2 POA

49% of POA is emitted as $EPOG_1$ with a saturation concentration (C*) of 1646 µg m^{-3} and 51% is emitted as $EPOG_2$ with C* of 20 µg m^{-3}. $EPOG_1$ and $EPOG_2$ reversibly partition to $EPOA_1$ and $EPOA_2$. $EPOG_1$ and $EPOG_2$ are aged in gas-phase via reaction with the OH radical (k_{OH} of 2 x 10^{-11}) to $OPOG_1$ and $OPOG_2$ with C* of 16.46 µg m^{-3} and 0.2 µg m^{-3} and respectively (Grieshop et al., 2009; Pye et al., 2010)

S2.3 SOA from Aromatic VOCs and Terpenes (Pye et al., 2010)

Gas-phase anthropogenic and select biogenic VOCs are oxidized (with oxidants - OH, O_3) to form alkyl peroxy (RO_2) radicals that then react with either HO_2 or NO to form second-generation aerosol products depending on the NOx regime – with high and low NOx yields and partitioning coefficients based on experimental fits from laboratory studies (See Table 1 in Pye et al., 2010). These second-generation products are assigned volatilities with C* ranging from 0.1,1,10 and 100 ug m^{-3} and partition between aerosol and gas phase based on the equations listed above. This framework is referred to as the 'Volatility Basis Set' (VBS) and its implementation in the GEOS-Chem model is outlined in Pye et al. (2010). Aromatic VOCs are simulated using benzene, toluene and xylene, which are oxidized to form 4 lumped semi-volatile products. Terpenoids (monoterpenes and sesquiterpenes) are also oxidized to form 4 lumped products with C* of 0.1,1,10,100. A detailed overview of the second-generation yields can be found in Pye et al. (2010).

S2.4 SOA from IVOCs (Pye et al., 2010)

Intermediate Volatility Organic Compounds (IVOCs) such as alcohols and phenols have been shown to form SOA on oxidation (Chan et al., 2009; Pye et al., 2010). Phenol and substituted phenol compounds have been shown to be major contributors to IVOC emissions (Schauer et al., 2001) and exhibit similar behavior to naphthalene in terms of their aerosol yields. Thus, IVOCs are represented as a naphthalene-like surrogate (Pye et al., 2010) and assumed to form SOA in accordance with the parameters derived from the chamber studies of Chan et al. 2009. Global IVOC emissions are uncertain but are assumed to have the spatial distribution of naphthalene. For biofuel and biomass burning, naphthalene emissions are approximated using CO as a proxy, with an emission ratio of 0.0602 and 0.0701 mmol naphthalene / mol CO for biomass and biofuel burning respectively (Andreae and Merlet, 2001; Pye et al., 2010). Anthropogenic IVOC emissions are estimated from the CEDS Inventory and were scaled from benzene emissions using the same scale factors used by Pye et al. (2010).

S2.5 Explicit Mechanism for SOA from Isoprene (Marais et al., 2016)

Isoprene oxidation occurs through an explicit mechanism outlined in Marais et al. (2016). In this mechanism most of the isoprene undergoes oxidation via OH to form a peroxy radical which in turn reacts with HO_2, NO, other peroxy radicals (RO_2) or undergoes isomerization. The HO_2 reaction pathway leads to the formation of hydroxyhydroperoxides (ISOPOOH) that are oxidized by OH to isoprene epoxydiol (IEPOX) and several low-volatility products, that are represented in the model as the C5-LVOC lumped product. The high-NOx (NO) pathway results in C_5 hydroxy carbonyls, methyl vinyl ketone, methacrolein, and first-generation isoprene nitrates (ISOPN). The first three products react with OH to produce glyoxal (GLYX) and methylglyoxal (MGLY). ISOPN is oxidized with OH to form dihydroxy dinitrates (DHDN) and IEPOX. Reaction of the peroxy radical with RO_2 is a minor pathway that ultimately leads to the formation of C_4 hydroxyepoxides (MEPOX) as well as GLYX and MGLY. Isomerization is a similarly minor pathway that leads to the formation of a hydroperoxyaldehyde that forms GLYX and MGLY when photolyzed. IEPOX also forms GLYX and MGLY on oxidation with OH.

In addition to the processes above, isoprene also undergoes ozonolysis and reaction with NO_3, forming MGLY and second generation hydroxy-nitrates (NT-ISOPN). IEPOX, GLYX, MGLY, C5-LVOC, MEPOX, ISOPN, DHDN, NT-ISOPN form non-volatile aerosols through an irreversible aqueous reactive uptake parametrization. A more detailed overview of the relevant mechanism, yields, reaction rates, branching ratios and uptake coefficients can be found in Marais et al. (2016).

S2.6 Explicit Mechanism for Organo-nitrates from Terpenes (Fisher et al., 2016)

Terpene species also form aerosol-phase organo-nitrates through an explicit mechanism defined in Fisher et al. (2016). During the day, terpene precursors react with OH to form peroxy radicals which then react with NO to form first generation monoterpene nitrates with a yield of 18%. These are then further oxidized to form second-generation monoterpene nitrates. At night, these terpenes react with NO_3 to form nitrooxy peroxy radicals that either decompose or form a more stable organo-nitrate with a predefined branching ratio based on the precursor. Formation of non-volatile aerosol from gas-phase organo-nitrate is modelled using an irreversible reactive uptake parameterization,

followed by particle-phase hydrolysis. A more detailed overview of the relevant mechanism, yields, reaction rates, branching ratios and uptake coefficients can be found in Fisher et al. (2016).

S3. OA Loss Processes: Dry and Wet Deposition

Organic Aerosol is deposited from the atmosphere through both wet deposition and dry deposition. Dry deposition is estimated using a parametrization described in Zhang et al. (2001) that calculates particle deposition velocities as a function of particle size, density and relevant meteorology and accounts for turbulent transfer, Brownian diffusion, impaction, interception, gravitational settling and particle rebound. Particle diameter and density is assumed to be 0.5 μm and 1500 kg m^{-3} respectively. Deposition velocities are calculated using the following relationship:

$$V_d = V_g + \frac{1}{(R_a + R_s)} \quad \text{(S4)}$$

where V_g is the gravitational settling velocity, R_a is the aerodynamic resistance above the canopy and R_s is the surface resistance. A more detailed derivation of the individual terms can be found in Section 2 of Zhang et al. (2001).

Wet deposition occurs through two processes – 'Rainout' defined by in-cloud scavenging and 'Washout' defined by below-cloud scavenging. Rainout scavenges aerosols efficiently and is sensitive to the fraction of the grid-box that experiences precipitation. This fraction is calculated online using the grid-scale precipitation formation rate (Q_k), cloud condensed water content (L), the duration of the model timestep, the duration of precipitation over the time step (T_c) and rate constant for conversion of cloud water to precipitation (C_1). See Liu et al. (2001) for more details. Below-cloud scavenging is calculated using a washout rate applied to the precipitation fraction described above. The model also simulates the release of aerosol during the re-evaporation of precipitation as it falls to the ground. Scavenging of aerosols is also modelled from cloud updrafts in moist convection and the fraction of aerosol tracer scavenged by the convective precipitation in the updraft is defined by the following relationship:

$$Conv_{frac} = 1 - e^{-\alpha \Delta z} \quad \text{(S5)}$$

where Δz is the thickness of the convective column and α is the scavenging efficiency.

The fraction of gas-phase OA precursors wet deposited is dictated by the liquid to gas ratio for a grid-box at any given timestep. For a soluble gas 'i', this ratio is calculated based on the following relationship:

$$\frac{C_{i,L}}{C_{i,G}} = K_i^* * L * R * T \quad \text{(S6)}$$

where K_i^* is the effective Henry's law constant that is calculated using the van't Hoff equation (Jacob et al., 2000), L is the cloud liquid water content, R is the ideal gas constant and T is the local temperature. Each organic gas-phase species has an associated Henry's law solubility constant (in M atm^{-1}), volatility constant (in K) and pH correction factor which is defined in the GEOS-Chem species database. A detailed overview of the wet deposition scheme can be found in Jacob et al. (2000), Liu et al. (2001) and Amos et al. (2012).

S4. Nomenclature: Oxygenated Primary Organic Aerosol (OPOA) vs Secondary Organic Aerosol (SOA)

The OPOA product is formed by the oxidation of EPOA. In the simple scheme, this process is approximated by a fixed lifetime of 1 day with no direct dependence on oxidant concentrations. In the complex scheme, EPOA is oxidized with OH to form oxygenated primary organic vapors. Many previous studies in the literature have represented the aerosol formed from these vapors as Oxygenated POA (Donahue et al., 2009; Pye et al., 2010; Shrivastava et al., 2008) but the nomenclature has been the topic of some contention, with other studies preferring to use the terminology of Secondary Organic Aerosol (SOA) to represent this aerosol product (Hayes et al., 2015; Murphy et al., 2014). For the purpose of this study we have chosen to refer to aerosol resulting from the oxidation of primary organic matter that is already semi-volatile as OPOA and reserve the term SOA exclusively for aerosol formed from the oxidation of volatile organic vapors. We are further motivated to maintain these labels given that this is how they are described in the GEOS-Chem model and the relevant model paper (Pye et al., 2010). We have separated the OPOA contribution and discussion whenever possible in this study to allow the reader to interpret the results as desired.

Campaign	Organic Aerosol	NO_x	Isoprene	CO
ARCPAC	**C-ToF-AMS** (A.M. Middlebrook)	**NOAA NO_yO_3** (T.B. Ryerson)	**PTR-MS** (J.A. de Gouw, C. Warneke)	**VUV Resonance Fluorescence** (J.S. Holloway)
ARCTAS	**HR-ToF-AMS** (J.L. Jimenez)	**NCAR 4 channel Chemiluminescence** (A.J. Weinheimer, F.M. Flocke, D.J. Knapp, D.D. Montzka, I.B. Pollack)	**TOGA** (E. Apel, R. Hornbrook)	**DACOM** (G.S. Diskin, G. Sachse)
EUCAARI	**C-ToF-AMS** (H. Coe)			
OP3	**C-ToF-AMS** (H. Coe)			
CalNex	**C-ToF-AMS** (A.M. Middlebrook)	**NOAA NO_yO_3** (T.B. Ryerson, I.B. Pollack)	**PTR-MS** (J.A. de Gouw, C. Warneke)	**VUV Resonance Fluorescence** (J.S. Holloway)
DC3	**HR-ToF-AMS** (J.L. Jimenez)	**NOAA NO_yO_3** (T.B. Ryerson, I.B. Pollack)	**PTR-MS** (T. Mikoviny, A. Wisthaler)	**DACOM** (G.S. Diskin, G Sachse)
SENEX	**C-ToF-AMS** (A.M. Middlebrook)	**NOAA NO_yO_3** (T.B. Ryerson, I.B. Pollack)	**PTR-MS** (M. Graus)	**VUV Resonance Fluorescence** (J.S. Holloway)
SEAC4RS	**HR-ToF-AMS** (J.L. Jimenez)	**NOAA NO_yO_3** (T.B. Ryerson, I.B. Pollack, J. Peischl)	**WAS** (D.R. Blake)	**DACOM** (G.S. Diskin, G. Sachse)
GoAmazon	**HR-ToF-AMS** (J.E. Shilling)		**PTR-MS** (J.E. Shilling)	**Los Gatos ICOS Analyzer** (S.R. Springston)
FRAPPE	**C-ToF-mAMS** (R. Bahreini)	**NCAR 2-channel Chemiluminescence** (A.J. Weinheimer, D.D. Montzka)	**TOGA** (E. Apel, R. Hornbrook)	**Aero-Laser VUV Fluorescence** (T.L. Campos and F.M. Flocke)
KORUS-AQ	**HR-AMS** (J.L. Jimenez, P. Campuzano-Jost)	**NCAR 4-channel Chemiluminescence** (A.J. Weinheimer, D.D. Montzka)	**PTR-MS** (P. Eichler, L. Kaser, T. Mikoviny, M. Müller, A. Wisthaler)	**DACOM** (G.S. Diskin, S.E. Pusede)
ATom	**HR-ToF-AMS** (J.L. Jimenez)	**NOAA NO_yO_3** (T.B. Ryerson, J. Peischl, C. Thompson)	**TOGA** (E. Apel, R. Hornbrook)	**QCLS** (B.C. Daube, S.C. Wofsy, R. Commane, E. Kort)

Table S2~~1~~. An overview of the instrumentation and associated primary investigators for the organic aerosol and trace gas observations used in this analysis.

Nitrogen oxides were measured using photolysis rates and NO/O_3 chemiluminescence techniques (Ryerson et al., 2000), carbon monoxide levels were measured using a Differential Absorption Carbon monOxide Measurement (DACOM) instrument (Sachse et al., 1987) or a VUV resonance fluorescence approach (Gerbig et al., 1999), isoprene concentrations were observed using a Proton Transfer Reaction Mass Spectrometer (de Gouw and Warneke, 2007), a Trace Organic Gas Analyzer (Apel et al., 2010) or a whole air sampling approach (Colman et al., 2001) and sulfate aerosol loadings were measured using an AMS.

Regime	Description	Percentage of Dataset	Mean OA	Median OA	Std. Dev. OA	Mean Isoprene	Mean NO_x	Mean CO
A	Dominant anthropogenic Influence	39.1%	1.9	0.6	3.2	0.05	0.96	144
F	Dominant pyrogenic Influence	7.3%	4.5	2.7	5.3	0.13	0.17	151
B	Dominant biogenic Influence	3.6%	3.1	2.6	2.6	1.46	0.16	122
AF	Anthropogenic and Pyrogenic Influence	6.8%	3.8	1.6	5.0	0.05	0.80	160
AB	Anthropogenic and Biogenic Influence	14.0%	4.1	2.7	4.0	0.60	0.35	115
AFB	No dominant influence from any one source category.	10.1%	3.2	2.5	2.9	0.10	0.38	115
R	Remote / Clean (concentrations under 0.2 µg / sm^3)	19.1%	0.1	0.1	0.3	0.05	0.08	71
Aggregate			2.4	0.7	3.6	0.24	0.55	126

Table S3~~2~~. An overview of the different regimes. Statistics (mean, median, standard deviation) are listed for the observational data categorized into the individual regimes. OA data is in units of µg sm^{-3}. Mean observations for isoprene, nitrogen oxides and carbon monoxide are in units of parts per billion (ppb).

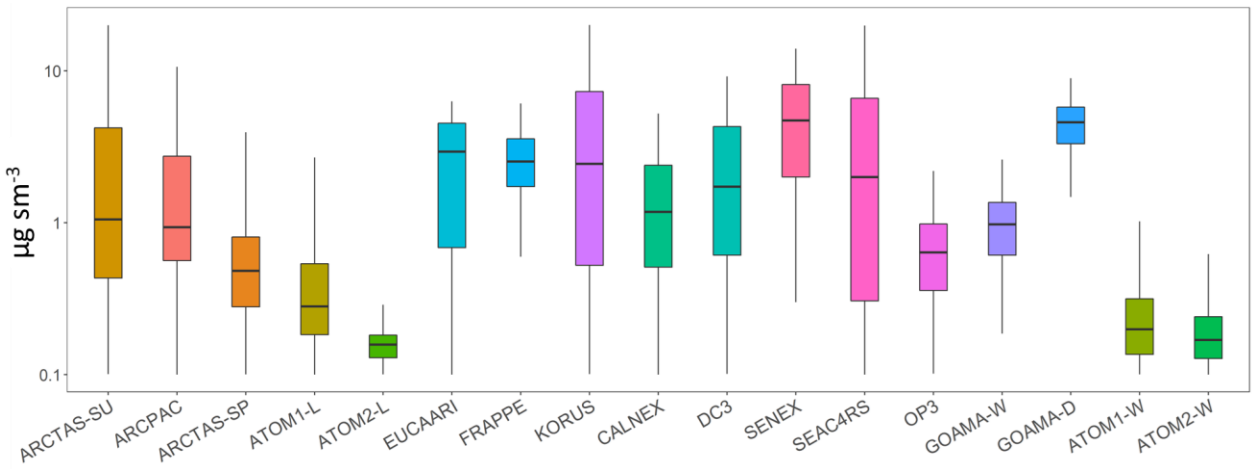

Figure S1. Distribution in the observed organic aerosol concentrations for each campaign. The boxes denote the 25th and 75th percentile of the distribution, while the whiskers denote the 5th and 95th percentile. Observations represented here have been filtered and averaged to the model timestep. Refer to Section 3 for more details.

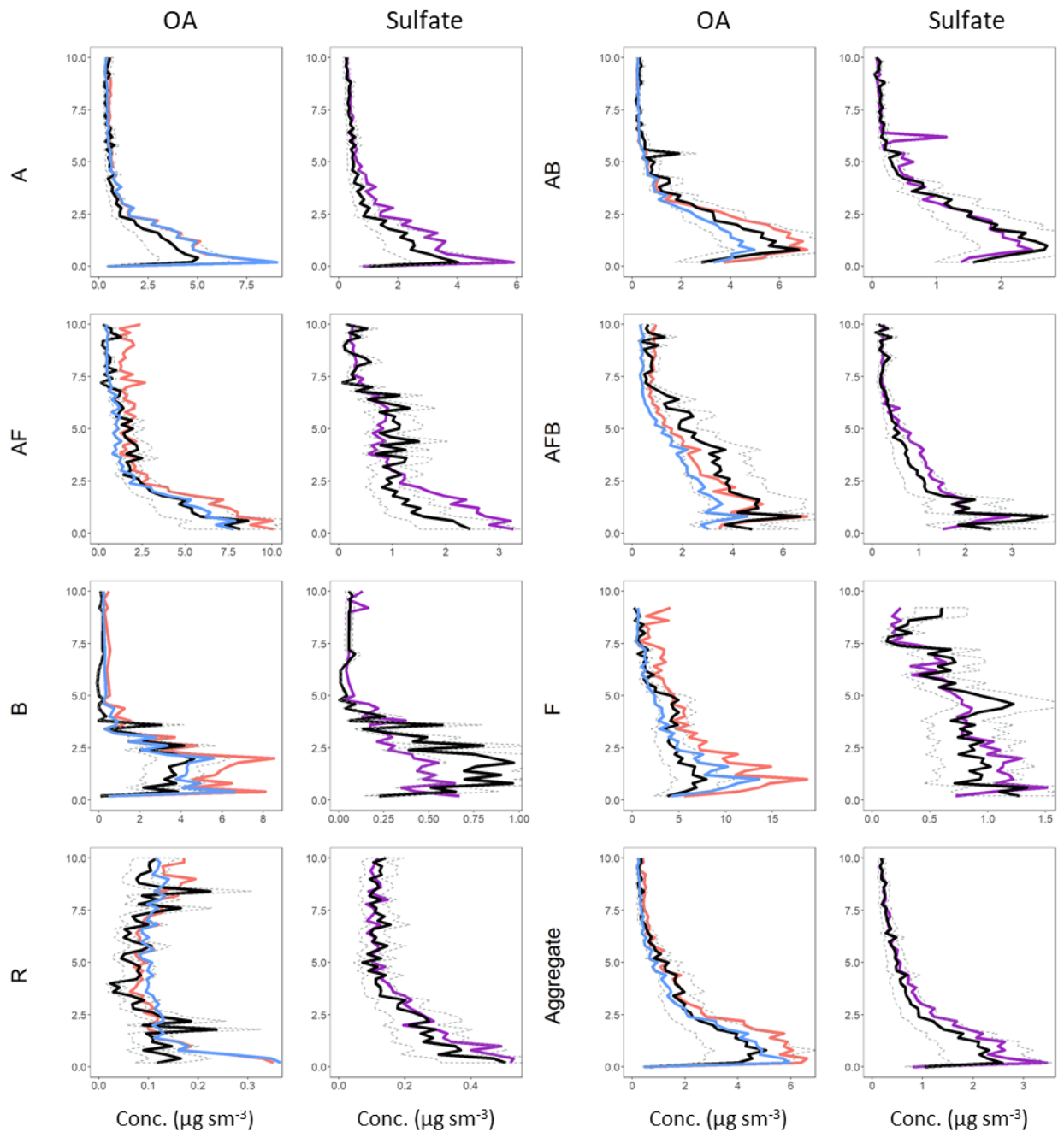

Figure S2. Mean vertical profiles (in km) for the observed and simulated OA and sulfate across the different regimes. The profiles are binned at 200m intervals. Observations are in black. For the OA, the complex scheme is in red while the simple scheme is in blue. Model sulfate is in purple.

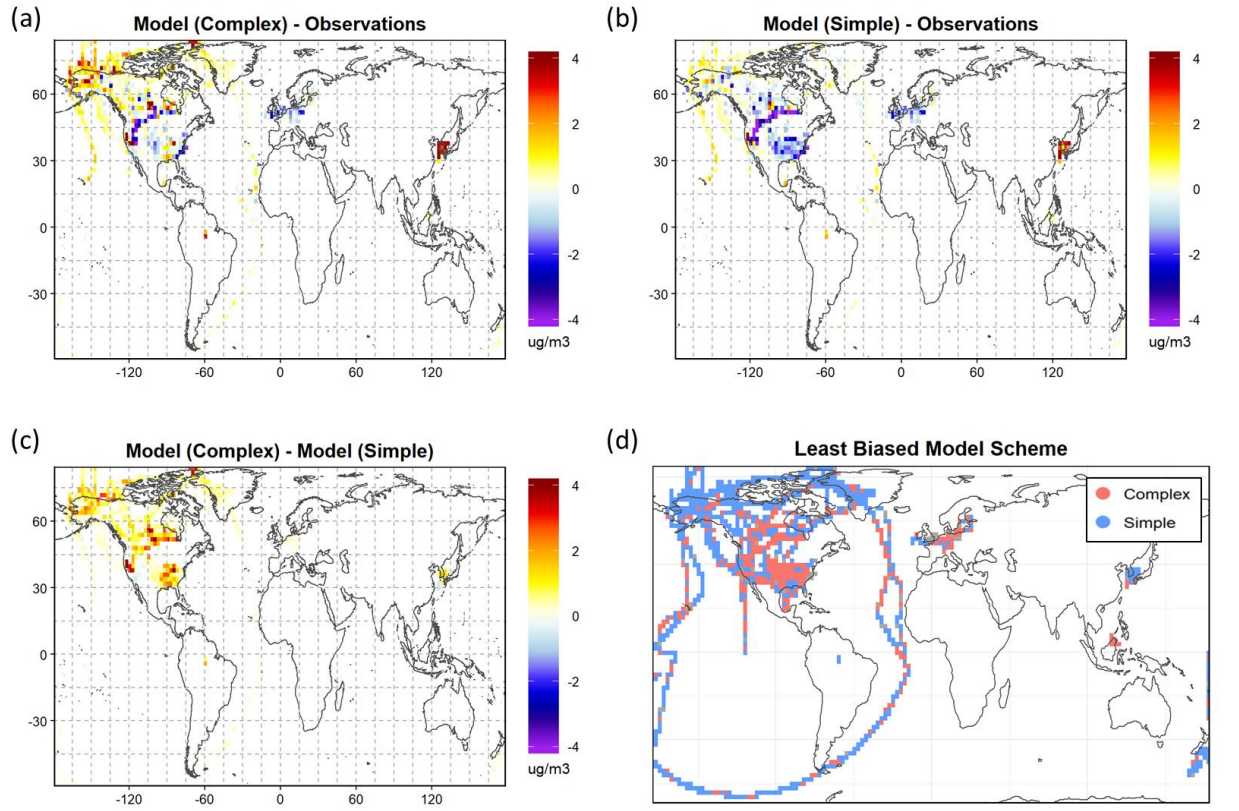

Figure S3. A comparison of the simulated OA loadings averaged by grid-box over the vertical dimension. Panel (d) provides an overview of the column-averaged 'best fit' scheme based on the ability to minimize the mean bias.

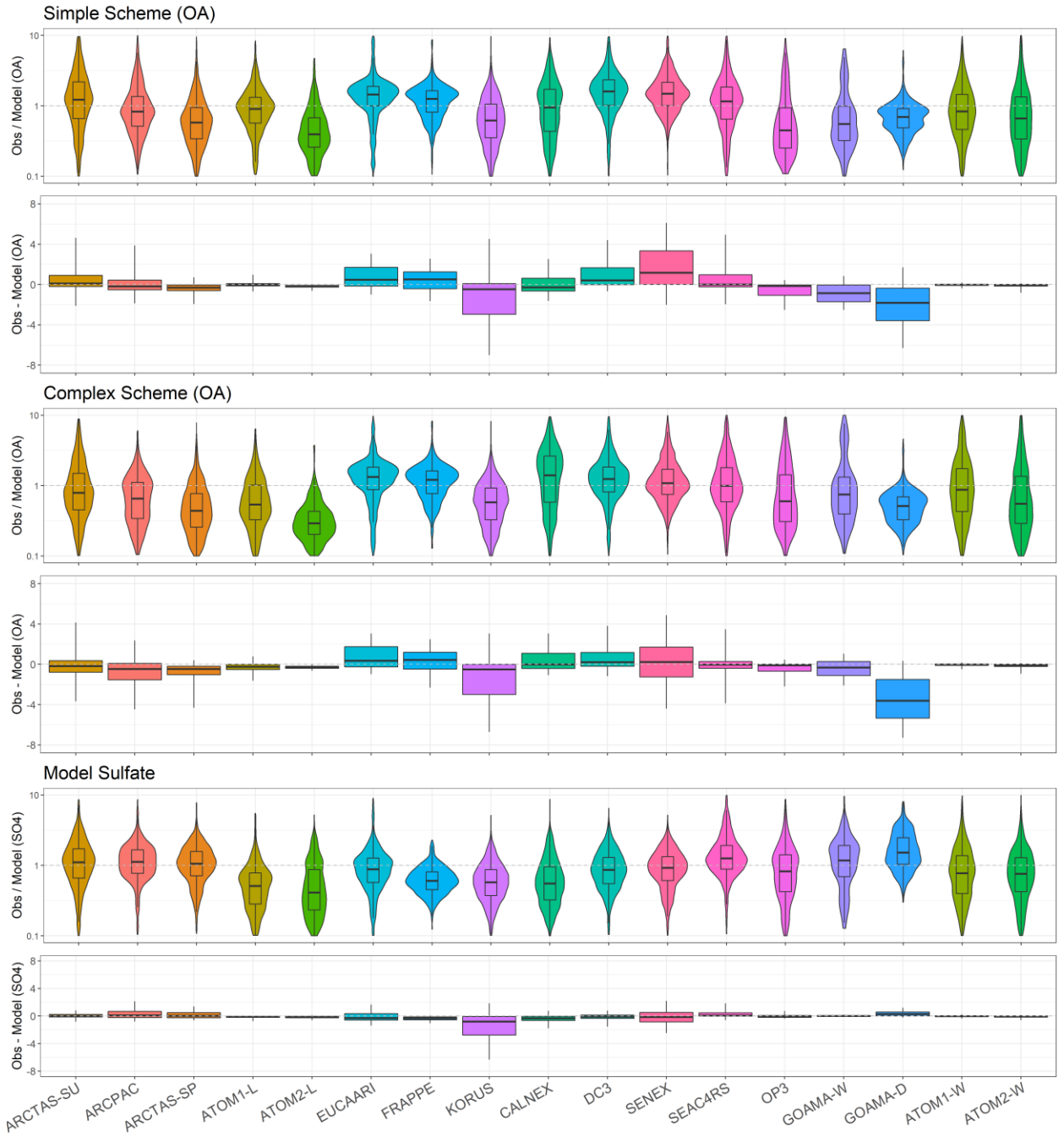

Figure S4. Distribution in the ratio and bias between the observed and modelled organic aerosol concentrations for each model scheme across the 17 campaigns. The boxes denote the 25th and 75th percentile of the distribution, while the whiskers denote the 5th and 95th percentile. The ratio plots have been overlaid with violin plots describing the entire distribution.

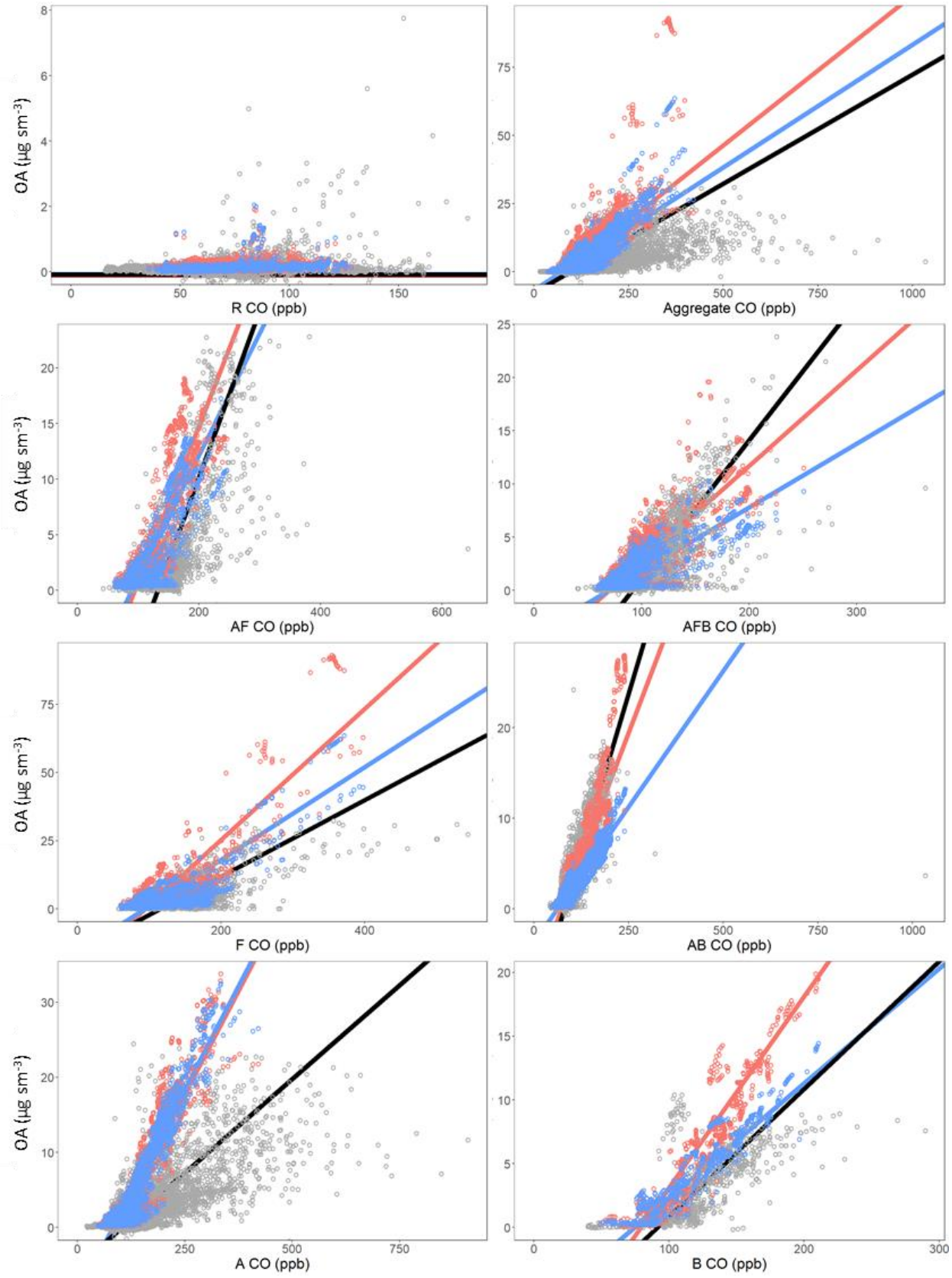

Figure S5. Comparison of complex (red), simple (blue) and observed (grey) organic aerosol to carbon monoxide.

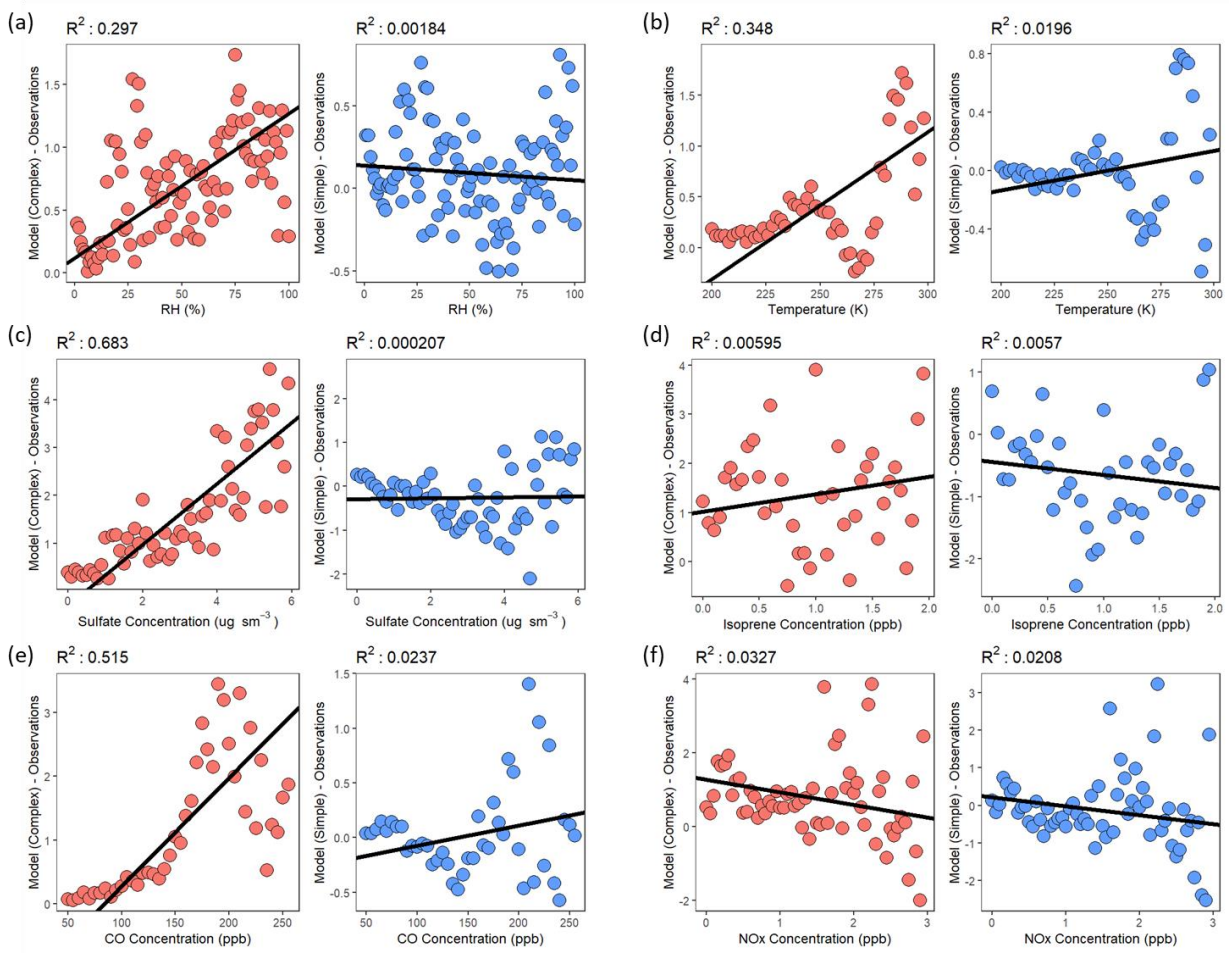

Figure S6. A comparison of model-observation OA bias and binned observations for a) relative humidity, b) Temperature, c) Sulfate, d) Isoprene, e) CO and f) NO_x for the complex (red) and simple (blue) schemes across the aggregate dataset. The best fit line is shown in black.

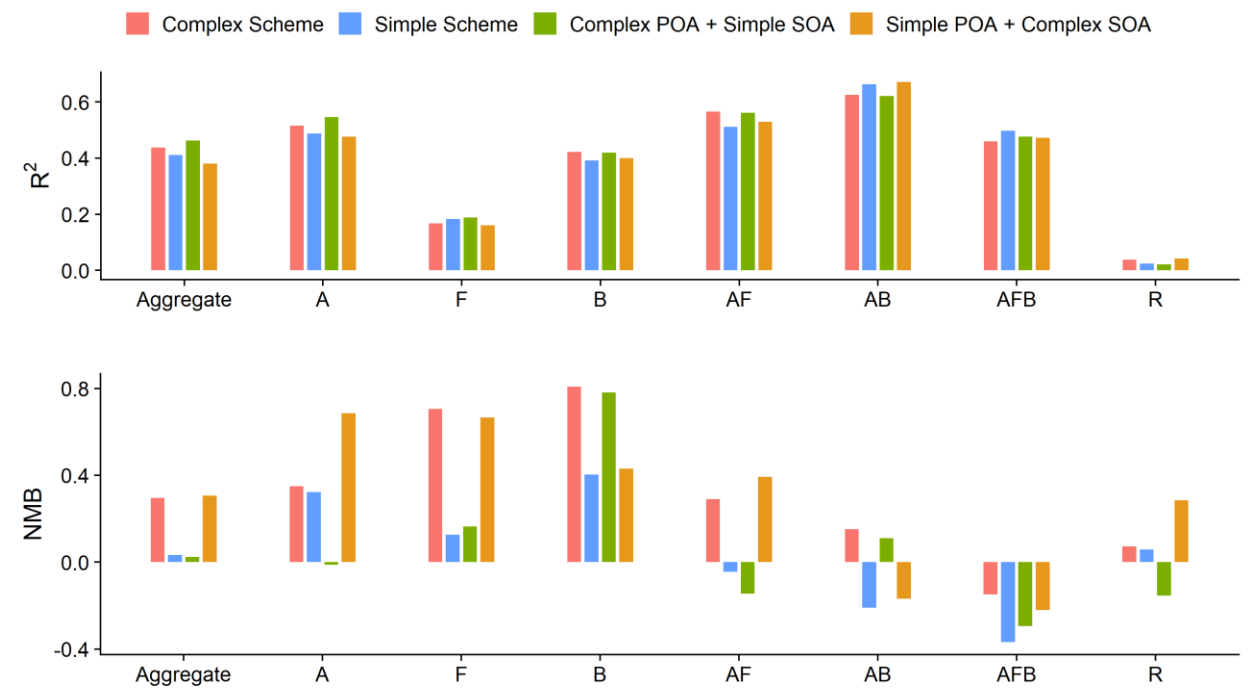

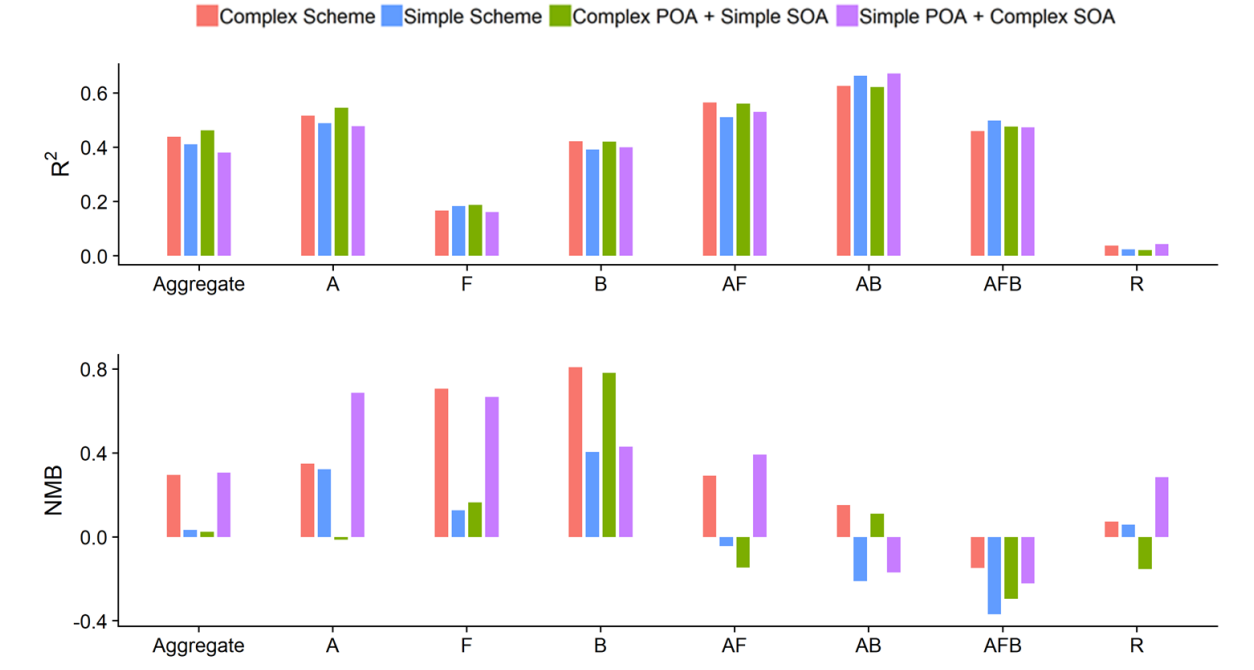

Figure S7. A statistical evaluation of the OA model skill for the complex and simple schemes against a modified treatment that interchanges the POA and SOA from both schemes.

References

Amos, H. M., Jacob, D. J., Holmes, C. D., Fisher, J. A., Wang, Q., Yantosca, R. M., Corbitt, E. S., Galarneau, E., Rutter, A. P., Gustin, M. S., Steffen, A., Schauer, J. J., Graydon, J. A., Louis, V. L. St., Talbot, R. W., Edgerton, E. S., Zhang, Y. and Sunderland, E. M.: Gas-particle partitioning of atmospheric Hg(II) and its effect on global mercury deposition, Atmospheric Chem. Phys., 12, 591–603, doi:10.5194/acp-12-591-2012, 2012.

Andreae, M. O. and Merlet, P.: Emission of trace gases and aerosols from biomass burning, Glob. Biogeochem. Cycles, 15(4), 955–966, doi:10.1029/2000GB001382, 2001.

Apel, E. C., Emmons, L. K., Karl, T., Flocke, F., Hills, A. J., Madronich, S., Lee-Taylor, J., Fried, A., Weibring, P., Walega, J., Richter, D., Tie, X., Mauldin, L., Campos, T., Weinheimer, A., Knapp, D., Sive, B., Kleinman, L., Springston, S., Zaveri, R., Ortega, J., Voss, P., Blake, D., Baker, A., Warneke, C., Welsh-Bon, D., de Gouw, J., Zheng, J., Zhang, R., Rudolph, J., Junkermann, W. and Riemer, D. D.: Chemical evolution of volatile organic compounds in the outflow of the Mexico City Metropolitan area, Atmospheric Chem. Phys., 10, 2353–2375, doi:https://doi.org/10.5194/acp-10-2353-2010, 2010.

Chan, A. W. H., Kautzman, K. E., Chhabra, P. S., Surratt, J. D., Chan, M. N., Crounse, J. D., Kürten, A., Wennberg, P. O., Flagan, R. C. and Seinfeld, J. H.: Secondary organic aerosol formation from photooxidation of naphthalene and alkylnaphthalenes: implications for oxidation of intermediate volatility organic compounds (IVOCs), Atmospheric Chem. Phys., 9(9), 3049–3060, doi:https://doi.org/10.5194/acp-9-3049-2009, 2009.

Chung, S. H. and Seinfeld, J. H.: Global distribution and climate forcing of carbonaceous aerosols, J. Geophys. Res., 107(D19), doi:10.1029/2001JD001397, 2002.

Colman, J. J., Swanson, A. L., Meinardi, S., Sive, B. C., Blake, D. R. and Rowland, F. S.: Description of the Analysis of a Wide Range of Volatile Organic Compounds in Whole Air Samples Collected during PEM-Tropics A and B, Anal. Chem., 73(15), 3723–3731, doi:10.1021/ac010027g, 2001.

Donahue, N. M., Robinson, A. L. and Pandis, S. N.: Atmospheric organic particulate matter: From smoke to secondary organic aerosol, Atmos. Environ., 43(1), 94–106, doi:10.1016/j.atmosenv.2008.09.055, 2009.

Fisher, J. A., Jacob, D. J., Travis, K. R., Kim, P. S., Marais, E. A., Chan Miller, C., Yu, K., Zhu, L., Yantosca, R. M., Sulprizio, M. P., Mao, J., Wennberg, P. O., Crounse, J. D., Teng, A. P., Nguyen, T. B., Clair, J. M. S., Cohen, R. C., Romer, P., Nault, B. A., Wooldridge, P. J., Jimenez, J. L., Campuzano-Jost, P., Day, D. A., Hu, W., Shepson, P. B., Xiong, F., Blake, D. R., Goldstein, A. H., Misztal, P. K., Hanisco, T. F., Wolfe, G. M., Ryerson, T. B., Wisthaler, A. and Mikoviny, T.: Organic nitrate chemistry and its implications for nitrogen budgets in an isoprene- and monoterpene-rich atmosphere: constraints from aircraft (SEAC^{4}RS) and ground-based (SOAS) observations in the Southeast US, Atmospheric Chem. Phys., 16(9), 5969–5991, doi:https://doi.org/10.5194/acp-16-5969-2016, 2016.

Gerbig, C., Schmitgen, S., Kley, D., Volz-Thomas, A., Dewey, K. and Haaks, D.: An improved fast-response vacuum-UV resonance fluorescence CO instrument, J. Geophys. Res. Atmospheres, 104(D1), 1699–1704, doi:10.1029/1998JD100031, 1999.

de Gouw, J. and Warneke, C.: Measurements of volatile organic compounds in the earth's atmosphere using proton-transfer-reaction mass spectrometry, Mass Spectrom. Rev., 26(2), 223–257, doi:10.1002/mas.20119, 2007.

Grieshop, A. P., Logue, J. M., Donahue, N. M. and Robinson, A. L.: Laboratory investigation of photochemical oxidation of organic aerosol from wood fires 1: measurement and simulation of organic aerosol evolution, Atmospheric Chem. Phys., 9(4), 1263–1277, doi:https://doi.org/10.5194/acp-9-1263-2009, 2009.

Hayes, P. L., Carlton, A. G., Baker, K. R., Ahmadov, R., Washenfelder, R. A., Alvarez, S., Rappenglück, B., Gilman, J. B., Kuster, W. C., de Gouw, J. A., Zotter, P., Prévôt, A. S. H., Szidat, S., Kleindienst, T. E., Offenberg, J. H., Ma,

P. K. and Jimenez, J. L.: Modeling the formation and aging of secondary organic aerosols in Los Angeles during CalNex 2010, Atmospheric Chem. Phys., 15(10), 5773–5801, doi:10.5194/acp-15-5773-2015, 2015.

Jacob, D. J., Liu, H., Mari, C. and Yantosca, R. M.: Harvard wet deposition scheme for GMI, , 6, 2000.

Liu, H., Jacob, D. J., Bey, I. and Yantosca, R. M.: Constraints from ^{210}Pb and ^{7}Be on wet deposition and transport in a global three-dimensional chemical tracer model driven by assimilated meteorological fields, J. Geophys. Res. Atmospheres, 106(D11), 12109–12128, doi:10.1029/2000JD900839, 2001.

Marais, E. A., Jacob, D. J., Jimenez, J. L., Campuzano-Jost, P., Day, D. A., Hu, W., Krechmer, J., Zhu, L., Kim, P. S., Miller, C. C., Fisher, J. A., Travis, K., Yu, K., Hanisco, T. F., Wolfe, G. M., Arkinson, H. L., Pye, H. O. T., Froyd, K. D., Liao, J. and McNeill, V. F.: Aqueous-phase mechanism for secondary organic aerosol formation from isoprene: application to the southeast United States and co-benefit of SO₂ emission controls, Atmospheric Chem. Phys., 16(3), 1603–1618, doi:10.5194/acp-16-1603-2016, 2016.

Murphy, B. N., Donahue, N. M., Robinson, A. L. and Pandis, S. N.: A naming convention for atmospheric organic aerosol, Atmospheric Chem. Phys., 14(11), 5825–5839, doi:10.5194/acp-14-5825-2014, 2014.

Pye, H. O. T., Chan, A. W. H., Barkley, M. P. and Seinfeld, J. H.: Global modeling of organic aerosol: the importance of reactive nitrogen (NO_x and NO_3), Atmospheric Chem. Phys., 10(22), 11261–11276, doi:10.5194/acp-10-11261-2010, 2010.

Ryerson, T. B., Williams, E. J. and Fehsenfeld, F. C.: An efficient photolysis system for fast-response NO_2 measurements, J. Geophys. Res. Atmospheres, 105(D21), 26447–26461, doi:10.1029/2000JD900389, 2000.

Sachse, G. W., Hill, G. F., Wade, L. O. and Perry, M. G.: Fast-response, high-precision carbon monoxide sensor using a tunable diode laser absorption technique, J. Geophys. Res. Atmospheres, 92(D2), 2071–2081, doi:10.1029/JD092iD02p02071, 1987.

Schauer, J. J., Kleeman, M. J., Cass, G. R. and Simoneit, B. R. T.: Measurement of Emissions from Air Pollution Sources. 3. C1−C29 Organic Compounds from Fireplace Combustion of Wood, Environ. Sci. Technol., 35(9), 1716–1728, doi:10.1021/es001331e, 2001.

Shrivastava, M. K., Lane, T. E., Donahue, N. M., Pandis, S. N. and Robinson, A. L.: Effects of gas particle partitioning and aging of primary emissions on urban and regional organic aerosol concentrations, J. Geophys. Res., 113(D18), D18301, doi:10.1029/2007JD009735, 2008.

Zhang, L., Gong, S., Padro, J. and Barrie, L.: A size-segregated particle dry deposition scheme for an atmospheric aerosol module, Atmos. Environ., 35(3), 549–560, doi:10.1016/S1352-2310(00)00326-5, 2001.